Decoherence of non-relativistic bosonic quantum fields

Der Fakultät für Physik
der Universität Duisburg-Essen

vorgelegte Dissertation

zum Erwerb des akademischen Grades eines
Doktors der Naturwissenschaft (Dr. rer. nat)

Marduk Bolaños Puchet
aus Mexiko Stadt, Mexiko

Tag der mündlichen Prüfung: 25.10.2019
Erstgutachter: Prof. Dr. Klaus Hornberger, Universität Duisburg-Essen
Zweitgutachter: Prof. Dr. Bassano Vacchini, Università degli Studi di Milano

DOI: 10.17185/duepublico/72927
URN: urn:nbn:de:hbz:464-20201103-113343-2

Dedicated to the memory of Sören Werneburg

Abstract

Contemporary experiments prepare and probe quantum superpositions in increasingly macroscopic and complex many-body systems subject to environmental interactions. Motivated by the fact that quantum systems with a large number of interacting constituents are often described in the framework of quantum field theory, in this thesis a minimal and generic field-theoretic model is developed, that appropriately accounts for the decoherence dynamics towards a corresponding classical field theory. The main result is a generic Markovian master equation that induces the gradual classicalization of non-relativistic bosonic quantum fields in one spatial dimension. It turns any quantum superposition of distinct field configurations into a mixture, while ensuring that the expectation values of the canonical field variables evolve according to the classical field equations. Once the quantum coherences have decayed considerably, the semiclassical field dynamics is indistinguishable from a classical linear Boltzmann-type equation in the functional phase space of field configurations. The effect of the master equation on the field is minimal in the sense that it leaves the first moments of the mode quadratures unaffected, while increasing the field energy with a small state-independent rate. Assuming that the initial state of the field is a superposition of single-mode coherent states, several analytical expressions for the purity are obtained, which are in remarkable agreement with numerical calculations. The latter are carried out using quasi-Monte Carlo integration based on generalized Faure sequences. As established here, this is an efficient and accurate method for calculating expectation values in a high-dimensional quantum phase space. The presented results can be applied to a wide range of quantum many-body systems, and they set the stage for generalizations to tensorial fields in higher spatial dimensions and relativistic quantum fields.

Zusammenfassung

Heutzutage lassen sich Quantensuperpositionen in zunehmend makroskopischen Vielteilchensystemen herstellen, die oft komplexen Wechselwirkungen mit der Umwelt ausgesetzt sind. Da Quantensysteme mit einer großen Anzahl wechselwirkender Bestandteile oft im Rahmen der Quantenfeldtheorie beschrieben werden, wird in dieser Dissertation ein minimales und generisches feldtheoretisches Modell entwickelt, das den Dekohärenz-bedingten Übergang zu einer entsprechenden klassischen Feldtheorie angemessen berücksichtigt. Das Hauptergebnis ist eine generische Markowsche Mastergleichung, die den allmählichen quanten-klassischen Übergang nicht-relativistischer bosonischer Quantenfelder in einer räumlichen Dimension induziert. Sie wandelt jede Quantensuperposition unterschiedlicher Feldkonfigurationen in eine Mischung um und gewährleistet, dass die Erwartungswerte der kanonischen Feldvariablen den klassischen Feldgleichungen genügen. Sobald die Quantenkohärenzen stark zerfallen sind, lässt sich die semiklassische Felddynamik von einer klassischen linearen Boltzmann-artigen Gleichung im funktionalen Phasenraum von Feldkonfigurationen nicht unterscheiden. Die Wirkung der Mastergleichung auf das Feld ist insofern minimal, als sie die ersten Momente der Quadraturen der Feldmoden unverändert lässt und gleichzeitig die Feldenergie mit einer niedrigen zustandsunabhängigen Rate erhöht. Für einen Anfangszustand des Feldes, der durch eine Superposition kohärenter Moden-Zustände beschrieben wird, werden mehrere analytische Ausdrücke für die Purity angegeben, die eine bemerkenswerte Übereinstimmung mit numerischen Simulationen zeigen. Diese Rechnungen werden mittels einer auf verallgemeinerten Faure-Sequenzen basierenden Quasi-Monte-Carlo-Integration durchgeführt, welche hier als eine effiziente und genaue Methode zur Berechnung von Erwartungswerten in einem hochdimensionalen Quanten-Phasenraum etabliert wird. Die hier vorgelegten Ergebnisse lassen sich auf zahlreiche quantenmechanische Vielteilchensysteme anwenden und können als Grundlage dienen für die Verallgemeinerung zu tensoriellen Feldern, auf höheren räumlichen Dimensionen und zu relativistischen Quantenfeldern.

Acknowledgments

First and foremost I want to express my gratitude to my *Doktorvater*, Klaus Hornberger, for proposing such an interesting and challenging project for my doctoral thesis. I also want to thank him for suggesting me to attend the International School of Physics "Enrico Fermi" in Varenna, Italy in 2016. It was a great experience to share a week with several experts in quantum physics at such a beautiful place. I also learned to improve my language-agnostic communication skills through our joint work. Danke Klaus!

Next, I want to express my gratitude for the joy of sharing almost 4 years of my life with such a lively and joyful group. For all the grill parties, the weddings, the *Mettwoch*, the concerts, the movies, the Matjes, the dinners, the piñata, the pizzas, the beers, the cakes and all the laughs we shared, ein ganz großes Dankeschön an Benjamin, Birthe, Björn, Filip, Henning, Jonas, Kai, Klaus, Lukas, Lutz, Sabine, Silas, Stefan, Tobias und Traudl.

Of course, none of this would have been possible without the generous support of a CONACYT-DAAD scholarship and two scholarships from the University of Duisburg–Essen.

Last, but not least, I am grateful for the continuous support of my parents throughout my life.

Table of contents

1 Introduction

A PhD is a ticket to a life of research and exploration, a life of learning for learning's sake, and a life of sharing the joy of discovery with like-minded people.

—Matthias Felleisen

This dissertation is the culmination of a research project that took more than three years. Like any endeavor worth undertaking, the path to the objective was sometimes uncertain but, in the end, the results are a tangible proof of achievement. In this introductory chapter I will describe the motivation behind this work, the goals that were pursued and what was accomplished. Moreover, I will lay out the structure of the remainder of the manuscript.

Motivation

The Schrödinger equation describes the unitary evolution of a closed quantum system. In practice, however, no quantum system is actually closed. It interacts with external degrees of freedom collectively called the environment. As a result, the quantum coherences in the system decay with time. This situation is dramatically illustrated by Schrödinger's cat, which is the paradigmatic example of a macroscopic system that immediately ceases to exhibit quantum coherence once it interacts with an environment.

The loss of quantum coherence and the emergence of classical behavior in systems with a *finite* number of degrees of freedom have been extensively and successfully studied using the framework of open quantum systems [1–4]. One of the most important results of this theory is the Lindblad–Gorini–Kossakowski–Sudarshan master equation, usually simply called Lindblad equation. It is the most general dynamical law for the non-unitary evolution of a quantum system in contact with a Markovian environment. That is, an environment that "forgets" the effect of the interaction with the system faster than the system evolves.

Understanding the phenomena of decoherence and the quantum-classical transition is of paramount importance for the development of quantum technologies, since their performance is ultimately limited by the coupling to the surrounding environment [5]. Moreover, there is an ongoing effort to prepare superpositions of increasingly more massive and complex systems with the aim of understanding how macroscopic a quantum system can be [6, 7]. Decoherence plays a central role in these experiments probing the physics at the quantum-classical border.

Quantum systems with a large number of interacting constituents are often described in terms of quantum fields, since an atomistic treatment of the combined dynamics becomes unwieldy. Therefore, one usually considers that the degrees of freedom of the system are the collective field modes. Examples include degenerate quantum gases and fluids [8, 9], collective degrees of freedom in strongly correlated solid-state systems [10, 11], acoustic vibrations in superfluid Helium [12–14], micromechanical oscillators [15, 16], and closely spaced chains of harmonic oscillators realized, for example, in ion traps [17] and superconducting circuits [18].

For these many-body systems a minimal and generic field-theoretic model that appropriately accounts for the decoherence dynamics toward the corresponding classical field theory is desirable. Previous works on the open-system dynamics of bosonic fields [19–23] considered the electromagnetic and the Klein–Gordon fields subject to interactions that lead to a master equation for quantum Brownian motion [24]. While such models are adequate when the environment induces small fluctuations in the field amplitude, they cannot appropriately describe the decoherence of macroscopic superpositions. One reason is that the obtained decay rates become unrealistically large, growing above all bounds as the separation between the superposed field states increases [25].

As mentioned in the beginning, macroscopic systems are never found in a quantum superposition. However, quantum theory does not exclude this possibility. Therefore, experimentally falsifiable stochastic nonlinear modifications of the Schrödinger equation have been proposed, whose predictions in the microscopic scale are in agreement with quantum theory, while prohibiting superpositions of macroscopically distinct states [26]. These models of wave-function collapse are being tested in experiments involving molecular interferometry and optomechanical systems [27]. Their field-theoretic extension becomes necessary as the number of constituents in the many-body system grows.

Objective

Motivated by the foundational issues expounded above and by the technological implications of a better understanding of decoherence in large quantum systems, this thesis presents a generic field-theoretic model for bosonic many-body systems that appropriately accounts for the decoherence dynamics towards a corresponding classical field theory, while minimally affecting the field. In order to simplify the exposition, a non-relativistic bosonic quantum field in *one* dimension is considered.

Results

In the following I summarize the results and contributions of this thesis.

LINDBLAD EQUATION. The main contribution of this work is a generic field-theoretic Lindblad equation that induces the gradual classicalization of a non-relativistic bosonic field. It induces a monotonic decay of the purity of any quantum

state of the field, thereby suppressing all quantum coherences. At the same time, it ensures that the expectation values of the canonical field variables, namely the field amplitude and its canonically conjugate momentum, evolve according to the corresponding classical linear field equations and thus the classical superposition principle is not affected. In this sense the master equation has a minimal impact on the bosonic field. Besides classicalizing the state of the field, the master equation also leads to a gradual increase of the field's energy with a constant rate that is independent of the state. The open field dynamics can be seen as a stochastic process in which the unitary evolution is interrupted at random times by simultaneous minimally imprecise generalized measurements of the canonical variables of the field, whose results are discarded.

Semiclassical dynamics. In the functional phase space of the canonical variables of the field the dynamics induced by the master equation correspond to a generalized linear Boltzmann equation that reduces to a Fokker–Planck equation in the diffusion limit. These equations, which describe the time evolution of the Wigner quasi-probability distribution functional, govern the semiclassical dynamics of the field once the quantum coherences have decayed appreciably. This occurs due to the field being subject to random phase-space kicks, which as mentioned above can be interpreted as generalized measurements.

Purity decay. The master equation turns any quantum superposition of different field configurations into a mixture. The classicalization dynamics is in general not amenable to analytic treatment. However, for certain limiting values of the parameters in the master equation and assuming a superposition of single-mode coherent states, I obtained approximate analytical expressions that are in excellent agreement with the numerical simulation of the exact dynamics. This proved more challenging than expected, since calculating integrals in a high-dimensional phase space requires a numerical method that converges faster than Monte Carlo methods. This work demonstrates that quasi-Monte Carlo integration is a valuable addition to the numerical toolbox of quantum physicists.

The road ahead

In the following chapters, I discuss in detail the model system, the master equation and its properties, the corresponding phase-space dynamics, the time evolution of the purity decay for a superposition of single-mode coherent states and the numerical integration method used for the calculations.

In **Chapter 2** I consider a linear harmonic chain subject to periodic boundary conditions and show that in the continuum limit this many-body bosonic system can be described in terms of a quantum field. This is the system whose classicalization is studied in subsequent chapters. Here I also present a short summary of the theory of field quantization, including the phase-space methods used in Chapter 4. Since this involves working with functional derivatives, a section will be devoted to the necessary mathematical background.

The generic field-theoretic Lindblad equation is introduced in **Chapter 3**. First, I will provide a brief summary of the theory of open quantum systems, including a discussion of the family of master equations generated by random unitary transformations. Then, I will present the master equation and discuss the physical requirements that lead to the specific form it has. Finally, after a short presentation of the framework of generalized measurements, I will show that the Lindblad equation presented here can be interpreted as a measurement master equation.

The phase-space dynamics induced by the master equation are described in **Chapter 4** using the Wigner representation. As will be shown, the Wigner functional in the phase space of the canonical variables of the field evolves with a generalized linear Boltzmann equation that reduces to a Fokker–Planck equation in the diffusion limit. Using the Wigner functional in the phase space of the mode variables the dynamics of the purity decay of the state of the field are studied analytically and numerically for a superposition of single-mode coherent states. Since functional integrals are used extensively in this chapter, their rigorous definition is discussed in Appendix A. Moreover, for the sake of reproducibility, in Appendix B I provide a Fortran program that performs the above numerical calculations.

The phase-space integrals in Chapter 4 are evaluated using a quasi-Monte Carlo method. This class of integration methods is not well known in the quantum optics community even though, as shown in this work, they are very useful for studying many-body quantum systems. **Chapter 5** provides a short introduction to digital sequences with a special emphasis on Faure sequences and their generalization. An illustration of the usage of a Java library to generate Faure sequences is provided in Appendix C.

The results and contributions of this research project are summarized in **Chapter 6**. Here I also discuss the perspectives for extending the decoherence model to relativistic, tensor and spinor fields.

2 Non-relativistic bosonic fields

The central topic of this dissertation is a generic model for the classicalization of a bosonic quantum field describing a many-body system. In this chapter, I first present a brief summary of the theory of classical scalar fields and afterwards I discuss several aspects of their quantization, including the Fock space and the phase-space representation. The objective is to show how the concepts and tools familiar from quantum mechanics with finitely many degrees of freedom generalize when describing systems with infinitely many degrees of freedom. In the final section, I introduce the model system that will be considered throughout the remaining chapters, a harmonic chain subject to periodic boundary conditions, which in the continuum limit is described by a bosonic quantum field.

2.1 Classical scalar fields

I start by providing a summary of the Lagrangian and Hamiltonian formulations of the theory of classical scalar fields. As will be shown, they are generalizations of the corresponding formulations for N degrees of freedom, obtained in the limit $N \to \infty$.

2.1.1 Lagrangian formalism

The configuration of a system of point-like particles may be specified by the *generalized coordinates*, usually denoted $q_i(t)$ with $i = 1, ..., N$, where N is the number of degrees of freedom of the system. In Lagrange's formalism the dynamics of the system of particles are obtained from the Lagrangian,

$$L = L(q_1(t), ..., q_N(t), \dot{q}_1(t), ..., \dot{q}_N(t), t), \tag{2.1}$$

a function of the generalized coordinates $q_i(t)$, their corresponding velocities $\dot{q}_i(t)$, and time t, using Hamilton's principle of stationary action [28],

$$\delta S = \int_{t_1}^{t_2} \mathrm{d}t \, \delta L(q_1(t), ..., q_N(t), \dot{q}_1(t), ..., \dot{q}_N(t), t) = 0. \tag{2.2}$$

For fixed t_1 and t_2 the action S is a functional of the generalized coordinates. That is, it maps a set of functions to a number. The symbol δS denotes the first variation of the functional, a generalization of the concept of total differential of a function, which will be discussed in Section 2.2. The variation of the Lagrangian is given by the total differential

$$\delta L(q_1(t), ..., q_N(t), \dot{q}_1(t), ..., \dot{q}_N(t), t) = \sum_{i=1}^{N} \left[\frac{\partial L}{\partial q_i} \delta q_i + \frac{\partial L}{\partial \dot{q}_i} \delta \dot{q}_i \right], \tag{2.3}$$

where the variations of the generalized coordinates satisfy

$$\delta q_i(t_1) = \delta q_i(t_2) = 0, \quad i = 1, 2, ..., N. \tag{2.4}$$

Integrating by parts the second term in the right side of (2.3) and using (2.4), the principle of stationary action yields the Euler–Lagrange equations

$$\frac{\partial L}{\partial q_i} \quad \partial_t \frac{\partial L}{\partial \dot{q}_i} = 0, \quad i = 1, 2, ..., N. \tag{2.5}$$

Given the initial values of the generalized coordinates and their time derivatives, these equations determine the time evolution of the system.

In the limit of infinitely many particles, $N \to \infty$, the index i is replaced by the continuous variable x and the generalized coordinates become fields. That is,

$$q_i(t) \equiv q(i,t) \quad \to \varphi(x,t). \tag{2.6}$$

The Lagrangian of the system at a given time t depends on the values of $\varphi(x,t)$ and $\dot{\varphi}(x,t)$ at every position x and is thus a functional,

$$L[\varphi, \dot{\varphi}, t] = \int \mathrm{d}x \, \mathcal{L}(\varphi(x,t), \partial_x \varphi(x,t), \dot{\varphi}(x,t); x, t), \tag{2.7}$$

defined in terms of the Lagrangian density $\mathcal{L}$, which for each x is a function of the values of the field and its spatial and temporal derivatives, and it may also depend explicitly on x and t.

The total differential of Eq. (2.3) generalizes to the first variation of the Lagrangian [29],

$$\delta L = \int \mathrm{d}x \left[\frac{\delta L}{\delta \varphi(x,t)} \delta\varphi(x,t) + \frac{\delta L}{\delta \dot{\varphi}(x,t)} \delta\dot{\varphi}(x,t) \right], \tag{2.8}$$

and the corresponding Euler–Lagrange equations are the $N \to \infty$ generalization of Eqs. (2.5) [29],

$$\frac{\delta L}{\delta \varphi(x,t)} \quad \partial_t \frac{\delta L}{\delta \dot{\varphi}(x,t)} = 0. \tag{2.9}$$

The functional derivatives in the last two equations, denoted with the Greek letter delta, correspond to a generalization of the directional derivative for the case of infinitely many variables. They are defined and discussed in Section 2.2.

2.1.2 Hamiltonian formalism

In Hamilton's formulation the dynamics of the system are obtained from the Hamiltonian,

$$H(\mathbf{q}, \boldsymbol{\pi}, t) = \sum_{i=1}^{N} \pi_i \dot{q}_i \quad L(\mathbf{q}, \dot{\mathbf{q}}, t), \tag{2.10}$$

a function of the generalized coordinates and the canonical momenta

$$\pi_i = \frac{\partial L}{\partial \dot{q}_i}, \quad i = 1, ..., N. \tag{2.11}$$

From the total differential of the Hamiltonian,

$$\begin{aligned} \mathrm{d}H &= \sum_{i=1}^{N} \frac{\partial H}{\partial \pi_i}\,\mathrm{d}\pi_i + \frac{\partial H}{\partial q_i}\,\mathrm{d}q_i + \frac{\partial H}{\partial t}\,\mathrm{d}t \\ &= \sum_{i=1}^{N} \dot{q}_i\,\mathrm{d}\pi_i \quad \sum_{i=1}^{N} \dot{\pi}_i\,\mathrm{d}q_i \quad \frac{\partial L}{\partial t}\,\mathrm{d}t, \end{aligned} \tag{2.12}$$

it follows that q_i and π_i evolve according to Hamilton's equations,

$$\dot{q}_i = \quad \frac{\partial H}{\partial \pi_i}, \tag{2.13}$$

$$\dot{\pi}_i = \quad \frac{\partial H}{\partial q_i}. \tag{2.14}$$

The *canonical coordinates* q_i and π_i specify at each time t the state of the mechanical system. Its time evolution generates a trajectory in a $2N$-dimensional space, called the *phase space*.

The dynamical variables of the system are functions $f(\mathbf{q}, \boldsymbol{\pi}, t)$, which in general have an explicit dependence on time. Calculating the total time derivative of f yields

$$\frac{\mathrm{d}}{\mathrm{d}t} f(\mathbf{q}, \boldsymbol{\pi}, t) = \frac{\partial f}{\partial t} + \{f, H\}_{P.B.}, \tag{2.15}$$

where

$$\{f, g\}_{P.B.} = \sum_{i=1}^{N} \frac{\partial f}{\partial q_i}\frac{\partial g}{\pi_i} \quad \frac{\partial f}{\partial \pi_i}\frac{\partial g}{q_i} \tag{2.16}$$

is the Poisson bracket between two functions of the canonical coordinates. It is antisymmetric under the exchange of its arguments and satisfies $\{f, f\}_{P.B.} = 0$. The Poisson brackets between the generalized coordinates and the canonical momenta are given by

$$\{q_i, \pi_j\} = \delta_{ij}, \tag{2.17}$$

$$\{q_i, q_j\} = \{\pi_i, \pi_j\} = 0. \tag{2.18}$$

In the limit of infinitely many particles, $N \to \infty$, the Hamiltonian becomes a functional,

$$H[\varphi, \pi, t] = \int \mathrm{d}x\, [\pi(x)\dot{\varphi}(x) \quad \mathcal{L}(x, t)], \tag{2.19}$$

of the field amplitude $\varphi(x, t)$ and the canonical momentum field

$$\pi(x, t) = \frac{\partial \mathcal{L}(x, t)}{\partial \dot{\varphi}(x, t)}, \tag{2.20}$$

which is defined in terms of the Lagrangian density in (2.7).

The corresponding generalization of Hamilton's equations is given by

$$\dot{\varphi}(x) = \frac{\delta H}{\delta \pi(x)}, \tag{2.21}$$

$$\dot{\pi}(x) = \frac{\delta H}{\delta \varphi(x)}. \tag{2.22}$$

The Poisson bracket (2.16) generalizes to [29]

$$\{F, G\}_{P.B.} = \int \mathrm{d}x \left[\frac{\delta F}{\delta \varphi(x)} \frac{\delta G}{\delta \pi(x)} \quad \frac{\delta F}{\delta \pi(x)} \frac{\delta G}{\delta \varphi(x)} \right], \tag{2.23}$$

where $F[\varphi, \pi]$ and $G[\varphi, \pi]$ are functionals of the canonical coordinates of the field. Using the identity (see Section 2.2)

$$\frac{\delta f(x,t)}{\delta f(x',t)} = \delta(x \quad x'), \tag{2.24}$$

it follows that $\varphi(x,t)$ and $\pi(x,t)$ satisfy the canonical relations

$$\{\varphi(x,t), \pi(x',t)\} = \delta(x \quad x'), \tag{2.25}$$

$$\{\varphi(x,t), \varphi(x',t)\} = \{\pi(x,t), \pi(x',t)\} = 0. \tag{2.26}$$

2.2 Functional differentiation

Before discussing the quantization of classical scalar fields, in this section I provide a short summary of functional calculus, which already appeared in Section 2.1 and will play an important role in Chapter 4. As will be shown, functional derivatives are the straightforward generalization of the directional derivative, familiar from the calculus of several variables, to the case of infinitely many variables. For a comprehensive discussion the reader is advised to consult [30].

2.2.1 Linear functionals

A real-valued function f of n real variables is defined as the map

$$\mathbb{R}^n \to \mathbb{R}, \quad \mathbf{x} = x_1, x_2, ..., x_n \overset{f}{\mapsto} f(\mathbf{x}). \tag{2.27}$$

A *linear functional* F is defined as the map

$$\mathcal{X} \to \mathbb{C}, \quad \alpha \overset{F}{\mapsto} F[\alpha], \tag{2.28}$$

where $\mathcal{X}$ is a normed linear space of functions. That is, F assigns to each element α of $\mathcal{X}$ the complex number $F[\alpha]$. It is customary to write the argument of a functional in square brackets to distinguish it from a function.

In general, given a set M equipped with a measure μ and a subspace X of the space of functions $h\colon M \to \mathbb{C}$, a linear functional $F[h]$ can be defined as

$$F[h] = \int \varrho(x) h(x)\, \mathrm{d}\mu(x), \quad \text{for all } h \in X, \tag{2.29}$$

for any given function $\varrho \in X$, called the *density function* of the functional. For example, the functional that associates a function f with its value at a point x_0 in its domain $\mathcal{D}$, $F[f] = f(x_0)$, has the Dirac delta distribution as its density function,

$$F[f] = \int_{\mathcal{D}} f(x)\, \delta(x \quad x_0)\, \mathrm{d}x. \tag{2.30}$$

This functional is sometimes denoted as $\delta_{x_0}[f]$.

2.2.2 Functional derivatives

The directional derivative of the function (2.27) along a vector $\mathbf{v} = (v_1, \ldots, v_n)$ is the function $D_{\mathbf{v}} f\colon \mathbb{R}^n \to \mathbb{R}$ defined by the limit

$$D_{\mathbf{v}} f(\mathbf{x}) = \lim_{t \to 0} \frac{f(\mathbf{x} + t\mathbf{v}) \quad f(\mathbf{x})}{t}. \tag{2.31}$$

Intuitively, this expression gives the rate of change of f at the point $\boldsymbol{x}$ with respect to a small change $\Delta\mathbf{x} = t\mathbf{v}$ of all the coordinates $\mathbf{x}$ in the direction $\mathbf{v}$. Since $f(\mathbf{x} + t\mathbf{v})$ is a function of t, (2.31) can also be stated in a form which is more convenient for calculations,

$$D_{\mathbf{v}} f(\mathbf{x}) = \frac{\mathrm{d}}{\mathrm{d}t} f(\mathbf{x} + t\mathbf{v})\bigg|_{t=0}. \tag{2.32}$$

Given two elements f and g of the function space $\mathcal{X}$, the *functional (or variational) derivative* of the functional (2.28) at the point f in the direction g is the map from $\mathcal{X}$ to $\mathbb{C}$ defined through the limit [31]

$$\frac{\delta F[f]}{\delta f}(g) = \lim_{t \to 0} \frac{F[f + tg] \quad F[f]}{t}. \tag{2.33}$$

Comparing this expression with (2.31) it becomes clear that the functional derivative can be seen as a generalization of the directional derivative. Moreover, considering $F[f + tg]$ as a function of t, from the Taylor series expansion of F it follows that (2.33) can be written in a form similar to (2.32),

$$\frac{\delta F[f]}{\delta f}(g) = \frac{\mathrm{d}}{\mathrm{d}t} F[f + tg]\bigg|_{t=0}. \tag{2.34}$$

Higher-order functional derivatives are defined by iterative application of (2.33). In particular, the second functional derivative of F at the point f is given by the map from $\mathcal{X} \times \mathcal{X}$ to $\mathbb{C}$ [31]

$$\frac{\delta^2 F[f]}{\delta f^2}(g, h) = \frac{\mathrm{d}}{\mathrm{d}t} \frac{\delta F[f + th]}{\delta f}(g)\bigg|_{t=0}. \tag{2.35}$$

2.2.3 Partial functional derivatives

The partial derivative of the function (2.27) at the point $(x_1, ..., x_n)$ with respect to a change of the k-th variable is defined as

$$\frac{\partial f}{\partial x_k}(x_1, ..., x_n) = \lim_{t\to 0} \frac{1}{t}[f(x_1 + t\delta_{1_k}, ..., x_n + t\delta_{nk}) \quad f(x_1, ..., x_n)]. \tag{2.36}$$

In particular, for $f(\mathbf{x}) = x_j$ this yields

$$\frac{\partial x_j}{\partial x_k} = \delta_{jk}. \tag{2.37}$$

In an analogous way, the *partial functional derivative* of the functional (2.28) at the point f with respect to a local change of f at x is defined as [31]

$$\frac{\delta F[f]}{\delta f(x)} = \frac{\mathrm{d}}{\mathrm{d}t} F[f + t\delta_x]\Big|_{t=0}, \tag{2.38}$$

where $\delta_x(y) \equiv \delta(y \quad x)$ is the Dirac delta centered at x. Using this definition, the functional generalization of (2.37) is given by

$$\frac{\delta}{\delta f(x)} \delta_y[f] = \delta(x \quad y), \tag{2.39}$$

which, since $\delta_y[f] = f(y)$, is commonly written as

$$\frac{\delta f(y)}{\delta f(x)} = \delta(x \quad y). \tag{2.40}$$

Higher-order partial functional derivatives are defined through repeated application of (2.38). In particular, the second partial functional derivative is given by

$$\frac{\delta^2 F[f]}{\delta f(y)\delta f(x)} = \frac{\mathrm{d}}{\mathrm{d}t} \frac{\delta F[f + t\delta_y]}{\delta f(x)}\Big|_{t=0}. \tag{2.41}$$

2.2.4 Variation of a functional

The total differential of the function (2.27) at the point $\mathbf{x} = (x_1, ..., x_n)$ is given by

$$\mathrm{d}f(\mathbf{x}, \Delta\mathbf{x}) = \sum_{j=1}^{n} \frac{\partial f}{\partial x_j}(\mathbf{x})\, \mathrm{d}x_j, \tag{2.42}$$

with $\Delta\mathbf{x} = (\Delta x_1, ..., \Delta x_n)$ and $\Delta x_j = \mathrm{d}x_j$. It can also be defined as a directional derivative,

$$\mathrm{d}f(\mathbf{x}, \Delta\mathbf{x}) = \lim_{t\to 0} \frac{f(\mathbf{x} + t\Delta\mathbf{x}) \quad f(\mathbf{x})}{t} = \frac{\mathrm{d}}{\mathrm{d}t} f(\mathbf{x} + t\Delta\mathbf{x})\Big|_{t=0}. \tag{2.43}$$

The n-th order total differential of the function f at the point $\mathbf{x}$ is defined as

$$\mathrm{d}^n f(\mathbf{x}, \Delta\mathbf{x}) = \frac{\mathrm{d}^n}{\mathrm{d}t^n} f(\mathbf{x} + t\Delta\mathbf{x})\Big|_{t=0}. \tag{2.44}$$

In terms of total differentials, the Taylor series of f at the point $\mathbf{x}$ is

$$f(\mathbf{x}+\Delta\mathbf{x}) \simeq f(\mathbf{x}) + \mathrm{d}f(\mathbf{x},\Delta\mathbf{x}) + \frac{1}{2}\mathrm{d}^2 f(\mathbf{x},\Delta\mathbf{x}) + \cdots + \frac{1}{n!}\mathrm{d}^n f(\mathbf{x},\Delta\mathbf{x}) + \cdots \tag{2.45}$$

The above definitions can be generalized to the case of functionals. The *first variation* of the functional (2.28) at the point f is given by [32]

$$\delta F[f,g] = \int \mathrm{d}x \, \frac{\delta F[f]}{\delta f(x)} \, g(x). \tag{2.46}$$

In terms of the functional derivative, it can be calculated as

$$\delta F[f,g] = \lim_{t\to 0} \frac{F[f+t\,g] \quad F[f]}{t} = \frac{\mathrm{d}}{\mathrm{d}t} F[f+t\,g]\bigg|_{t=0}. \tag{2.47}$$

From the last two expressions it follows that the functional derivative of F at the point f in the direction g can be written as

$$\frac{\delta F[f]}{\delta f}(g) = \int \mathrm{d}x \, \frac{\delta F[f]}{\delta f(x)} \, g(x). \tag{2.48}$$

Since the n-th order variation of the functional F at the point f is given by

$$\delta^n F[f,g] = \frac{\mathrm{d}^n}{\mathrm{d}t^n} F[f+t\,g]\bigg|_{t=0}, \tag{2.49}$$

in terms of variations the Taylor series of F at the point f is

$$F[f+g] \simeq F[f] + \delta F[f,g] + \frac{1}{2}\delta^2 F[f,g] + \cdots + \frac{1}{n!}\delta^n F[f,g] + \cdots \tag{2.50}$$

2.2.5 Product rule and chain rule

Since the functional derivative generalizes the derivative of a function of several variables, there are a corresponding product rule and a chain rule. Given two functionals F_1 and F_2, applying the definition (2.38) to the product F_1F_2 yields [32]

$$\frac{\delta(F_1[f]F_2[f])}{\delta f(x)} = \frac{\delta F_1[f]}{\delta f(x)} F_2[f] + F_1[f] \frac{\delta F_2[f]}{\delta f(x)}. \tag{2.51}$$

For a scalar function

$$f\colon \mathbf{y} = (y_1, \ldots, y_n) \mapsto g(x_1(\mathbf{y}), \ldots, x_n(\mathbf{y})), \tag{2.52}$$

which is the composition of the scalar function g with the coordinate functions $\mathbf{x}$, the partial derivative of f with respect to y_j at the point $\mathbf{y}$ is given by the chain rule

$$\frac{\partial f(\mathbf{y})}{\partial y_j} = \sum_{i=1}^{n} \frac{\partial g(\mathbf{x}(\mathbf{y}))}{\partial x_i} \frac{\partial x_i(\mathbf{y})}{\partial y_j}. \tag{2.53}$$

The chain rule for functionals must be stated carefully. The crucial point is to note that the generalization of the coordinate functions $x_1, ..., x_n$ to the case of a continuous index is a one-parameter family of functionals,

$$\lambda(s) = X_s[f], \quad s \in \mathbb{R}. \tag{2.54}$$

That is, the function λ maps each $s \in \mathbb{R}$ onto a functional $X_s[f]$. Given a functional G acting on λ, from (2.54) it follows that

$$G[\lambda] = G[X_s[f]] \equiv F[f]. \tag{2.55}$$

It is important to remark that $G[X_s[f]]$ does not denote the composition of two functionals, because that is not possible. It is rather a functional F of f, since a variation of f changes the value of λ, which in turn produces a variation of G. The partial functional derivative of F with respect to a local change of f at x is given by [32]

$$\frac{\delta F[f]}{\delta f(x)} = \int \mathrm{d}s \, \frac{\delta G[\lambda]}{\delta \lambda(s)} \frac{\delta X_s[f]}{\delta f(x)}. \tag{2.56}$$

This equation is the generalization of the chain rule (2.53) for functionals.

2.2.6 Functional Wirtinger derivatives

In complex analysis, a complex-valued function of a complex variable is complex-differentiable if and only if it is real-differentiable and a pair of partial differential equations, the Cauchy–Riemann equations, are satisfied [33].

For a complex function α that is real-differentiable but not complex-differentiable, one can define generalized complex derivatives known as *Wirtinger derivatives*. In this so-called Wirtinger calculus, α is formally regarded as a function of two independent complex variables, z and z^*, with $z = x + \mathrm{i}y$ and z^* its complex conjugate. The Wirtinger derivatives are implemented by the generalized complex differential operators

$$\frac{\partial}{\partial z} = \frac{1}{2}\left(\frac{\partial}{\partial x} \quad \mathrm{i}\frac{\partial}{\partial y} \right), \tag{2.57}$$

and

$$\frac{\partial}{\partial z^*} = \frac{1}{2}\left(\frac{\partial}{\partial x} + \mathrm{i}\frac{\partial}{\partial y} \right). \tag{2.58}$$

In terms of them, the Cauchy–Riemann equations have the simple expression [33]

$$\frac{\partial \alpha}{\partial z^*} = 0. \tag{2.59}$$

As an illustration of the Wirtinger calculus consider the function $\alpha(z) = z z^* = |z|^2$. Regarding z and z^* as two independent variables, the Wirtinger derivatives of α are given by

$$\frac{\partial \alpha}{\partial z} = z^* \quad \text{and} \quad \frac{\partial \alpha}{\partial z^*} = z. \tag{2.60}$$

This can be verified by writing α in terms of x and y.

The Wirtinger calculus can be generalized to the case of linear functionals. Considering the functional (2.28) as formally depending on two independent complex functions α and α^*, with $\alpha = f + \mathrm{i}g$, the *functional Wirtinger derivatives* are implemented by the generalized functional differential operators

$$\frac{\delta}{\delta\alpha} = \frac{1}{2}\left(\frac{\delta}{\delta f} \quad \mathrm{i}\frac{\delta}{\delta g}\right), \tag{2.61}$$

and

$$\frac{\delta}{\delta\alpha^*} = \frac{1}{2}\left(\frac{\delta}{\delta f} + \mathrm{i}\frac{\delta}{\delta g}\right). \tag{2.62}$$

These functional derivatives are commonly used in the description of the dynamics of open quantum systems in the phase-space representation, which will be introduced in section 2.6, as will be shown in Chapter 4.

2.3 Field quantization in an arbitrary basis

Non-relativistic quantum scalar fields can be considered as the limit $N \to \infty$ of a sequence of discrete models with N canonical quantum degrees of freedom. It is reasonable to assume that the larger N, the better the sequence approximates the actual field. In the limit of infinitely many degrees of freedom the fields $\varphi(x,t)$ and $\pi(x,t)$ can be written in a countable basis of real orthonormal functions $h_j(x)$,

$$\varphi(x,t) = \sum_{j=1}^{\infty} \phi_j(t)\, h_j(x), \tag{2.63}$$

$$\pi(x,t) = \sum_{j=1}^{\infty} \pi_j(t)\, h_j(x). \tag{2.64}$$

In the final section of this chapter I will discuss a discrete model and obtain the corresponding quantum field in the limit $N \to \infty$.

The canonical quantization or Dirac quantization of the classical fields $\varphi(x,t)$ and $\pi(x,t)$ consists in promoting the real sequences $\{\phi_j\}$ and $\{\pi_j\}$ in (2.63) and (2.64) to corresponding sequences of Hermitian operators, $\{\Phi_j\}$ and $\{\Pi_j\}$, satisfying the *canonical commutation relations*

$$[\Phi_j, \Pi_{j'}] = \mathrm{i}\hbar\delta_{jj'}, \tag{2.65}$$

obtained by replacing the Poisson bracket in (2.17) with the Lie bracket or commutator.

The quantized fields are thus given by

$$\Phi(x) = \sum_{j=1}^{\infty} \Phi_j\, h_j(x), \tag{2.66}$$

and

$$\Pi(x) = \sum_{j=1}^{\infty} \Pi_j\, h_j(x). \tag{2.67}$$

Actually, these are only formal expressions since, in general, for fixed x the sums in (2.66) and (2.67) do not converge to an operator. They define so-called *local operators*, which become true operators only when smeared with appropriate test functions [34, 35]. Denoting with f and g two real test functions, the *smeared field operators* are defined as

$$\Phi[f] = \int \mathrm{d}x\, \Phi(x) f(x) = \sum_{j=1}^{\infty} \Phi_j \int \mathrm{d}x\, h_j(x) f(x), \tag{2.68}$$

and

$$\Pi[g] = \int \mathrm{d}x\, \Pi(x) g(x) = \sum_{j=1}^{\infty} \Pi_j \int \mathrm{d}x\, h_j(x) g(x). \tag{2.69}$$

With a proper choice of test-function space the integrals in the right side fall rapidly to zero as $j \to \infty$, thereby ensuring that the sums in (2.68) and (2.69) converge to operators.

The local field operators (2.66) and (2.67) satisfy the commutation relations

$$\begin{aligned}[\Phi(x), \Pi(y)] &= \sum_{i,j=1}^{\infty} [\Phi_i, \Pi_j]\, h_i(x) h_j(y) \\ &= \mathrm{i}\hbar \sum_{i=1}^{\infty} h_i(x) h_i(y).\end{aligned} \tag{2.70}$$

Recalling the completeness relation of a countable orthonormal basis, given in terms of the Dirac delta as

$$\sum_{i=1}^{\infty} h_i(x) h_i(y) = \delta(x \quad y), \tag{2.71}$$

Eq. (2.70) yields the formal expression for the canonical commutation relations of the fields

$$[\Phi(x), \Pi(y)] = \mathrm{i}\hbar\, \delta(x \quad y). \tag{2.72}$$

A well-defined expression is obtained by taking the commutator of the smeared field operators (2.68) and (2.69),

$$\big[\Phi[f], \Pi[g]\big] = \mathrm{i}\hbar \langle f, g \rangle, \tag{2.73}$$

where the right side involves the inner product in the space of test functions,

$$\langle f, g \rangle = \int \mathrm{d}x\, f(x) g(x). \tag{2.74}$$

The canonical commutation relations define the algebra of the canonical variables, which provide a complete description of the system at any given time. Therefore, any observable of the system can be expressed as a function of Φ and Π. However, the Hamiltonian, which is the generator of time translations, can be written as a well-defined operator only after specifying the representation of the canonical variables as operators in a Hilbert space.

For a finite number of degrees of freedom the canonical variables admit a unique physically relevant representation. The uniqueness is guaranteed by the Stone–von Neumann theorem on the unitary equivalence of the representations of the canonical commutation relations [36, 37]. Since the representation space is the tensor product of the Hilbert spaces associated with the pairs of canonical variables, the resulting Hilbert space is separable, that is, it has a countable orthonormal basis.

For quantum systems with infinitely many degrees of freedom, however, there exist a large number of unitarily inequivalent representations of the canonical variables. Remarkably, the dynamics of the field determine the choice of representation [36, 38]. Even though an infinite tensor product of Hilbert spaces with dimension larger than one is non-separable, that is, in such a space complete orthonormal sets are not countable, there usually is an observable of the field that can be defined on a separable subspace of the infinite tensor product, thus providing a representation space [38, 39]. The most common example is the number operator, which will be introduced in the next section.

2.4 Fock representation of bosonic fields

The Fock representation for infinitely many degrees of freedom, which was rigorously constructed by Cook [40], is the standard description of both fermionic and bosonic free fields. However, this representation is in general unsuitable for interacting fields and one must resort to using so-called non-Fock representations [10, 41].

Remarkably, the Fock representation of quantum fields also provides a convenient mathematical framework for classical statistical mechanics [42, 43]. Moreover, it affords a natural description of stochastic processes with non-commutative random variables. This so-called quantum stochastic calculus is the mathematical framework used in the theory of quantum noise [44, 45].

The quantum fields with which this thesis is concerned can be represented in a bosonic Fock space. For the sake of generality, in the following I discuss this representation without considering a particular basis.

Given a separable Hilbert space $\mathfrak{h}$, the corresponding *bosonic Fock space* is constructed as

$$\mathcal{F}(\mathfrak{h}) = \bigoplus_{n=0}^{\infty} \mathfrak{h}^{\otimes_s^n} = \mathfrak{h}^{\otimes_s^0} \oplus \mathfrak{h}^{\otimes_s^1} \oplus \mathfrak{h}^{\otimes_s^2} \oplus \mathfrak{h}^{\otimes_s^3} \oplus \cdots, \tag{2.75}$$

where $\oplus$ denotes the direct sum of two vector spaces and the component subspaces are given by

$$\begin{aligned} \mathfrak{h}^{\otimes_s^0} &= \mathbb{C}, \\ \mathfrak{h}^{\otimes_s^1} &= \mathfrak{h}, \\ \mathfrak{h}^{\otimes_s^2} &= \mathfrak{h} \otimes_s \mathfrak{h}, \\ \mathfrak{h}^{\otimes_s^3} &= \mathfrak{h} \otimes_s \mathfrak{h} \otimes_s \mathfrak{h}. \end{aligned} \tag{2.76}$$

The symbol $\otimes_s$ denotes the *symmetric tensor product* of two vector spaces, which is spanned by permutation-symmetric linear combinations of tensor products of basis elements of both spaces. Since the spaces $\mathfrak{h}^{\otimes_s^n}$ are separable, their direct sum yields the separable Hilbert space $\mathcal{F}(\mathfrak{h})$, which for historical reasons is called the *second quantization* of $\mathfrak{h}$.

An arbitrary permutation-symmetric state in $\mathfrak{h}^{\otimes_s^n}$ is given by [46]

$$|Y^{(n)}\rangle = \frac{1}{\sqrt{n!}} \sum_{P(n)} |Y_{p_1} Y_{p_2} ... Y_{p_n}\rangle, \tag{2.77}$$

where $P(n)$ is the set of permutations of n indices and p_i are the indices corresponding to a given permutation. The operators

$$\mathrm{a}[f]|Y^{(n)}\rangle = \frac{1}{\sqrt{(n-1)!}} \sum_{P(n)} \langle f|Y_{p_1}\rangle |Y_{p_2} ... Y_{p_n}\rangle, \tag{2.78}$$

and

$$\mathrm{a}^\dagger[f]|Y^{(n)}\rangle = \frac{1}{\sqrt{(n+1)!}} \sum_{P(n+1)} |f_{p_0} Y_{p_1} Y_{p_2} ... Y_{p_n}\rangle, \tag{2.79}$$

where $|f\rangle$ is an arbitrary normalized element of $\mathfrak{h}$, map $\mathfrak{h}^{\otimes_s^n}$ onto $\mathfrak{h}^{\otimes_s^{n-1}}$ and onto $\mathfrak{h}^{\otimes_s^{n+1}}$, respectively. Since $|f\rangle$ can be expressed in terms of an orthonormal basis $\{|h_n\rangle\}_{n=1}^\infty$ as

$$|f\rangle = \sum_{n=1}^{\infty} \langle h_n|f\rangle |h_n\rangle, \tag{2.80}$$

the operators (2.78) and (2.79) can be alternatively written as [47, 48]

$$\mathrm{a}[f] = \sum_{n=1}^{\infty} \langle f|h_n\rangle \mathrm{a}_n, \tag{2.81}$$

and

$$\mathrm{a}^\dagger[f] = \sum_{n=1}^{\infty} \langle h_n|f\rangle \mathrm{a}_n^\dagger, \tag{2.82}$$

with $\mathrm{a}_n = \mathrm{a}[h_n]$. These operators satisfy the commutation relations

$$\big[\mathrm{a}[f], \mathrm{a}^\dagger[g]\big] = \langle f|g\rangle \mathrm{I}, \tag{2.83}$$

where

$$\langle f|g\rangle = \int \mathrm{d}x\, f^*(x) g(x) \tag{2.84}$$

is the inner product in $\mathfrak{h}$. In particular,

$$\langle f|f\rangle \equiv \|f\|^2. \tag{2.85}$$

The Fock representation is characterized by the existence of a unique vector $|0\rangle$, which has the property that for every normalized $|f\rangle$ in $\mathfrak{h}$

$$\mathrm{a}[f]|0\rangle = 0. \tag{2.86}$$

From Eq. (2.79) it follows that

$$|f\rangle = \mathrm{a}^\dagger[f]|0\rangle, \tag{2.87}$$

and

$$|f_1 f_2\rangle = \mathrm{a}^\dagger[f_1]\,\mathrm{a}^\dagger[f_2]|0\rangle. \tag{2.88}$$

It is clear that any other element of $\mathfrak{H}$ can be constructed like this. Therefore, $|0\rangle$ is called the cyclic state of the Fock representation [46].

The states (2.87) and (2.88) are eigenvectors of the total number operator N, defined as

$$\mathrm{N} = \sum_{n=1}^{\infty} \mathrm{a}_n^\dagger \mathrm{a}_n. \tag{2.89}$$

The operators $\mathrm{a}[f]$, $\mathrm{a}^\dagger[f]$ and N satisfy the commutation relations

$$[\mathrm{N}, \mathrm{a}^\dagger[f]] = \mathrm{a}^\dagger[f], \tag{2.90}$$

and

$$[\mathrm{N}, \mathrm{a}[f]] = -\mathrm{a}[f]. \tag{2.91}$$

From these commutators it follows that $|f\rangle$ has unit eigenvalue,

$$\mathrm{N}\,\mathrm{a}^\dagger[f]|0\rangle = \mathrm{a}^\dagger[f]|0\rangle, \tag{2.92}$$

and $|f_1 f_2\rangle$ has eigenvalue two,

$$\mathrm{N}\,\mathrm{a}^\dagger[f_1]\,\mathrm{a}^\dagger[f_2]|0\rangle = 2\,\mathrm{a}^\dagger[f_1]\,\mathrm{a}^\dagger[f_2]|0\rangle. \tag{2.93}$$

Therefore, $|f\rangle$ and $|f_1 f_2\rangle$ represent, respectively, one and two excitations of the field, whereas $|0\rangle$ is called the vacuum state of the field.

From Eqs. (2.78) and (2.79) it follows that monomials of $\mathrm{a}[f]$ and $\mathrm{a}^\dagger[f]$ transfer excitations between the component subspaces of $\mathfrak{H}$. For this reason $\mathrm{a}[f]$ and $\mathrm{a}^\dagger[f]$ are called annihilation and creation operators, respectively. The eigenvectors of the number operator N are called *Fock states* and are labeled with the corresponding eigenvalue. For example, the one-excitation state is usually denoted as

$$|1_f\rangle \equiv |f\rangle. \tag{2.94}$$

2.5 Coherent states: quantum-classical connection

Among the states that can be constructed in the bosonic Fock space, the eigenvectors of the annihilation operators $\mathrm{a}[f]$, called *coherent states*, are of fundamental physical importance. As will be shown in this section, they lie at the heart of a correspondence principle between classical and quantum scalar fields, and they are in many respects the most classical quantum states.

Note that the creation operators have no eigenvectors in Fock space [49]. However, in the Bargmann–Segal representation of the canonical commutation relations, which is realized in a Hilbert space of holomorphic functions, the creation operators act on functions multiplying them by a complex number [50, 51]. This representation is useful, for example, when dealing with infinite systems of harmonic oscillators for which the state operator is not trace-class, that is, its trace diverges [52].

For the algebra of canonical commutation relations the coherent states are defined as

$$|\{\alpha\}\rangle = \mathrm{D}[\alpha]|0\rangle, \tag{2.95}$$

resulting from the action of the Weyl operator

$$\mathrm{D}[\alpha] = \exp(\mathrm{a}^\dagger[\alpha] \quad \mathrm{a}[\alpha]), \tag{2.96}$$

on the vacuum state. This operator satisfies the Weyl form of the canonical commutation relations [46, 48],

$$\mathrm{D}[\alpha]\mathrm{D}[\beta] = \mathrm{D}[\alpha+\beta]\exp\Big(\tfrac{1}{2}[\langle\beta|\alpha\rangle \quad \langle\alpha|\beta\rangle]\Big). \tag{2.97}$$

Using the Kermack-McCrae identity [53]

$$e^{\mathrm{A}+\mathrm{B}} = e^{\mathrm{A}}\, e^{\mathrm{B}}\, e^{\ \frac{1}{2}[\mathrm{A},\mathrm{B}]}, \tag{2.98}$$

which requires $[\mathrm{A},[\mathrm{A},\mathrm{B}]] = [\mathrm{B},[\mathrm{A},\mathrm{B}]] = 0$, the Weyl operator can be disentangled as [54]

$$\mathrm{D}[\alpha] = \exp\Big(\ \ \tfrac{1}{2}\|\alpha\|^2\Big)\exp(\mathrm{a}^\dagger[\alpha])\exp(\ \ \mathrm{a}[\alpha]). \tag{2.99}$$

Using this expression, it follows that the coherent states satisfy the relation

$$\mathrm{a}[\alpha]|\{\beta\}\rangle = \langle\alpha|\beta\rangle|\{\beta\}\rangle. \tag{2.100}$$

That is, they are eigenvectors of the annihilation operator corresponding to an arbitrary $|\alpha\rangle$ in $\mathfrak{h}$. Since this operator is not Hermitian, its eigenvectors are not orthonormal. The inner product of two coherent states is given by [48]

$$\langle\{\beta\}|\{\alpha\}\rangle = \exp\Big[\ \ \tfrac{1}{2}(\|\alpha\|^2 + \|\beta\|^2) + \langle\beta|\alpha\rangle\Big]. \tag{2.101}$$

The coherent states reveal the geometrical meaning of Eq. (2.97). Acting with $\mathrm{D}[\alpha]$ on $|\{\beta\}\rangle$ yields

$$\mathrm{D}[\alpha]|\{\beta\}\rangle = \exp\Big(\tfrac{1}{2}[\langle\beta|\alpha\rangle \quad \langle\alpha|\beta\rangle]\Big)|\{\alpha+\beta\}\rangle, \tag{2.102}$$

that is, the Weyl operator acts on a coherent state as a *displacement operator* [55]. In the literature it is sometimes claimed that the complex phase in the right side of (2.102) is physically irrelevant. However, this is only true when it is a global phase of the quantum state of the field. In a superposition of a displaced coherent state with an arbitrary state this phase is measurable and plays an important role in several experiments [56].

The Weyl operator (2.96) can also be written in the basis of the smeared field operators $\Phi[\varphi]$ and $\Pi[\pi]$ from (2.68) and (2.69). It is given by [57]

$$\mathrm{D}[\varphi,\pi]=\exp\!\left(\frac{\mathrm{i}}{\hbar}\big[\,\Phi[\pi]\quad\Pi[\varphi]\,\big]\right), \tag{2.103}$$

where $\varphi(x)$ and $\pi(x)$ are, respectively, the classical field and its canonically conjugate momentum field. The relationship between (2.96) and (2.103) is established by defining the smeared creation operator

$$\mathrm{a}^{\dagger}[\alpha]=\int \mathrm{d}x\,\alpha(x)\mathrm{a}^{\dagger}(x), \tag{2.104}$$

where

$$\alpha(x)=\frac{1}{\sqrt{2\hbar}}\;\big(\varphi(x)+\mathrm{i}\pi(x)\big) \tag{2.105}$$

and

$$\mathrm{a}^{\dagger}(x)=\frac{1}{\sqrt{2\hbar}}\;\big(\Phi(x)\quad\mathrm{i}\Pi(x)\big). \tag{2.106}$$

The coherent states generated by $\mathrm{D}[\varphi,\pi]$,

$$|\{\varphi,\pi\}\rangle=\mathrm{D}[\varphi,\pi]|0\rangle, \tag{2.107}$$

are eigenstates of $\mathrm{a}(x)$ with eigenvalue $\alpha(x)$. Moreover, they allow establishing a connection between classical and quantum scalar fields, as will be shown next.

The *weak correspondence principle* for a scalar field states that the diagonal matrix element

$$G[\varphi,\pi]=\langle\{\varphi,\pi\}|\mathrm{G}|\{\varphi,\pi\}\rangle \tag{2.108}$$

of a quantum generator G of the symmetry group of the field yields the corresponding classical generator G [57]. Klauder proved this relationship for the six generators of an Euclidean-invariant field theory plus the Hamiltonian, and for the ten generators of a Lorentz-invariant field theory. This correspondence principle was rediscovered later, but it was considered merely ‘‘a curiosity’’ [58].

Remarkably, this association between quantum and classical quantities does not involve the usual limit $\hbar\to 0$. However, it requires that the quantum operators are normal-ordered. That is, all creation operators should appear to the left of the annihilation operators. For example, consider the free field Hamiltonian

$$\mathrm{H}=\frac{1}{2}\iint \mathrm{d}x\,\mathrm{d}y\,:[\Pi(x)\delta(x\quad y)\Pi(y)+\Phi(x)W(x\quad y)\Phi(y)]:, \tag{2.109}$$

where the colons (:) indicate normal ordering and W is a distribution (or generalized function) chosen such that the Hamiltonian is a well-defined positive-definite operator. Then the coherent-state expectation value yields the corresponding classical Hamiltonian

$$\langle\{\varphi,\pi\}|\mathrm{H}|\{\varphi,\pi\}\rangle=\frac{1}{2}\int \mathrm{d}x\,\pi^2(x)+\frac{1}{2}\iint \mathrm{d}x\,\mathrm{d}y\,\varphi(x)W(x\quad y)\varphi(y). \tag{2.110}$$

Figure 2.1. Free quantum scalar field in a coherent state. The solid line corresponds to the expectation value $\langle\{\varphi,\pi\}|\Phi(x)|\{\varphi,\pi\}\rangle$, which yields the classical field $\varphi(x)$. The blurred region shows the quantum uncertainty $\Delta\Phi[f]$ for a Gaussian f.

Likewise, the expectation values of the local field operators $\Phi(x)$ and $\Pi(x)$ in the coherent state $|\{\varphi,\pi\}\rangle$ are given by the classical field amplitude and its canonically conjugate momentum,

$$\langle\{\varphi,\pi\}|\Phi(x)|\{\varphi,\pi\}\rangle = \varphi(x), \tag{2.111}$$

and

$$\langle\{\varphi,\pi\}|\Pi(x)|\{\varphi,\pi\}\rangle = \pi(x). \tag{2.112}$$

They are calculated using the commutation relation (2.72) and the identity [59]

$$e^{s\mathrm{A}}\mathrm{B}e^{\ \ s\mathrm{A}} = \mathrm{B} + \sum_{n=1}^{\infty} \frac{s^n}{n!} C^n(\mathrm{A},\mathrm{B}), \tag{2.113}$$

with $C(\mathrm{A},\mathrm{B}) = [\mathrm{A},\mathrm{B}]$ and for $n \geq 2$ $C^n(\mathrm{A},\mathrm{B}) = [\mathrm{A}, C^{n\ \ 1}(\mathrm{A},\mathrm{B})]$.

As mentioned in the beginning of this section, the coherent states are the most classical quantum states. Recalling the Robertson–Schrödinger uncertainty relation,

$$\Delta\mathrm{X}\,\Delta\mathrm{Y} \geq \frac{1}{2}\big|\langle[\mathrm{X},\mathrm{Y}]\rangle\big|, \tag{2.114}$$

where X and Y are dimensionless observables whose variance is defined as

$$\Delta\mathrm{O} = \sqrt{\langle\psi|\mathrm{O}^2|\psi\rangle \quad \langle\psi|\mathrm{O}|\psi\rangle^2}, \tag{2.115}$$

it can be shown that for $\mathrm{X} = \Phi[f]/\hbar$ and $\mathrm{Y} = \Pi[g]/\hbar$, and taking the expectations with respect to the coherent states $|\{\varphi,\pi\}\rangle$, the inequality (2.114) is saturated,

$$\Delta\Phi[f]\,\Delta\Pi[g] = \frac{1}{2}\langle f|g\rangle, \tag{2.116}$$

with

$$\Delta\Phi[f] = \Delta\Pi[g]. \tag{2.117}$$

Therefore, when a free scalar quantum field is in the state $|\{\varphi,\pi\}\rangle$, the field canonical variables have equal dimensionless variances and the uncertainty product achieves its minimum value. That is, in such a state, the field observables behave as close as possible to their classical counterparts, as depicted in Figure 2.1. While this plot is only illustrative, a more accurate representation can be obtained using a recently introduced method for visualizing any state of a scalar quantum field as an ensemble of field configurations [60].

2.6 Phase-space representation of bosonic fields

In the previous section it was shown that the Weyl operators, through their action on the vacuum state, allow establishing a connection between normal-ordered field observables and the corresponding classical functionals of the canonical field variables in phase space. In general, these operators allow associating to *every* observable of the field a phase-space functional. This will be the subject of this section.

As pointed out in Section 2.3, any observable of a quantum field is a function of the canonical field operators Φ and Π. In the Fock representation these operators can be expressed in terms of the creation and annihilation operators, $\mathrm{a}[f]$ and $\mathrm{a}^\dagger[f]$, from (2.81) and (2.82). An operator-valued function of a and $\mathrm{a}^\dagger$, $\mathrm{G}(\mathrm{a},\mathrm{a}^\dagger)$, satisfying

$$\mathrm{Tr}\Big(\mathrm{G}\ \mathrm{a},\mathrm{a}^\dagger\big)\mathrm{G}^\dagger\ \mathrm{a},\mathrm{a}^\dagger\big)\Big)<\infty, \tag{2.118}$$

can be uniquely expressed in the form [61]

$$\mathrm{G}(\mathrm{a},\mathrm{a}^\dagger)=\int\mathcal{D}^2[\alpha]\,g[\alpha,\alpha^*]\,\mathrm{D}[\alpha], \tag{2.119}$$

where

$$g[\alpha,\alpha^*]=\mathrm{Tr}\ \ \mathrm{D}^\dagger[\alpha]\,\mathrm{G}(\mathrm{a},\mathrm{a}^\dagger)\big). \tag{2.120}$$

The integration in (2.119) is a *functional integral*, defined as (see Appendix A)

$$\int\mathcal{D}^2[\alpha]\,f[\alpha]=\lim_{n\to\infty}\int\frac{\mathrm{d}^2\alpha_1}{\pi}\cdots\frac{\mathrm{d}^2\alpha_n}{\pi}\,f(\alpha_1,...,\alpha_n). \tag{2.121}$$

It is customary to omit the second argument in $g[\alpha,\alpha^*]$ except when calculating functional Wirtinger derivatives of it (see Section 2.2.6). Since α can be expressed in terms of the classical canonical variables (see Eq. (2.105)), the functional g is called the *phase-space representation* of the observable G.

As shown in [61], the representation (2.119) is established by considering the coherent-state matrix elements of the operator-valued function

$$\mathrm{M}(\mathrm{a},\mathrm{a}^\dagger)=\int\mathcal{D}^2[\alpha]\,\mathrm{Tr}\ \ \mathrm{D}^\dagger[\alpha]\,\mathrm{G}(\mathrm{a},\mathrm{a}^\dagger)\big)\mathrm{D}[\alpha], \tag{2.122}$$

which turn out to be equal to the coherent-state matrix elements of $\mathrm{G}(\mathrm{a},\mathrm{a}^\dagger)$. Thus, $\mathrm{M}(\mathrm{a},\mathrm{a}^\dagger)=\mathrm{G}(\mathrm{a},\mathrm{a}^\dagger)$. Therefore, the Weyl operators $\mathrm{D}[\alpha]$ establish a correspondence between an operator-valued function of the creation and annihilation operators and a complex-valued functional of their complex eigenvalues, α,

$$\mathrm{a}[\alpha]|\{\alpha\}\rangle=\alpha|\{\alpha\}\rangle, \tag{2.123}$$

and α^*,

$$\langle\{\alpha\}|\,\mathrm{a}^\dagger[\alpha]=\alpha^*\langle\{\alpha\}|. \tag{2.124}$$

This so-called Weyl correspondence affords a representation of the state operator of the field, ρ, as a functional of α,

$$\chi[\alpha]=\mathrm{Tr}\ \ \rho\mathrm{D}[\alpha]\big), \tag{2.125}$$

called the *characteristic functional* of the state. It satisfies

$$\chi[0] = 1, \tag{2.126}$$

and

$$\left|\chi[\alpha]\right| \leq 1, \tag{2.127}$$

just like the characteristic function of a probability distribution. However, the Fourier transform of (2.125),

$$W[\eta] = \int \mathcal{D}^2[\alpha]\, \chi[\alpha] \exp\left(\int \mathrm{d}x \, [\eta^*(x)\alpha(x) \quad \eta(x)\alpha^*(x)] \right), \tag{2.128}$$

which involves a functional integration, see (2.121), is a quasiprobability distribution called the *Wigner functional* [62]. It satisfies

$$\int \mathcal{D}^2[\eta]\, W[\eta] = 1, \tag{2.129}$$

and

$$\left|W[\eta]\right| \leq 2, \tag{2.130}$$

but, in general, it is not positive definite. In fact, it can be shown that the only pure state that has a non-negative Wigner functional is a coherent state [63].

The Wigner functional of a coherent state can easily be obtained from that for the vacuum state. The latter is the Fourier transform of

$$\chi_{|0\rangle\langle 0|}[\alpha] = \mathrm{Tr}(\mathrm{D}[\alpha]\, |0\rangle\langle 0|) = \langle 0|\mathrm{D}[\alpha]|0\rangle, \tag{2.131}$$

which using (2.99) has the explicit expression

$$\chi_{|0\rangle\langle 0|}[\alpha] = e^{\ \frac{1}{2}\|\alpha\|^2}, \tag{2.132}$$

with $\|\alpha\|^2 = \langle \alpha|\alpha\rangle$. The Wigner functional of the vacuum state is thus

$$W_{|0\rangle\langle 0|}[\eta] = 2e^{\ 2\|\eta\|^2}. \tag{2.133}$$

Since the coherent state $|\{\xi\}\rangle$ results from displacing the vacuum state (2.95), the corresponding Wigner functional is the displacement of (2.133),

$$W_{|\xi\rangle\langle\xi|}[\eta] = 2e^{\ 2\|\eta \quad \xi\|^2}. \tag{2.134}$$

Due to Heisenberg's uncertainty principle the Wigner functional cannot be localized in a phase-space region with a volume smaller than $\hbar$ [64].

The Wigner functional can also be calculated as

$$W[\eta] = 2\mathrm{Tr}(\rho \mathrm{T}[\eta]), \tag{2.135}$$

that is, the expectation value of the Fourier transform of the Weyl operator, $\mathrm{T}[\eta]$, also called the displaced parity operator, since it has the explicit expression [65]

$$\mathrm{T}[\eta] = \mathrm{D}[\eta]\Pi_0\, \mathrm{D}^\dagger[\eta], \tag{2.136}$$

in terms of the parity operator

$$\Pi_0|\{\alpha\}\rangle = |\{\ \ \alpha\}\rangle. \tag{2.137}$$

Convolving the Wigner functional with any functional $\theta[\xi]$ such that its Fourier transform satisfies

$$\hat{\theta}[\mathrm{Re}\,\xi, 0] = \hat{\theta}[0, \mathrm{Im}\,\xi] = 1, \tag{2.138}$$

yields Cohen's class of quasiprobability distributions [66]. They allow calculating quantum expectation values in a similar manner to how it is done in classical statistical mechanics. That is, given a classical functional $g[\eta]$ of the canonical coordinates, the expectation value of its quantization, the operator G, is given by the phase-space integral

$$\langle \mathrm{G} \rangle = \int \mathcal{D}^2[\eta]\, g[\eta] F[\eta], \tag{2.139}$$

where F is an element of Cohen's class. Any such functional F has the property that integrating it with respect to one canonical variable yields the probability distribution of the canonically conjugate variable.

For a free scalar field with mass density μ and Hamiltonian

$$\mathrm{H} = \frac{1}{2}\int \mathrm{d}x \left[\frac{\Pi^2(x)}{\mu} + \mu v^2 [\,\partial_x \Phi(x)]^2 + \mu \omega^2 \Phi^2(x) \right], \tag{2.140}$$

where v has dimension of speed and ω is a frequency, it can be shown that the time evolution of the Wigner functional is given by the classical Liouville equation for a probability distribution in phase space [62],

$$\partial_t W_t[\varphi, \pi] = \int \mathrm{d}x \left[\frac{\delta H[\varphi,\pi]}{\delta \varphi(x)} \frac{\delta}{\delta \pi(x)} \quad \frac{\delta H[\varphi,\pi]}{\delta \pi(x)} \frac{\delta}{\delta \varphi(x)} \right] W_t[\varphi, \pi], \tag{2.141}$$

where

$$H[\varphi, \pi] = \langle \{\varphi, \pi\} | \mathrm{H} | \{\varphi, \pi\} \rangle. \tag{2.142}$$

However, Eq. (2.141) does not represent classical behavior unless the Wigner functional is positive. Therefore, this equation governs the so-called semiclassical dynamics of the field. Note that for a Hamiltonian with a non-quadratic potential the equation of motion for the Wigner functional is more complicated than (2.141). In general, it is an infinite power series in $\hbar$, where terms proportional to a power of the Planck constant are called quantum corrections to the classical dynamics [64].

2.7 From a harmonic chain to a quantum field

The bosonic quantum field whose classicalization will be studied in the subsequent chapters can be considered as the limit $N \to \infty$ of a sequence of discrete quantum harmonic oscillators forming a chain with N degrees of freedom. In this section I will describe this limit process.

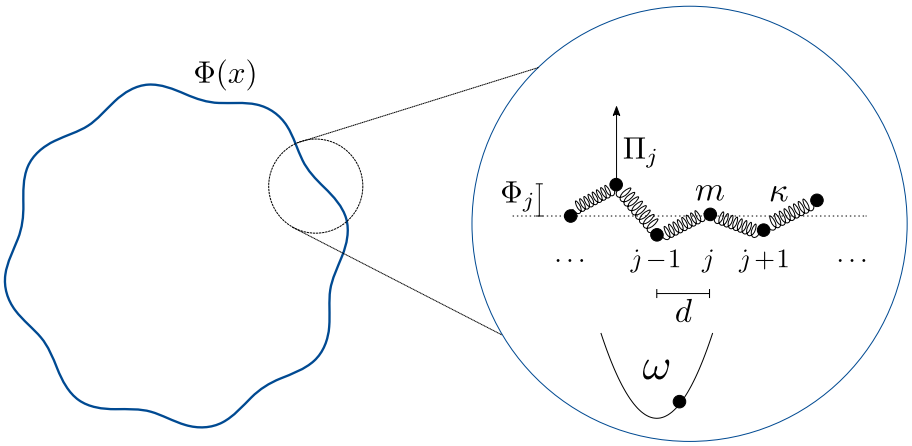

Figure 2.2. A scalar quantum field $\Phi(x)$ in a finite region of space can be considered the limit $N \to \infty$ of a sequence of N discrete harmonic chains with lattice constant d, which are subject to periodic boundary conditions. Each oscillator in the chain, with operator-valued canonical coordinates Φ_j and Π_j, has mass m and is subject to a local harmonic potential of frequency ω; the coupling strength between the oscillators is given by κ.

Consider a harmonic chain consisting of N identical particles of mass m, located at the sites of a one-dimensional lattice subject to periodic boundary conditions, as depicted in Figure 2.2. The lattice constant is d. The particles vibrate harmonically in a direction orthogonal to the lattice with frequency ω. In addition, they are harmonically coupled to their nearest neighbors with frequency Ω.

The operator-valued canonical coordinates of each particle are the amplitude of vibration Φ_j and its conjugate momentum Π_j, which satisfy the conditions $\Phi_{N+1} = \Phi_1$ and $\Pi_{N+1} = \Pi_1$, as well as the canonical commutation relations

$$[\Phi_j, \Pi_{j'}] = \mathrm{i}\hbar\delta_{jj'}. \tag{2.143}$$

The Hamiltonian of the system is given by

$$\mathrm{H} = \sum_{j=1}^{N} \frac{\Pi_j^2}{2m} + \frac{m\omega^2}{2}\Phi_j^2 + \frac{\kappa}{2}(\Phi_j \quad \Phi_{j+1})^2, \tag{2.144}$$

where $\kappa = m\Omega^2$ is the coupling strength between nearest neighbors.

Due to the periodic boundary conditions, the Hamiltonian is invariant with respect to lattice translations. This means that it has the structure of a circulant matrix and, therefore, it can be diagonalized using the discrete Fourier transform [67]. All such matrices have the same eigenvectors. The n-th eigenvector $|q_n\rangle$ has entries

$$\langle j\,|q_n\rangle = \frac{1}{\sqrt{N}}\, e^{\ \mathrm{i}q_n j}, \quad q_n = \frac{2\pi n}{N}, \tag{2.145}$$

where $|j\rangle = e_j$ correspond to the canonical basis vectors of the N-dimensional Euclidean space and, due to the periodic boundary conditions, the integer index n takes the values [68]

$$\begin{aligned} \frac{N}{2} < n \leq \frac{N}{2}, &\qquad \text{for } N \text{ even}, \\ \frac{N-1}{2} < n \leq \frac{N-1}{2}, &\quad \text{for } N \text{ odd}. \end{aligned} \tag{2.146}$$

The eigenvectors $|q_n\rangle$ are orthonormal,

$$\begin{aligned} \langle q_n | q_m \rangle &= \sum_{j=1}^{N} \langle q_n | j \rangle \langle j | q_m \rangle \\ &= \frac{1}{N} \sum_{j=1}^{N} e^{\mathrm{i} j (q_n - q_m)} = \delta_{q_n q_m}, \end{aligned} \tag{2.147}$$

and provide a resolution of the identity,

$$\sum_{n=1}^{N} |q_n\rangle \langle q_n| = \mathrm{I}. \tag{2.148}$$

The corresponding eigenvalues λ_n are given by the Fourier transform of the unique entries a_n of the circulant matrix,

$$\lambda_n = \sum_{j=1}^{N} a_j e^{\mathrm{i}(2\pi/N) jn}. \tag{2.149}$$

In terms of their Fourier components the canonical coordinates of the particles are given by

$$\Phi_j = \tfrac{1}{\sqrt{N}} \sum_{q \in Q_N} e^{-\mathrm{i} q j} \tilde{\Phi}_q \tag{2.150}$$

and

$$\Pi_j = \tfrac{1}{\sqrt{N}} \sum_{q \in Q_N} e^{\mathrm{i} q j} \tilde{\Pi}_q, \tag{2.151}$$

where

$$Q_N = \left\{ q_n = \frac{2\pi n}{N};\, n \in \mathbb{Z} \text{ determined by (2.146)} \right\}. \tag{2.152}$$

For $q \in Q_N$ the normal coordinates $\tilde{\Phi}_q$ and their conjugate momenta $\tilde{\Pi}_q$ satisfy

$$\tilde{\Phi}_q^\dagger = \tilde{\Phi}_{-q}, \quad \tilde{\Pi}_q^\dagger = \tilde{\Pi}_{-q}, \tag{2.153}$$

as well as the canonical commutation relations

$$[\tilde{\Phi}_q, \tilde{\Pi}_{q'}] = \mathrm{i}\hbar \delta_{qq'}. \tag{2.154}$$

In the Fourier basis, the Hamiltonian (2.144) describes a system of N uncoupled harmonic oscillators with canonical coordinates $\tilde{\Phi}_q$ and $\tilde{\Pi}_q^\dagger$,

$$\mathrm{H} = \tfrac{1}{2} \sum_{q \in Q_N} \tilde{\Pi}_q \tilde{\Pi}_q^\dagger + \omega_q^2 \tilde{\Phi}_q \tilde{\Phi}_q^\dagger, \tag{2.155}$$

with the nonlinear dispersion relation

$$\omega_q^2 = \Omega^2\Big(2\sin\frac{q}{2}\Big)^2 + \omega^2. \tag{2.156}$$

Introducing the dimensionless bosonic operators

$$\mathrm{c}_q = \frac{1}{\sqrt{2}}\Big(\frac{1}{\lambda_q}\tilde{\Phi}_q + \mathrm{i}\,\frac{\lambda_q}{\hbar}\tilde{\Pi}_q^\dagger\Big), \quad \lambda_q = \sqrt{\frac{\hbar}{m\omega_q}}, \tag{2.157}$$

satisfying the canonical commutation relations

$$\big[\mathrm{c}_q, \mathrm{c}_{q'}^\dagger\big] = \delta_{qq'}, \tag{2.158}$$

the Hamiltonian can be written as

$$\mathrm{H} = \sum_{q\in Q_N} \hbar\omega_q\Big(\mathrm{c}_q^\dagger\mathrm{c}_q + \tfrac{1}{2}\Big). \tag{2.159}$$

As discussed in Section 2.3, the continuum limit of a sequence of harmonic chains with N degrees of freedom yields a quantum field. That is, for $N\to\infty$, and $d\to 0$, while keeping the length $L = Nd$ constant, the vibration amplitude of the harmonic chain and its canonically conjugate momentum become continuous degrees of freedom, $\Phi(x)$ and $\Pi(x)$ respectively.

With the replacements

$$\Phi_j \to \Phi(x_j), \quad \Pi_j \to d\cdot\Pi(x_j), \tag{2.160}$$

the Hamiltonian of the system in this limit takes the form

$$\mathrm{H} = \lim_{d\to 0, N\to\infty} d\sum_{j=1}^{N} \frac{\Pi^2(x_j)}{2m/d} + \frac{\kappa d}{2}\Big(\frac{\Phi(x_j) \quad \Phi(x_{j+1})}{d}\Big)^2 + \frac{m\omega^2}{2d}\Phi^2(x_j). \tag{2.161}$$

Upon taking the limits, the sum is replaced with an integral,

$$d\sum_j \to \int_0^L \mathrm{d}x, \tag{2.162}$$

yielding the Hamiltonian of the quantum field,

$$\mathrm{H} = \frac{1}{2}\int_0^L \mathrm{d}x\left[\frac{\Pi^2(x)}{\mu} + \tau\Big(\frac{\partial\Phi(x)}{\partial x}\Big)^2 + \mu\omega^2\Phi^2(x)\right]. \tag{2.163}$$

Here, the parameters characterizing the field are the mass density

$$\mu = \frac{m}{d} \tag{2.164}$$

and the tension

$$\tau = \kappa d. \tag{2.165}$$

The commutation relations between the canonical coordinates are obtained in a similar way,

$$\begin{aligned}[\Phi(x),\Pi(x')] &= \lim_{d\to 0,N\to\infty}[\Phi(x_j),\Pi(x_{j'})]\\ &= \lim_{d\to 0,N\to\infty}\mathrm{i}\hbar\frac{\delta_{jj'}}{d}\\ &= \mathrm{i}\hbar\delta(x\quad x'). \end{aligned} \tag{2.166}$$

This equation follows from considering (2.30) as the continuum limit of

$$\sum_{n\in\mathbb{Z}} f_n\delta_{nn_0} = f_{n_0}. \tag{2.167}$$

The field $\Phi(x)$ and its canonically conjugate momentum $\Pi(x)$ are operator-valued functions on a circle of length L. A periodic function can be written as a Fourier series,

$$f(x) = \frac{1}{\sqrt{L}}\sum_{k\in K_L} e^{\mathrm{i}kx} f_k, \tag{2.168}$$

where

$$K_L = \left\{\frac{2\pi n}{L}, n\in\mathbb{Z}\right\}, \tag{2.169}$$

and

$$\langle x|k\rangle = L^{\ 1/2}\, e^{\mathrm{i}kx} \tag{2.170}$$

are the normalized eigenfunctions $|k\rangle$ of the circular convolution operator [69] evaluated at x. They are orthonormal,

$$\langle k|k'\rangle = \frac{1}{L}\int_0^L \mathrm{d}x\, e^{\mathrm{i}(k'\ \ k)x} = \delta_{kk'}, \tag{2.171}$$

and satisfy the completeness relation

$$\delta(x\quad y) = \frac{1}{L}\sum_{k\in K_L} e^{\mathrm{i}kx} e^{\ \mathrm{i}ky}, \tag{2.172}$$

where the series converges in the distribution sense [70].

Therefore, the canonical coordinates of the quantum field can be written as

$$\Phi(x) = \frac{1}{\sqrt{L}}\sum_{k\in K_L} e^{\mathrm{i}kx}\,\Phi_k, \tag{2.173}$$

and

$$\Pi(x) = \frac{1}{\sqrt{L}}\sum_{k\in K_L} e^{\ \mathrm{i}kx}\,\Pi_k, \tag{2.174}$$

where Φ_k and Π_k are, respectively, the normal coordinates and their conjugate momenta, which for $k,k'\in K_L$ satisfy

$$\Phi_k^\dagger = \Phi_{\ k}, \quad \Pi_k^\dagger = \Pi_{\ k}, \tag{2.175}$$

and the canonical commutation relations

$$[\Phi_k,\Pi_{k'}] = \mathrm{i}\hbar\delta_{kk'}. \tag{2.176}$$

In this representation the Hamiltonian of the system is given by

$$\mathrm{H} = \frac{1}{2} \sum_{k \in K_L} \Pi_k \Pi_k^\dagger + \omega_k^2 \Phi_k \Phi_k^\dagger, \tag{2.177}$$

with the nonlinear dispersion relation

$$\omega_k^2 = v^2 k^2 + \omega^2, \quad v^2 = \frac{\tau}{\mu}. \tag{2.178}$$

That is, it describes a system of infinitely many independent harmonic oscillators.

In terms of the dimensionless bosonic operators

$$\mathrm{c}_k = \frac{1}{\sqrt{2}} \left(\frac{1}{\lambda_k} \Phi_k + \mathrm{i} \frac{\lambda_k}{\hbar} \Pi_k^\dagger \right), \quad \lambda_k = \sqrt{\frac{\hbar}{\mu \omega_k}}, \tag{2.179}$$

satisfying the canonical commutation relations

$$[\mathrm{c}_k, \mathrm{c}_{k'}^\dagger] = \delta_{kk'}, \tag{2.180}$$

the Hamiltonian can be written as

$$\mathrm{H} = \sum_{k \in K_L} \hbar \omega_k \left(\mathrm{c}_k^\dagger \mathrm{c}_k + \tfrac{1}{2} \right). \tag{2.181}$$

The infinite contribution of the second term in (2.181) does not represent a problem, since it has no effect on the time evolution generated by the Hamiltonian. However, this does not imply that it has no physical consequences. This so-called zero-point energy plays an important role in superfluidity [13] and many other quantum phenomena.

Writing (2.173) in terms of the Heisenberg-picture bosonic operators

$$\mathrm{c}_k(t) = e^{\mathrm{i}\mathrm{H}t/\hbar} \mathrm{c}_k e^{-\mathrm{i}\mathrm{H}t/\hbar}, \tag{2.182}$$

it follows that the equation of motion of the field $\Phi(x,t)$ is given by

$$\partial_t \Phi(x,t) = \frac{\mathrm{i}}{\sqrt{L}} \sum_{k \in K_L} \sqrt{\frac{\hbar \omega_k}{2\mu}} \left[\mathrm{c}_k^\dagger(t) e^{-\mathrm{i}kx} - \mathrm{c}_k(t) e^{\mathrm{i}kx} \right]. \tag{2.183}$$

From the discussion of the weak correspondence principle in Section 2.5, it follows that the coherent-state expectation value of (2.183) yields the equation of motion of the classical field $\varphi(x,t)$.

3 Master equation for bosonic fields

This chapter introduces the main result of this thesis, a generic Lindblad master equation that induces the classicalization of a non-relativistic bosonic field. As will be shown, it induces a monotonic decay of the purity of any state of the quantum field, while the corresponding Ehrenfest equations for the canonical field variables are identical to the classical field equations. In addition to producing decoherence, the master equation increases the field energy with a constant rate that is independent of the quantum state of the field.

The master equation belongs to the class of quantum dynamical semigroups generated by stochastic unitary transformations. In fact, the open field dynamics considered here may be viewed as a stochastic process in which the unitary evolution is interrupted by phase-space kicks. The interpretation of the master equation in the framework of generalized measurements is discussed in the final section.

3.1 Open quantum systems

The Schrödinger equation describes the unitary evolution of a closed quantum system. Such quantum systems can often be divided into a small number of degrees of freedom of interest, collectively called the open system S, and an in general infinite number of degrees of freedom R, acting as an environment or as a reservoir.

Denoting the state of the combined system with ρ, the reduced state operator of the open system S is obtained by taking the partial trace of ρ over the degrees of freedom of R,

$$\rho_s = \mathrm{Tr}_R\, \rho. \tag{3.1}$$

Since ρ evolves unitarily with the total Hamiltonian

$$\mathrm{H} = \mathrm{H}_S + \mathrm{H}_R + \mathrm{H}_I, \tag{3.2}$$

where H_I describes the interaction between S and R, the reduced state operator ρ_S at time t is given by

$$\rho_S(t) = \mathrm{Tr}_R\ \big(\mathrm{U}(t)\rho(0)\mathrm{U}^\dagger(t)\big), \tag{3.3}$$

where $\mathrm{U}(t) = e^{\ \mathrm{i}\mathrm{H}t/\hbar}$ is the unitary evolution operator.

In general, determining the state of the open system through Eq. (3.3) is unfeasible. However, if the correlation functions of the reservoir decay on a time scale which is much shorter than the time scale of the evolution of the open system, the time evolution of the reduced state operator can be described approximately in terms of a *quantum dynamical semigroup*,

$$\rho_S(t) \simeq \mathcal{V}(t)\rho_S(0), \tag{3.4}$$

where $\mathcal{V}(t)$ is a continuous, one-parameter family of dynamical maps satisfying the semigroup or Markov property

$$\mathcal{V}(t_1)\mathcal{V}(t_2) = \mathcal{V}(t_1 + t_2), \quad t_1, t_2 \geq 0. \tag{3.5}$$

Since $\mathcal{V}(t)$ maps a state operator onto a state operator, it is a completely positive, trace-preserving operator transformation [1].

Quantum dynamical semigroups are contracting. That is, they do not increase the trace norm $\|\mathrm{A}\|_1 \equiv \mathrm{Tr}\,|\mathrm{A}|$ of a Hermitian operator A acting on the Hilbert space of the open quantum system S. In particular, this holds for ρ_S. Due to this property they can be represented in terms of a generator $\mathcal{L}$ [1],

$$\mathcal{V}(t) = \exp(\mathcal{L}t). \tag{3.6}$$

As shown by Lindblad [71] and Gorini, Kossakowski and Sudarshan [72], the most general form of the generator of a quantum dynamical semigroup is

$$\mathcal{L}\rho_S = \frac{1}{\mathrm{i}\hbar}[\mathrm{H}, \rho_t] + \sum_j \left[\mathrm{L}_j \rho_t \mathrm{L}_j^\dagger \quad \frac{1}{2}\left\{ \mathrm{L}_j^\dagger \mathrm{L}_j, \rho_t \right\} \right], \tag{3.7}$$

where H is a Hermitian operator with dimension of energy, the operators L_j are arbitrary and have dimension of square root of frequency, and $\{\mathrm{A}, \mathrm{B}\} = \mathrm{AB} + \mathrm{BA}$ is the anticommutator of two operators. The corresponding dynamical equation for ρ_S is called the *Lindblad master equation*,

$$\frac{\mathrm{d}}{\mathrm{d}t}\rho_S(t) = \mathcal{L}\rho_S(t). \tag{3.8}$$

For a comprehensive treatment of the theory of open quantum systems, including the microscopic derivation of Lindblad equations starting from the Hamiltonian of a closed quantum system, the reader is referred to [1].

3.1.1 Randomly generated semigroups

A relevant class of quantum dynamical semigroups are the so-called random unitary maps, which can be expressed as convex combinations of unitary transformations [73]. They are defined quite generally in terms of a projective representation U of a locally compact group G and a convolution semigroup μ_t of probability measures on the group satisfying [74]

$$\mu_t * \mu_s = \mu_{t+s}, \quad t, s \geq 0. \tag{3.9}$$

The semigroup of measures

$$\mu_t = e^{\ \gamma t} \sum_{n=0}^{\infty} \frac{(\gamma t)^n}{n!} \mu^{*n}, \quad t \geq 0, \tag{3.10}$$

where μ^{*n} is the n-fold convolution of a probability measure μ on G, is called the Poisson stochastic process in G with rate γ. It induces the quantum dynamical semigroup [74]

$$\mathcal{V}(t)\rho = \exp \quad \gamma t(\mathcal{I} \quad \mathcal{Z})\big)\rho, \tag{3.11}$$

where $\mathcal{I}$ is the identity map and

$$\mathcal{Z}\rho = \int_G \mathrm{U}(g)\rho\,\mathrm{U}^\dagger(g)\,\mathrm{d}\mu(g). \tag{3.12}$$

The corresponding Lindblad equation is

$$\frac{\mathrm{d}}{\mathrm{d}t}\rho_t = \gamma\bigg(\int_G \mathrm{U}(g)\rho_t\mathrm{U}^\dagger(g)\,\mathrm{d}\mu(g) \quad \rho_t\bigg). \tag{3.13}$$

It has the form of the master equation that will be introduced in the next section.

3.2 Field-theoretic Lindblad equation

In this section I introduce a Lindblad equation describing the open-system dynamics of a bosonic quantum field confined to a one-dimensional region of length L, subject to periodic boundary conditions [75]. Since the master equation is model-independent, it has a wide range of applicability.

The physical intuition behind it is the following. It is assumed that the quantum field is subject to certain interactions with another quantum system, that change both the field amplitude and its canonically conjugate momentum by a random amount. Since a local interaction confined to an infinitely small region would affect all the field modes, it could result in an infinitely large energy transfer. Therefore, the interaction is assumed to be non-local so that all degrees of freedom of the field within a region of finite extent are involved. On the other hand, if the perturbation is large enough, a linear field equation might no longer be an appropriate description of the quantum system. Therefore, the probability distribution of the strength of the random kicks should have a finite second moment. Finally, the interaction should not distinguish any region of the field.

The assumed perturbation of the canonical variables of the field is naturally described as a phase-space displacement,

$$\mathrm{U}_x(\xi) = \exp\bigg(\int_0^L \mathrm{d}y\, f\bigg(\frac{y \quad x}{L}\bigg)\big[\xi\Psi^\dagger(y) \quad \xi^*\Psi(y)\big]\bigg). \tag{3.14}$$

As mentioned above, it should only affect the degrees of freedom within a finite region centered at the position x. This is taken care of by the *spread function* f of width σ/L. This real-valued function is square-integrable and L-periodic. Moreover, it is normalized such that $f(0) = 1$. Therefore, the kick strength (or displacement amplitude) is given by the complex number ξ, characterized by a probability distribution $g(\xi)$, with vanishing odd moments and a finite second moment σ_g. In the following, the function g will be called the *kick-strength distribution*.

Following the discussion in the previous section on quantum dynamical semigroups generated by stochastic unitary transformations, in the Schrödinger picture the master equation is given by

$$\dot\rho_t = \frac{\mathrm{i}}{\hbar}[\mathrm{H},\rho_t] + \gamma\int_0^L \frac{\mathrm{d}x}{L}\int \mathrm{d}^2\xi\, g(\xi)\Big[\mathrm{U}_x(\xi)\rho_t\mathrm{U}_x^\dagger(\xi) \quad \rho_t\Big]. \tag{3.15}$$

Since the phase-space displacement induced by $\mathrm{U}_x(\xi)$ should be the same at any location x within the region $[0, L]$, this parameter has the uniform distribution $1/L$.

The complex field operators $\Psi(y)$ in (3.14) are related to the canonical coordinates in the usual way,

$$\Psi(y) = \frac{1}{\sqrt{2}}\left(\frac{\Phi(y)}{\Lambda} + \mathrm{i}\,\frac{\Lambda}{\hbar}\,\Pi(y)\right), \quad \Lambda = \sqrt{\frac{\hbar}{\mu\omega}}. \tag{3.16}$$

From (2.166) it follows that they satisfy the commutation relation

$$[\Psi(y), \Psi^\dagger(y')] = \delta(y \quad y'). \tag{3.17}$$

Using (2.173) and (2.179) they can be written in terms of the bosonic mode operators c_k as

$$\Psi(y) = \tfrac{1}{\sqrt{L}} \sum_{k\in K} e^{\mathrm{i}ky}\,\Omega_k^+ \mathrm{c}_k + e^{\ \mathrm{i}ky}\,\Omega_k\,\mathrm{c}_k^\dagger, \tag{3.18}$$

where

$$\Omega_k^\pm = \frac{1}{2}\left(\sqrt{\frac{\omega}{\omega_k}} \pm \sqrt{\frac{\omega_k}{\omega}}\right), \tag{3.19}$$

and $K = \{2\pi j/L, j \in \mathbb{Z}\}$. That is, k runs over all integer multiples of $2\pi/L$.

Eq. (3.18) shows that, from dimensional considerations, the function f and the parameter ξ in Eq. (3.14) must have dimension of inverse square root of length. Inserting the former expression into the latter yields the displacement operators in the mode basis,

$$\mathrm{U}_x(\xi) = \exp\left(\sum_{k\in K} \frac{1}{\sqrt{L}} \int_0^L \mathrm{d}y\, f\Big(\frac{y \quad x}{L}\Big)\, e^{\ \mathrm{i}ky}\ \xi\Omega_k^+ \quad \xi^*\Omega_k\ )\,\mathrm{c}_k^\dagger \quad \text{h.c.}\right). \tag{3.20}$$

Using the change of variables $z = y \quad x$, the integral in the argument of the exponential can be written as

$$\frac{1}{\sqrt{L}} \int_0^L \mathrm{d}y\ f\Big(\frac{y \quad x}{L}\Big)\, e^{\ \mathrm{i}ky} = e^{\ \mathrm{i}kx}\, \frac{1}{\sqrt{L}} \int_x^{L\ \ x} \mathrm{d}z\ f\Big(\frac{z}{L}\Big)\, e^{\ \mathrm{i}kz}. \tag{3.21}$$

The integral on the right side can in turn be decomposed into a sum of two integrals,

$$\int_x^{L\ \ x} \mathrm{d}z\ f\Big(\frac{z}{L}\Big)\, e^{\ \mathrm{i}kz} = \int_0^{L\ \ x} \mathrm{d}z\ f\Big(\frac{z}{L}\Big)\, e^{\ \mathrm{i}kz} + \int_x^{0} \mathrm{d}z\ f\Big(\frac{z}{L}\Big)\, e^{\ \mathrm{i}kz}. \tag{3.22}$$

With the change of variables $z = z' \quad L$, since $f\Big(\frac{z' \quad L}{L}\Big) = f\Big(\frac{z'}{L}\Big)$, it follows that

$$\int_x^0 \mathrm{d}z\ f\Big(\frac{z}{L}\Big)\, e^{\ \mathrm{i}kz} = \int_{L\ \ x}^{L} \mathrm{d}z'\ f\Big(\frac{z'}{L}\Big)\, e^{\ \mathrm{i}kz'}. \tag{3.23}$$

Therefore, due to the periodicity of the spread function the operators (3.20) can be written compactly as

$$\mathrm{U}_x(\xi) = \exp\left(\sum_{k\in K} f_k e^{\ \mathrm{i}kx}\ \ \xi\Omega_k^+ \quad \xi^*\Omega_k \,)\, \mathrm{c}_k^\dagger \quad f_k\, e^{\mathrm{i}kx}\ \ \xi^*\Omega_k^+ \quad \xi\Omega_k \,)\, \mathrm{c}_k \right), \tag{3.24}$$

in terms of the real-valued Fourier coefficients of the spread function,

$$f_k = \frac{1}{\sqrt{L}} \int_0^L \mathrm{d}y\, f\Big(\frac{y}{L}\Big)\, e^{\mathrm{i}ky}. \tag{3.25}$$

In the following sections I will discuss some of the physical consequences of the master equation (3.15). Namely, the Ehrenfest equations for the canonical variables of the field are identical to the classical equations of motion, the purity of any quantum state of the field decreases monotonically with time, and the mean energy of the field increases with a constant rate which is independent from the state. The classicalization of a quantum superposition of field configurations will be discussed in detail in Chapter 4, where also the phase-space representation of the dynamics of the field will be derived.

3.2.1 Ehrenfest equations

For a non-relativistic quantum particle of mass m subject to a potential $V(\mathrm{x})$, Ehrenfest obtained the equations of motion for the expectation value of the position and the momentum [76],

$$\begin{aligned} m\frac{\mathrm{d}}{\mathrm{d}t}\langle\psi(t)|\mathrm{x}|\psi(t)\rangle &= \ \langle\psi(t)|\mathrm{p}|\psi(t)\rangle, \\ \frac{\mathrm{d}}{\mathrm{d}t}\langle\psi(t)|\mathrm{p}|\psi(t)\rangle &= \ \langle\psi(t)|V'(\mathrm{x})|\psi(t)\rangle, \end{aligned} \tag{3.26}$$

which are now called *Ehrenfest equations* or Ehrenfest's theorem. While these equations can be derived using the Schrödinger equation, it was shown recently that from them and the canonical commutation relations one can obtain the Schrödinger equation [77].

When the potential is quadratic in the position, the following equality holds

$$\langle\psi(t)|V'(\mathrm{x})|\psi(t)\rangle = \ V'(\langle\psi(t)|\mathrm{x}|\psi(t)\rangle), \tag{3.27}$$

and the equations (3.26) coincide with the classical equations of motion. Since the quantum field considered in this thesis is described by a potential quadratic in the field amplitude, the corresponding Ehrenfest equations for the canonical field variables coincide with the classical equations of motion, as was shown at the end of Section 2.7. However, it should be noted that this correspondence is neither a necessary nor a sufficient condition for a quantum system to behave classically [78].

As will be shown next, the Ehrenfest equations for the canonical variables of the quantum field, resulting from the master equation (3.15), coincide with the corresponding classical equations of motion. In this sense, the master equation effects a minimal modification of the unitary dynamics of the quantum field.

From the master equation (3.15), the expectation value of the mode operators c_k evolves as

$$\frac{\mathrm{d}}{\mathrm{d}t}\langle \mathrm{c}_k\rangle(t) = \frac{\mathrm{i}}{\hbar}\mathrm{Tr}([\mathrm{H},\rho_t]\mathrm{c}_k) + \gamma\int_0^L \frac{\mathrm{d}x}{L}\int \mathrm{d}^2\xi\, g(\xi)\mathrm{Tr}\Big(\mathrm{U}_x(\xi)\rho_t\mathrm{U}_x^\dagger(\xi)\mathrm{c}_k\Big) \quad \gamma\langle \mathrm{c}_k\rangle(t). \tag{3.28}$$

The trace in the first term,

$$\mathrm{Tr}\ \ [\mathrm{H},\rho_t]\mathrm{c}_k\big) = \mathrm{Tr}\ \ \rho_t\,[\mathrm{c}_k,\mathrm{H}]\big) = \hbar\omega_k\langle \mathrm{c}_k\rangle(t), \tag{3.29}$$

follows from the canonical commutation relations $[\mathrm{c}_k,\mathrm{c}_{k'}^\dagger] = \delta_{kk'}$ and the commutator identity $[\mathrm{A},\mathrm{BC}] = [\mathrm{A},\mathrm{B}]\mathrm{C} + \mathrm{B}[\mathrm{A},\mathrm{C}]$. The trace in the second term of (3.28),

$$\mathrm{Tr}\ \ \rho_t\mathrm{U}_x^\dagger(\xi)\mathrm{c}_k\mathrm{U}_x(\xi)\big) = \langle \mathrm{c}_k\rangle(t) + f_k\, e^{\ \mathrm{i}kx}\ \ \xi\Omega_k^+ \quad \xi^*\Omega_k\ \big), \tag{3.30}$$

is calculated using the identity (2.113).

Since $g(\xi)$ is an even function, the second term in (3.30) does not contribute to the dynamics of $\langle \mathrm{c}_k\rangle(t)$. Therefore, Eq. (3.28) corresponds to the Ehrenfest equation of c_k,

$$\frac{\mathrm{d}}{\mathrm{d}t}\langle \mathrm{c}_k\rangle(t) = \ \mathrm{i}\omega_k\langle \mathrm{c}_k\rangle(t). \tag{3.31}$$

From Eq. (3.18), the expectation value of the field operators (3.16) evolves as

$$\frac{\mathrm{d}}{\mathrm{d}t}\langle \Psi(y)\rangle(t) = \frac{1}{\sqrt{L}}\sum_{k\in K}\Big[\ \ e^{\mathrm{i}ky}\,\Omega_k^+\,\mathrm{i}\omega_k\langle \mathrm{c}_k\rangle(t) + e^{\ \mathrm{i}ky}\,\Omega_k\ \mathrm{i}\omega_k\langle \mathrm{c}_k^\dagger\rangle(t)\Big], \tag{3.32}$$

where Eq. (3.31) has been used. It follows that the Ehrenfest equation for the field amplitude,

$$\frac{\mathrm{d}}{\mathrm{d}t}\langle \Phi(y)\rangle(t) = \frac{\mathrm{i}}{\sqrt{L}}\sum_{k\in K}\sqrt{\frac{\hbar\omega_k}{2\mu}}\Big[e^{\ \mathrm{i}ky}\langle \mathrm{c}_k^\dagger\rangle(t) \quad e^{\mathrm{i}ky}\langle \mathrm{c}_k\rangle(t)\Big], \tag{3.33}$$

corresponds to the classical equation of motion, as discussed below Eq. (2.183).

In a bosonic system with periodic boundary conditions the generator of translations is the quasimomentum

$$\mathrm{Q} = \sum_{k\in K}\hbar k\,\mathrm{c}_k^\dagger\mathrm{c}_k. \tag{3.34}$$

From the master equation (3.15), the expectation value of Q evolves as

$$\frac{\mathrm{d}}{\mathrm{d}t}\langle \mathrm{Q}\rangle(t) = \frac{\mathrm{i}}{\hbar}\mathrm{Tr}\ \ [\mathrm{H},\rho_t]\mathrm{Q}\big) + \gamma\int_0^L \frac{\mathrm{d}x}{L}\int \mathrm{d}^2\xi\, g(\xi)\mathrm{Tr}\Big(\mathrm{U}_x(\xi)\rho_t\mathrm{U}_x^\dagger(\xi)\mathrm{Q}\Big) \quad \gamma\langle \mathrm{Q}\rangle(t). \tag{3.35}$$

It involves the unitary transformation of the quasimomentum operator

$$\begin{aligned}\mathrm{U}_x^\dagger(\xi)\,\mathrm{Q}\,\mathrm{U}_x(\xi) = &\sum_k \hbar k f_k\, e^{\mathrm{i}kx}(\xi^*\Omega_k^+ \quad \xi\Omega_k\ )\mathrm{c}_k + \mathrm{h.c.}\\ &+\sum_k \hbar k f_k f_k\ \ \xi\Omega_k^+ \quad \xi^*\Omega_k\ \big)\ \ \xi^*\Omega_k^+ \quad \xi\Omega_k\ \big) + \mathrm{Q},\end{aligned} \tag{3.36}$$

which is obtained using Eq. (2.113). Since the odd moments of $g(\xi)$ vanish, the first sum in (3.36) does not contribute to the dynamics of $\langle \mathrm{Q} \rangle(t)$. The summand in the second sum is an odd function of k and vanishes due to symmetry. Therefore, Eq. (3.34) yields the Ehrenfest equation for Q,

$$\frac{\mathrm{d}}{\mathrm{d}t}\langle \mathrm{Q} \rangle(t) = \frac{1}{\mathrm{i}\hbar}\big\langle [\mathrm{Q}, \mathrm{H}] \big\rangle(t). \tag{3.37}$$

Given that the Hamiltonian of the field (2.163) is translation-invariant, it commutes with the quasimomentum and thus Eq. (3.37) reduces to

$$\frac{\mathrm{d}}{\mathrm{d}t}\langle \mathrm{Q} \rangle(t) = 0. \tag{3.38}$$

As discussed in [79], an observable Q is a conserved quantity of a given open quantum dynamics if (i) it is the generator of a symmetry of the adjoint Lindblad equation, i.e.

$$e^{\ \mathrm{i}\mathrm{Q}y/\hbar}\ \mathcal{L}^{\#}\,\mathrm{Q}_t)\,e^{\mathrm{i}\mathrm{Q}y/\hbar} = \mathcal{L}^{\#}\Big(e^{\ \mathrm{i}\mathrm{Q}y/\hbar}\mathrm{Q}_t\,e^{\mathrm{i}\mathrm{Q}y/\hbar}\Big), \tag{3.39}$$

with

$$\mathcal{L}^{\#}\,\mathrm{Q}_t = \frac{\mathrm{i}}{\hbar}[\mathrm{H}, \mathrm{Q}_t] + \gamma\int_0^L \frac{\mathrm{d}x}{L}\int \mathrm{d}^2\xi\, g(\xi)\Big[\mathrm{U}_x^{\dagger}(\xi)\mathrm{Q}_t\mathrm{U}_x(\xi) \quad \mathrm{Q}_t\Big], \tag{3.40}$$

and (ii) $\mathcal{L}^{\#}\,\mathrm{Q}_t = 0$. In order to verify that Eq. (3.39) holds, note that

$$e^{\ \mathrm{i}\mathrm{Q}y/\hbar}\mathrm{U}_x^{\dagger}(\xi)\mathrm{Q}\mathrm{U}_x(\xi)e^{\mathrm{i}\mathrm{Q}y/\hbar} = \mathrm{U}_{x\ \ y}^{\dagger}(\xi)\mathrm{Q}\mathrm{U}_{x\ \ y}(\xi), \tag{3.41}$$

which follows from Eq. (3.36). In addition, the periodicity arguments leading to Eq. (3.24) yield the identity

$$\int_0^L \frac{\mathrm{d}x}{L}\,\mathrm{U}_{x\ \ y}^{\dagger}(\xi)\mathrm{Q}\mathrm{U}_{x\ \ y}(\xi) = \int_0^L \frac{\mathrm{d}z}{L}\,\mathrm{U}_z^{\dagger}(\xi)\mathrm{Q}\mathrm{U}_z(\xi). \tag{3.42}$$

Therefore, Q is a symmetry generator of the adjoint Lindblad equation (3.40). Moreover, the right side of this equation vanishes. This follows from $[\mathrm{H}, \mathrm{Q}_t] = 0$ and Eq. (3.36). In conclusion, the quasimomentum is a conserved quantity of the open field dynamics (3.15).

3.2.2 Purity decay

The purity of the state operator ρ_t is defined as

$$p_t = \mathrm{Tr}(\rho_t^2). \tag{3.43}$$

It is a simple measure of the degree of quantum coherence present in a state, and satisfies $p_t = 1$ for a pure state $\rho_t = |\psi_t\rangle\langle\psi_t|$ and $p_t < 1$ for a mixed state (that is, a convex combination of pure states). The rate of change of the purity is

$$\dot{p}_t = 2\,\mathrm{Tr}(\rho_t\dot{\rho}_t). \tag{3.44}$$

From the master equation (3.15) it follows that

$$\mathrm{Tr}(\rho_t\dot{\rho}_t) = \mathrm{Tr}\ \ \rho_t\,[\mathrm{H}, \rho_t]\big) + \gamma\int_0^L \frac{\mathrm{d}x}{L}\int \mathrm{d}^2\xi\ g(\xi)\Big[\mathrm{Tr}\ \ \rho_t\,\mathrm{U}_x(\xi)\rho_t\mathrm{U}_x^{\dagger}(\xi)\big) \quad p_t\Big]. \tag{3.45}$$

Using the cyclic property of the trace the first term vanishes. Following [80], the integrand in the second term can be written as

$$\begin{aligned} \mathrm{Tr}\ \ \rho_t \mathrm{U}_x(\xi)\rho_t \mathrm{U}_x^\dagger(\xi)\big) \quad p_t = \quad & \frac{1}{2}\mathrm{Tr}\ \ (\rho_t \mathrm{U}_x(\xi) \quad \mathrm{U}_x(\xi)\rho_t)^\dagger(\rho_t \mathrm{U}_x(\xi) \quad \mathrm{U}_x(\xi)\rho_t)\big), \\ = \quad & \frac{1}{2}\big\|[\rho_t, \mathrm{U}_x(\xi)]\big\|^2, \end{aligned} \tag{3.46}$$

in terms of the Hilbert–Schmidt norm $\|\mathrm{A}\|^2 = \mathrm{Tr}(\mathrm{A}^\dagger \mathrm{A})$.

Therefore, under the open-system dynamics (3.15) the purity of the state of the field decreases monotonically with time,

$$\dot{p}_t = \quad \gamma \int_0^L \frac{\mathrm{d}x}{L} \int \mathrm{d}^2\xi\ g(\xi) \big\|[\rho_t, \mathrm{U}_x(\xi)]\big\|^2 < 0. \tag{3.47}$$

This equation implies that any initially pure state of the field will become mixed. The functional dependence of the purity decay on the parameters of the master equation (3.15) as well as on the structure of the initial state of the field will be studied in detail in the next chapter.

3.2.3 Mean energy increase

In addition to inducing decoherence, a classicalizing non-unitary evolution will in general also affect the dynamics of otherwise conserved quantities, such as the energy [26]. As will be shown below, the master equation (3.15) leads to an increase of the mean field energy, with a rate that is independent from the state of the field and is finite even in the limit $L \to \infty$.

The time evolution of the expectation value of the energy follows from the master equation (3.15),

$$\frac{\mathrm{d}}{\mathrm{d}t}\langle \mathrm{H}\rangle(t) = \quad \frac{\mathrm{i}}{\hbar}\mathrm{Tr}\ \ [\mathrm{H}, \rho_t]\mathrm{H}\big) + \gamma \int_0^L \frac{\mathrm{d}x}{L} \int \mathrm{d}^2\xi\, g(\xi) \mathrm{Tr}\Big(\mathrm{U}_x(\xi)\rho_t \mathrm{U}_x^\dagger(\xi)\mathrm{H}\Big) \quad \gamma \langle \mathrm{H}\rangle(t). \tag{3.48}$$

It involves the unitary transformation of the field Hamiltonian,

$$\mathrm{U}_x^\dagger(\xi)\mathrm{H}\mathrm{U}_x(\xi) = \sum_{k\in K} \hbar\omega_k \Big[\mathrm{c}_k^\dagger \mathrm{c}_k + \beta_k(x,\xi)\mathrm{c}_k^\dagger + \beta_k^*(x,\xi)\mathrm{c}_k + |\beta_k(x,\xi)|^2\Big], \tag{3.49}$$

where

$$\beta_k(x,\xi) = e^{\ \mathrm{i}kx} f_k\,(\xi\,\Omega_k^+ \quad \xi^*\,\Omega_k\,), \tag{3.50}$$

which is calculated using Eq. (2.113). As before, since the odd moments of $g(\xi)$ vanish the terms linear in c_k and $\mathrm{c}_k^\dagger$ in (3.49) do not contribute to the dynamics of $\langle \mathrm{H}\rangle_t$. Therefore, the mean energy of the field increases with the constant rate

$$\frac{\mathrm{d}}{\mathrm{d}t}\langle \mathrm{H}\rangle(t) = \gamma \int \mathrm{d}^2\xi\ g(\xi) \sum_{k\in K} \hbar\omega_k \big| f_k\,(\xi\,\Omega_k^+ \quad \xi^*\,\Omega_k\,)\big|^2. \tag{3.51}$$

Writing $\xi = r e^{\mathrm{i}\theta}$ then

$$\big| f_k\,(\xi\,\Omega_k^+ \quad \xi^*\,\Omega_k\,)\big|^2 = r^2 |f_k|^2 \ \ \cos^2\theta\,(\Omega_k^+ \quad \Omega_k\,)^2 + \sin^2\theta\,(\Omega_k^+ + \Omega_k\,)^2\big). \tag{3.52}$$

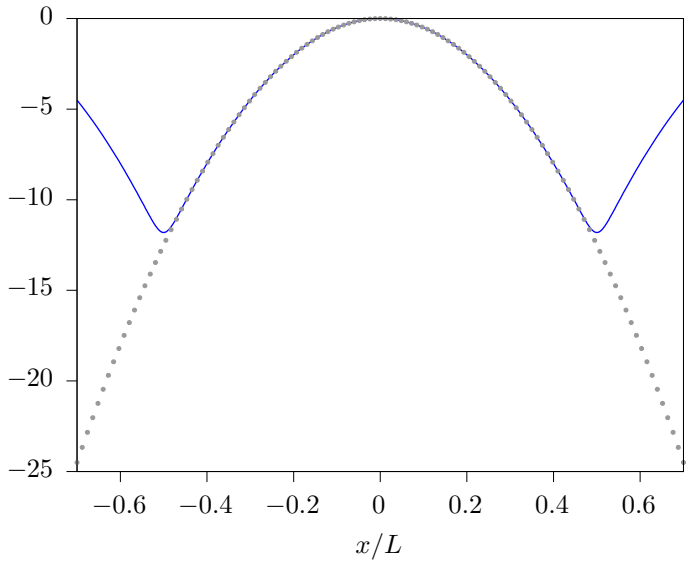

Figure 3.1. Comparison between $\log f(x/L)$, with f the periodic quasi-Gaussian function defined by the Fourier coefficients in Eq. (3.55), and $\log\exp(\quad (x/L)^2/2\sigma^2)$.

Using the identity

$$\Omega_k^+)^2 + \quad \Omega_k\,)^2 = \frac{1}{2}\,\frac{\omega^2+\omega_k^2}{\omega_k\,\omega}, \tag{3.53}$$

the θ-integral can be calculated and Eq. (3.51) simplifies to

$$\frac{\mathrm{d}}{\mathrm{d}t}\langle \mathrm{H}\rangle(t) = \gamma\,\hbar \int_0^\infty \mathrm{d}r\, G(r)\, r^3 \sum_{k\in K} |f_k|^2 \left[\omega + \frac{v^2k^2}{2\,\omega}\right], \tag{3.54}$$

where $G(r)$ is the radial component of the complex function $g(\xi)$.

In order to calculate the rate of energy increase, the spread function f and the kick-strength distribution g must be specified. Since they are generic representatives of even, square-integrable functions and to simplify the calculations, one would like to use Gaussian functions. However, the function f must be L-periodic. Therefore, it is constructed as a periodic quasi-Gaussian (shown in Fig. 3.1), with Fourier coefficients

$$f_k = \frac{\sqrt{L}\exp\left(\quad \sigma^2k^2/2\right)}{\vartheta_3\;\; 0, \exp\quad\; 2\pi^2\sigma^2/L^2\big)\big)}, \tag{3.55}$$

given in terms of the Jacobi theta function

$$\vartheta_3(z;q) = 1 + 2\sum_{n=1}^{\infty} q^{n^2}\cos(2\pi n\, z). \tag{3.56}$$

The kick-strength distribution is assumed to be isotropic, $g(\xi) = G(|\xi|)/2\pi$, with

$$G(r) = \frac{\exp\left(\quad r^2/2\,\sigma_g^2\right)}{\sigma_g^2}. \tag{3.57}$$

In the limit $L \to \infty$ the following substitution can be made

$$\sum_{k \in K} \quad \to L \int_{\infty}^{\infty} \frac{\mathrm{d}k}{2\pi}, \tag{3.58}$$

which, using $k = 2\pi n / L$ with $n \in \mathbb{Z}$, allows calculating

$$\vartheta_3\Big(0, \exp \quad 2\pi^2\sigma^2 / L^2\Big) = \frac{L}{\sqrt{2\pi\sigma^2}}, \tag{3.59}$$

as well as

$$\int \frac{\mathrm{d}k}{2\pi} |f_k|^2 \left[\omega + \frac{v^2 k^2}{2\,\omega}\right] = 2\pi\sigma^2 \left[\frac{\omega}{\sqrt{4\pi\sigma^2}} + \frac{v^2}{2\omega\sqrt{16\,\pi\sigma^6}}\right]. \tag{3.60}$$

The rate of energy increase is thus given by

$$\frac{\mathrm{d}}{\mathrm{d}t}\langle \mathrm{H} \rangle(t) = 2\sqrt{\pi}\,\gamma\hbar\omega\,\sigma\sigma_g^2 \left[1 + \frac{v^2}{(2\sigma\omega)^2}\right]. \tag{3.61}$$

This equation shows that the finite width $\sigma > 0$ of the spread function in position space ensures that the energy does not increase without bounds, as discussed at the beginning of Section 3.2.

3.3 Measurement interpretation

In the framework of quantum measurements Eq. (3.15) can be interpreted as arising from a measurement master equation involving the generalized simultaneous measurement of both canonical variables of the field. In this section I provide a brief introduction to the theory of generalized measurements and obtain the master equation (3.15) within this framework. For a comprehensive treatment of quantum measurement theory the reader is advised to consult [81]. For a pedagogical introduction to measurement master equations see [82].

3.3.1 Generalized measurements

In the axiomatization of quantum mechanics carried out by John von Neumann (born Neumann János Lajos) [83], given an observable with a discrete non-degenerate spectrum,

$$\mathrm{O} = \sum_n \lambda_n |\lambda_n\rangle\langle\lambda_n|, \tag{3.62}$$

the probability that a measurement of O yields the result λ_n is

$$\mathrm{Prob}(\lambda_n) = \mathrm{Tr} \quad \rho|\lambda_n\rangle\langle\lambda_n|\big). \tag{3.63}$$

After the measurement, the state of the system is the corresponding eigenstate of O,

$$\rho_n = |\lambda_n\rangle\langle\lambda_n|. \tag{3.64}$$

This projection postulate lies at the heart of the measurement problem in quantum mechanics [84]. If the measurement result is not recorded, the state of the system is consistently described as a probabilistic mixture of all the eigenstates of O,

$$\bar{\rho} = \sum_n \mathrm{Prob}(\lambda_n) |\lambda_n\rangle\langle\lambda_n|. \tag{3.65}$$

Instead of associating a projector with each measurement result n, in general one may associate a positive operator π_n with it. This allows accounting for imprecise or unsharp measurements. Such generalized measurements are described by an operator-valued probability measure called a positive-operator-valued measure (POVM) [81].

The operators π_n provide a resolution of the identity,

$$\sum_n \pi_n = \mathrm{I}. \tag{3.66}$$

Moreover, each operator can be written in terms of pairs of operators, A_j and $\mathrm{A}_j^\dagger$, called *effects*, as

$$\pi_n = \sum_j \mathrm{A}_{nj}^\dagger \mathrm{A}_{nj}. \tag{3.67}$$

This decomposition is not unique. The probability that a measurement yields the result n is

$$\mathrm{Prob}(n) = \mathrm{Tr}(\rho\, \pi_n). \tag{3.68}$$

The state of the system after the measurement is

$$\rho_n = \frac{1}{\mathrm{Tr}(\rho \pi_n)} \sum_j \mathrm{A}_{nj}\, \rho\, \mathrm{A}_{nj}^\dagger. \tag{3.69}$$

If the measurement result is not recorded, then the measurement is uninformative and the subsequent state of the system is given by the probabilistic mixture

$$\bar{\rho} = \sum_n \mathrm{Prob}(n)\, \rho_n = \sum_{n,j} \mathrm{A}_{nj}\, \rho\, \mathrm{A}_{nj}^\dagger. \tag{3.70}$$

This formalism is quite general. If the measurement result is a continuous value, the sums must be replaced by integrals. This will be the case in what follows.

3.3.2 Measurement master equation

The time evolution of the state of a quantum system continuously subject to generalized measurements whose outcome is disregarded can be modeled as a Poisson process with rate γ. Given a short time interval Δt, if a generalized measurement is performed and the result is not recorded, the state of the system at time $t + \Delta t$ is given by (3.70). Otherwise, the system evolves unitarily,

$$\rho_{t+\Delta t} = e^{\ \mathrm{i}\mathrm{H}\Delta t/\hbar} \rho_t\, e^{\mathrm{i}\mathrm{H}\Delta t/\hbar}. \tag{3.71}$$

Assuming that the probability of a measurement occurring during the time interval Δt is $\gamma \Delta t$, to first order in Δt this stochastic process is described by

$$\rho_{t+\Delta t} = (1 \quad \gamma \Delta t)\, \rho_t \quad \frac{\mathrm{i}}{\hbar}[\mathrm{H}, \rho_t]\Delta t + \gamma \Delta t\, \bar{\rho}_t. \tag{3.72}$$

In the limit $\Delta t \to 0$ the *measurement master equation* is obtained [85],

$$\dot{\rho}_t = \quad \frac{\mathrm{i}}{\hbar}[\mathrm{H}, \rho_t] + \gamma(\bar{\rho}_t \quad \rho_t). \tag{3.73}$$

As will be shown below, the master equation (3.15) is a generalization of Eq. (3.73) arising from a decomposition of the elements of a POVM in terms of an ensemble of operators with a given probability distribution. Correspondingly, the state of the field after an uninformative measurement is a random mixture of state transformations of the form (3.70).

The elements of the POVM corresponding to the simultaneous measurement of both canonical field variables are coherent-state projectors (see Section 2.5),

$$\pi[\alpha] = |\{\alpha\}\rangle\langle\{\alpha\}|. \tag{3.74}$$

Actually, it can be shown that every POVM is related to a set of generalized coherent states [86]. The operators $\pi[\alpha]$ yield a resolution of the identity,

$$\int \mathcal{D}^2[\alpha]\, |\{\alpha\}\rangle\langle\{\alpha\}| = \mathrm{I}, \tag{3.75}$$

where the functional integral is defined as [87] (see Appendix A)

$$\int \mathcal{D}^2[\alpha]\, f[\alpha] = \lim_{n\to\infty} \int \frac{\mathrm{d}^2\alpha_1 \cdots \mathrm{d}^2\alpha_n}{\pi^n}\, f(\alpha_1, \cdots, \alpha_n). \tag{3.76}$$

As implied by the notation used in (3.74), the measurement results are functions of the spatial coordinates. Namely, the field amplitude and its canonical conjugate momentum. In fact, the operators $\pi[\alpha]$ are approximately sharp observables [88]. That is, for any neighborhood B of a point in the set of possible measurement outcomes, one can construct a state such that the probability that the measurement result is in B is approximately 1. This shows that such observables do not have intrinsic unsharpness. Therefore, the uncertainty in the measurement outcome comes solely from the measured state. Indeed, the probability distribution is

$$\mathrm{Prob}[\alpha] = \mathrm{Tr}(\rho_t\, \pi[\alpha]) = \langle\{\alpha\}|\rho_t|\{\alpha\}\rangle. \tag{3.77}$$

It should be noted that this is the functional generalization of the Q-distribution introduced by Husimi [89].

The POVM elements can be written as

$$\pi[\alpha] = \mathrm{A}^\dagger_{x,\xi}[\alpha]\mathrm{A}_{x,\xi}[\alpha], \tag{3.78}$$

with

$$\mathrm{A}_{x,\xi}[\alpha] = \mathrm{D}[\alpha + \xi f_x]|0\rangle\langle 0|\mathrm{D}^\dagger[\alpha]. \tag{3.79}$$

The operators $\mathrm{A}_{x,\xi}[\alpha]$ are chosen from an ensemble according to the probability distribution $g(\xi)/L$, which is uniform in the position x. Therefore, the state of the field after having performed a measurement that yielded the result α is given by the stochastic mixture of state transformations

$$\rho_\alpha = \frac{1}{\langle\{\alpha\}|\rho|\{\alpha\}\rangle} \int \frac{\mathrm{d}x}{L} \int \mathrm{d}^2\xi\, g(\xi)\, \mathrm{A}_{x,\xi}[\alpha]\, \rho\, \mathrm{A}^\dagger_{x,\xi}[\alpha]. \tag{3.80}$$

When the measurement results are discarded, the state of the field after the measurement is

$$\bar{\rho} = \int \frac{\mathrm{d}x}{L} \int \mathrm{d}^2\xi\; g(\xi)\mathrm{U}_x(\xi)\rho'\mathrm{U}^\dagger_x(\xi), \tag{3.81}$$

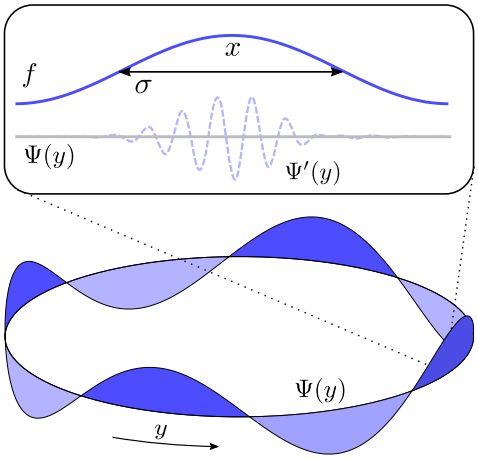

Figure 3.2. The open field dynamics governed by the master equation (3.15) can be viewed as a stochastic process in which the unitary evolution is interrupted by generalized simultaneous measurements of the field canonical variables, described by $\Psi(y)$, whose outcomes are discarded. These fictitious measurements have finite spatial resolution, as characterized by the spread function f of width σ.

where ρ' is the state of the system after an uninformative measurement of $\pi[\alpha]$,

$$\rho' = \int \mathcal{D}^2[\alpha]\, |\{\alpha\}\rangle\langle\{\alpha\}|\rho|\{\alpha\}\rangle\langle\{\alpha\}|. \tag{3.82}$$

This follows from the identity

$$\mathrm{D}[\alpha + \xi f_x]|0\rangle\langle\{\alpha\}|\rho|\{\alpha\}\rangle\langle 0|\mathrm{D}^\dagger[\alpha + \xi f_x] = \mathrm{U}_x(\xi)|\{\alpha\}\rangle\langle\{\alpha\}|\rho|\{\alpha\}\rangle\langle\{\alpha\}|\,\mathrm{U}_x^\dagger(\xi). \tag{3.83}$$

Inserting (3.81) into Eq. (3.73) yields the master equation corresponding to this measurement process,

$$\dot\rho_t = \frac{\mathrm{i}}{\hbar}[\mathrm{H}, \rho_t] + \gamma \int_0^L \frac{\mathrm{d}x}{L} \int \mathrm{d}^2\xi\, g(\xi) \Big[\mathrm{U}_x(\xi)\rho_t' \mathrm{U}_x^\dagger(\xi) \quad \rho_t \Big]. \tag{3.84}$$

Since the state transformation (3.82) does not affect qualitatively the decoherence dynamics and moreover $\rho' \simeq \rho$ for states such that the Husimi Q-distribution is approximately equal to the Glauber–Sudarshan P-distribution [87], ρ_t' may be replaced with ρ_t in (3.84) to yield the master equation (3.15).

In conclusion, the master equation can be viewed as describing a quantum field whose unitary evolution is randomly interrupted by stochastic phase-space displacements. As illustrated in Fig. 3.2, given a neighborhood of width σ around position $x \in [0, L]$, the field degrees of freedom located at any point y within this region experience a random phase-space kick of strength $\xi f(y/L \quad x/L)$. This displacement, implemented by the unitary operators $\mathrm{U}_x(\xi)$, occurs with the probability distribution $g(\xi)/L$. As will be shown in the next chapter, the corresponding stochastic state transformation turns a superposition of single-mode coherent states into a mixture.

4 Classicalization of a bosonic field

In this chapter I show that the dynamics described by the master equation introduced in Chapter 3 are given semiclassically by a linear Boltzmann equation in the functional phase space of field configurations. I also show that quantum superpositions of distinct field configurations are gradually turned into mixtures. Assuming that the initial state of the field is a superposition of single-mode coherent states I obtain approximate analytical expressions for the purity decay in different time scales. They are in excellent agreement with numerical calculations of the exact dynamics carried out using an integration method described in Chapter 5. Throughout the chapter the dynamics of the quantum field are considered in the interaction picture with respect to the free field Hamiltonian.

4.1 Master equation in the interaction picture

The master equation introduced in Chapter 3,

$$\partial_t \rho_t = \frac{\mathrm{i}}{\hbar}[\mathrm{H}, \rho_t] + \gamma \int_0^L \frac{\mathrm{d}x}{L} \int \mathrm{d}^2\xi \; g(\xi)\big[\mathrm{U}_x(\xi)\rho_t \mathrm{U}_x^\dagger(\xi) \quad \rho_t\big], \tag{4.1}$$

can be solved straightforwardly in the interaction picture with respect to the field Hamiltonian

$$\mathrm{H} = \sum_{k\in K} \hbar\omega_k \mathrm{c}_k^\dagger \mathrm{c}_k, \quad \text{with } \omega_k^2 = v^2k^2 + \omega^2, \tag{4.2}$$

where $K = \{2\pi j / L, j \in \mathbb{Z}\}$, and the mode operators c_k are defined in (2.179). In this basis the phase-space displacement operators are given by

$$\mathrm{U}_x(\xi) = \exp\left(\sum_{k\in K} f_k e^{\ \mathrm{i}kx} (\xi\Omega_k^+ \quad \xi^*\Omega_k)\, \mathrm{c}_k^\dagger \quad f_k e^{\mathrm{i}kx} (\xi^*\Omega_k^+ \quad \xi\Omega_k)\, \mathrm{c}_k \right), \tag{4.3}$$

with

$$\Omega_k^\pm = \tfrac{1}{2}\Big(\sqrt{\tfrac{\omega}{\omega_k}} \pm \sqrt{\tfrac{\omega_k}{\omega}} \Big). \tag{4.4}$$

In Eq. (4.3) the spread function f is specified by its Fourier coefficients,

$$f_k = \frac{1}{\sqrt{L}} \int_0^L \mathrm{d}z\, f\Big(\frac{z}{L}\Big)\, e^{\ \mathrm{i}kz}. \tag{4.5}$$

An operator $\tilde{\mathrm{O}}$ in the interaction picture with respect to (4.2) is related to an operator O in the Schrödinger picture through the unitary transformation

$$\mathrm{O} = e^{\ \mathrm{i}\mathrm{H}t/\hbar}\,\tilde{\mathrm{O}}\,e^{\mathrm{i}\mathrm{H}t/\hbar}. \tag{4.6}$$

Inserting the interaction-picture state operator $\tilde{\rho}_t$ in the master equation (4.1) yields

$$e^{\ \mathrm{i}\mathrm{H}t/\hbar}\,\partial_t\tilde{\rho}_t\,e^{\mathrm{i}\mathrm{H}t/\hbar} = \gamma\int_0^L\frac{\mathrm{d}x}{L}\int\mathrm{d}^2\xi\ g(\xi)\Big[\mathrm{U}_x(\xi)e^{\ \mathrm{i}\mathrm{H}t/\hbar}\,\tilde{\rho}_t\,e^{\mathrm{i}\mathrm{H}t/\hbar}\,\mathrm{U}_x^\dagger(\xi)\quad e^{\ \mathrm{i}\mathrm{H}t/\hbar}\,\tilde{\rho}_t\,e^{\mathrm{i}\mathrm{H}t/\hbar}\Big]. \tag{4.7}$$

Applying the inverse of the transformation (4.6) to this equation yields the master equation in the interaction picture,

$$\partial_t\tilde{\rho}_t = \gamma\int_0^L\frac{\mathrm{d}x}{L}\int\mathrm{d}^2\xi\ g(\xi)\big[\tilde{\mathrm{U}}_x(\xi)\tilde{\rho}_t\,\tilde{\mathrm{U}}_x^\dagger(\xi)\quad\tilde{\rho}_t\big], \tag{4.8}$$

where the unitary operators

$$\tilde{\mathrm{U}}_x(\xi) = \exp\left(\sum_{k\in K} f_k e^{\ \mathrm{i}(kx+\omega_k t)}\ \xi\Omega_k^+\quad\xi^*\Omega_k\ )\,\mathrm{c}_k^\dagger\quad f_k e^{\mathrm{i}(kx+\omega_k t)}\ \xi^*\Omega_k^+\quad\xi\Omega_k\ )\,\mathrm{c}_k\right), \tag{4.9}$$

are obtained using the identity [59]

$$e^{z\mathrm{c}_k^\dagger\mathrm{c}_k}F(\mathrm{c}_k,\mathrm{c}_k^\dagger)e^{\ z\mathrm{c}_k^\dagger\mathrm{c}_k} = F(\mathrm{c}_k e^{\ z},\mathrm{c}_k^\dagger e^z), \tag{4.10}$$

valid for any function F of c_k and $\mathrm{c}_k^\dagger$ that can be written as a power series. Since these operators do not commute the operator monomials in the series can be written either in normal order or in antinormal order. In the former, all creation operators are written to the left of the annihilation operators, whereas in the latter, all annihilation operators are written to the left of the creation operators. The identity (4.10) holds regardless of the ordering used.

4.1.1 Solution of the master equation

In order to solve an operator differential equation, it is convenient to choose a basis in operator space and obtain the corresponding equation of motion for the coefficients. The Weyl operators introduced in Chapter 2 form a basis of the space of bounded operators [37]. As will be shown below, the interaction-picture master equation (4.8) can be readily solved in this representation, which also provides the foundation for the quantitative analysis of the classicalization of a superposition state in the final section of the present chapter.

In the basis of the mode operators c_k the state operator is written as

$$\tilde{\rho}_t = \int\mathcal{D}^2[\{\eta_k\}]\ \tilde{\chi}_t[\{\eta_k\}]\,\mathrm{D}^\dagger[\{\eta_k\}], \tag{4.11}$$

where the coefficients are given by the *characteristic functional*

$$\tilde{\chi}_t[\{\eta_k\}] = \mathrm{Tr}(\tilde{\rho}_t \, \mathrm{D}[\{\eta_k\}]), \tag{4.12}$$

defined in terms of the Weyl operators

$$\mathrm{D}[\{\eta_k\}] = \exp\left(\sum_{k\in K} \eta_k \, \mathrm{c}_k^\dagger \quad \eta_k^* \, \mathrm{c}_k \right). \tag{4.13}$$

The functional integral in (4.11) is defined as (see Appendix A)

$$\int \mathcal{D}^2[\{\eta_k\}] \, F[\{\eta_k\}] = \lim_{N\to\infty} \int \frac{\mathrm{d}^2\eta_1 \cdots \mathrm{d}^2\eta_N}{\pi^N} \, F(\eta_1, ..., \eta_N). \tag{4.14}$$

Using the Weyl form of the canonical commutation relations,

$$\mathrm{D}^\dagger[\{\alpha_k\}]\mathrm{D}[\{\zeta_k\}]\mathrm{D}[\{\alpha_k\}] = \mathrm{D}[\{\zeta_k\}] \exp\left(\sum_{k\in K} \alpha_k^* \zeta_k \quad \alpha_k \zeta_k^* \right), \tag{4.15}$$

to simplify the operator transformation $\mathrm{U}_x^\dagger(\xi)\mathrm{D}[\{\zeta_k\}]\mathrm{U}_x(\xi)$, the equation of motion for $\tilde{\chi}_t[\{\eta_k\}]$ follows from the master equation (4.8) as

$$\partial_t \tilde{\chi}_t[\{\eta_k\}] = \quad {}_t[\{\eta_k\}] \tilde{\chi}_t[\{\eta_k\}]. \tag{4.16}$$

Integrating this equation yields the exact solution of the master equation (4.1) in the phase-space representation (4.12),

$$\tilde{\chi}_t[\{\eta_k\}] = \exp\left(\quad \gamma \int_0^t \mathrm{d}\tau \quad {}_\tau[\{\eta_k\}] \right) \chi_0[\{\eta_k\}]. \tag{4.17}$$

As will be shown below, the time-dependent decay rate

$${}_t[\{\eta_k\}] = \gamma \quad \gamma \int_0^L \frac{\mathrm{d}x}{L} \int \mathrm{d}^2\xi \, g(\xi) \exp\left(\sum_{k\in K} f_k e^{\mathrm{i}(kx+\omega_k t)} (\xi^* \Omega_k^+ \quad \xi \Omega_k \,) \eta_k \quad \text{c.c.} \right), \tag{4.18}$$

is real and positive.

For an isotropic distribution

$$g(\xi) = \frac{1}{2\pi} G(|\xi|), \tag{4.19}$$

the ξ-integral in Eq. (4.18) can be calculated using the polar representation $\xi = re^{\mathrm{i}\theta}$, $\mathrm{d}^2\xi = r\,\mathrm{d}r\,\mathrm{d}\theta$. In order to carry out the θ-integral, it is convenient to rewrite the argument of the exponential in (4.18) as

$$\begin{aligned} \xi^* z_t[\{\eta_k\}, x] \quad \xi z_t^*[\{\eta_k\}, x] &= r \big| z_t[\{\eta_k\}, x] \big| \Big(e^{\ \mathrm{i}(\theta \quad \varphi_z)} \quad e^{\mathrm{i}(\theta \quad \varphi_z)} \Big), \\ &= \quad \mathrm{i}2r \big| z_t[\{\eta_k\}, x] \big| \cos\Big(\theta \quad \varphi_z \quad \frac{\pi}{2} \Big), \end{aligned} \tag{4.20}$$

with

$$z_t[\{\eta_k\},x] = \big|z_t[\{\eta_k\},x]\big|\, e^{\mathrm{i}\varphi_z} = \sum_{k\in K} \Omega_k^+ f_k\, e^{\mathrm{i}kx} e^{\mathrm{i}\omega_k t}\eta_k + \Omega_k\, f_k\, e^{\ \mathrm{i}kx} e^{\ \mathrm{i}\omega_k t}\eta_k^*. \tag{4.21}$$

Using the Jacobi–Anger formula

$$e^{\mathrm{i}w\cos\theta} = J_0(w) + 2\sum_{n=1}^{\infty} \mathrm{i}^n J_n(w)\cos(n\theta), \tag{4.22}$$

and the invariance of the integral

$$\frac{1}{2\pi}\int_0^{2\pi} \mathrm{d}\theta\, e^{\mathrm{i}w\cos\theta} = J_0(w), \tag{4.23}$$

under translations of θ, Eq.(4.18) simplifies to

$$_t[\{\eta_k\}] = \gamma \quad \gamma\int_0^L \frac{\mathrm{d}x}{L}\int_0^{\infty} \mathrm{d}r\, G(r) r J_0\ \ r s_t[\{\eta_k\},x]\big), \tag{4.24}$$

with

$$s_t[\{\eta_k\},x] = 2\left|\sum_{k\in K} \Omega_k^+ f_k\, e^{\mathrm{i}kx} e^{\mathrm{i}\omega_k t}\eta_k + \Omega_k\, f_k\, e^{\ \mathrm{i}kx} e^{\ \mathrm{i}\omega_k t}\eta_k^*\right|. \tag{4.25}$$

The r-integral in (4.24) corresponds to the Hankel transform of G,

$$\hat{G}(s) = \int_0^{\infty} \mathrm{d}r\, G(r) r J_0(rs). \tag{4.26}$$

Being the characteristic function of a probability distribution, it satisfies $|\hat{G}| \le 1$. In terms of it Eq.(4.18) can be expressed compactly as

$$_t[\{\eta_k\}] = \gamma \quad \gamma\int_0^L \frac{\mathrm{d}x}{L}\, \hat{g}_r\left(2\left|\sum_{k\in K} \Omega_k^+ f_k\, e^{\mathrm{i}kx} e^{\mathrm{i}\omega_k t}\eta_k + \Omega_k\, f_k\, e^{\ \mathrm{i}kx} e^{\ \mathrm{i}\omega_k t}\eta_k^*\right|\right). \tag{4.27}$$

This expression shows that the decay rate in the equation of motion (4.16) for the characteristic functional is real and positive.

4.2 Equation of motion of the Wigner functional

As discussed in Chapter 2, the dynamics of a quantum system can be described in terms of the time evolution of the Wigner functional, which is defined on the phase space of the canonical variables of the system. This representation is particularly convenient for the semiclassical analysis of the dynamics. In this section I obtain the equation of motion of the Wigner functional from the master equation in the interaction picture (4.8). As will be shown, it is a generalization of the linear Boltzmann equation, and in the diffusion limit it reduces to a Fokker–Planck equation.

Defining the characteristic functional

$$\tilde{\chi}_t[\eta] = \mathrm{Tr}(\tilde{\rho}_t \, \mathrm{D}[\eta]), \tag{4.28}$$

in terms of the Weyl operators

$$\mathrm{D}[\eta] = \exp\Big(\int \mathrm{d}y \, \big[\eta(y)\Psi^\dagger(y) \quad \eta^*(y)\Psi(y) \big] \Big), \tag{4.29}$$

the *Wigner functional* is the Fourier transform of $\tilde{\chi}_t[\eta]$ [8],

$$\widetilde{W}_t[\lambda] = \int \mathcal{D}^2[\eta] \, \tilde{\chi}_t[\eta] \exp\Big(\int \mathrm{d}y \, \big[\lambda(y)\eta^*(y) \quad \lambda^*(y)\eta(y) \big] \Big). \tag{4.30}$$

The functional integral is defined as (see Appendix A)

$$\int \mathcal{D}^2[\eta] \, F[\eta] = \lim_{n\to\infty} \int \frac{\mathrm{d}^2\eta_1 \cdots \mathrm{d}^2\eta_n}{\pi^n} \, F(\eta_1, ..., \eta_n). \tag{4.31}$$

The properties of the Wigner functional were discussed in Section 2.6.

As shown in Section 2.7, the operators $\Psi(y)$ are defined as a linear combination of the canonical coordinates of the field. The displacement amplitudes $\eta(y)$ correspond to their coherent-state expectation values and are given by a linear combination of the classical canonical variables of the field. Since the equation of motion for $\widetilde{W}_t[\lambda]$ is the Fourier transform of the dynamical equation for $\tilde{\chi}_t[\eta]$, this will be obtained next.

From the discussion in Section 2.7, the bosonic operators c_k are related to the field operators $\Psi(y)$ through

$$\mathrm{c}_k = \Omega_k^+ \frac{1}{\sqrt{L}} \int_0^L \mathrm{d}y \, e^{\ \mathrm{i}ky} \, \Psi(y) \quad \Omega_k \frac{1}{\sqrt{L}} \int_0^L \mathrm{d}y \, e^{\ \mathrm{i}ky} \, \Psi^\dagger(y). \tag{4.32}$$

Inserting this expression into (4.9) yields the displacement operators in the basis of the field operators $\Psi(y)$,

$$\tilde{\mathrm{U}}_x(\xi) = \exp\Big(\int_0^L \mathrm{d}y \, \big[\Lambda_t(\xi, x; y)\Psi^\dagger(y) \quad \Lambda_t^*(\xi, x; y)\Psi(y) \big] \Big), \tag{4.33}$$

where the displacement amplitude

$$\Lambda_t(\xi, x; y) = a_t(x; y)\,\xi \quad b_t(x; y)\xi^*, \tag{4.34}$$

is a transformation of the kick strength ξ involving the time- and space-dependent coefficients

$$\begin{aligned} a_t(x; y) &= \frac{1}{\sqrt{L}} \sum_k f_k \, e^{\mathrm{i}k(x \ \ y)} \ e^{\mathrm{i}\omega_k t}(\Omega_k^+)^2 \quad e^{\ \mathrm{i}\omega_k t}(\Omega_k)^2 \big), \\ b_t(x; y) &= \frac{2\mathrm{i}}{\sqrt{L}} \sum_k f_k \, e^{\mathrm{i}k(x \ \ y)} \Omega_k \, \Omega_k^+ \sin(\omega_k t). \end{aligned} \tag{4.35}$$

The equation of motion for $\tilde{\chi}_t[\eta]$ is obtained from the master equation (4.8) in a way analogous to the previous section, but with $\tilde{\mathrm{U}}_x(\xi)$ given by (4.33). It is given by

$$\partial_t \tilde{\chi}_t[\eta] = \quad {}_t[\eta]\tilde{\chi}_t[\eta], \tag{4.36}$$

with the decay rate

$${}_t[\eta] = \gamma \quad \gamma \int_0^L \frac{\mathrm{d}x}{L} \int \mathrm{d}^2\xi g(\xi) \exp\Big(\int_0^L \mathrm{d}y \left[\eta(y)\Lambda_t^*(\xi, x; y) \quad \eta^*(y)\Lambda_t(\xi, x; y) \right] \Big). \tag{4.37}$$

This expression is the analog of (4.27) for the canonical variables of the field.

The Fourier transform of (4.36) yields the equation of motion for the Wigner functional,

$$\partial_t \widetilde{W}_t[\lambda] = \gamma \int_0^L \frac{\mathrm{d}x}{L} \int \mathrm{d}^2\xi \; g(\xi) \Big(\widetilde{W}_t[\lambda \quad \Lambda_t(\xi, x)] \quad \widetilde{W}_t[\lambda] \Big). \tag{4.38}$$

It describes the time evolution of a quasiprobability distribution in a functional phase space. Each point λ therein, which is a complex linear combination of the classical canonical variables of the field, is subject to random kicks that occur with rate γ and whose strength depends on the spatial position x, as given by the function $\Lambda_t(\xi, x)$.

As may be expected from the discussion in Chapter 3, Eq. (4.38) has the form of the forward Kolmogorov equation of a compound Poisson process with constant rate γ and jump-size distribution $g(\xi)/L$ [90]. In physical terms, this is a transport equation that has the form of a generalized linear Boltzmann equation. Correspondingly, the master equation (4.1) can be considered the field-theoretic generalization of a quantum linear Boltzmann equation [91].

4.2.1 Diffusion limit

As shown in [92], the integral operator in the linear Boltzmann equation can be properly approximated only by a second-order differential operator, thus yielding a Fokker–Planck equation. Physically, this corresponds to the diffusion limit of small and frequent kicks. In the present case it amounts to approximating all functions of ξ with a second-order polynomial in this parameter.

In order to obtain the diffusion approximation to Eq. (4.38), I will first approximate Eq. (4.36) for the characteristic functional $\tilde{\chi}_t[\eta]$ to second order in ξ and then take the Fourier transform. For this purpose, it is convenient to rewrite this equation as

$$\partial_t \tilde{\chi}_t[\eta] = \quad \gamma + \gamma \int_0^L \frac{\mathrm{d}x}{L} \int \mathrm{d}^2\xi \; g(\xi) \exp \; \xi^* z_t[\eta; x] \quad \xi z_t^*[\eta; x] \big), \tag{4.39}$$

with

$$z_t[\eta;x]=\int_0^L \mathrm{d}y\,\big[\,\eta(y)a_t(x;y)+\eta^*(y)b_t(x;y)\,\big]. \tag{4.40}$$

To second order in ξ the exponential is approximated by a polynomial,

$$\exp(\xi^* z_t[\eta;x] \quad \xi z_t^*[\eta;x]) \simeq 1+\xi^* z_t[\eta;x] \quad \xi z_t^*[\eta;x]+\tfrac{1}{2}\ \xi^* z_t[\eta;x] \quad \xi z_t^*[\eta;x]\big)^2. \tag{4.41}$$

Writing $\xi=|\xi|e^{\mathrm{i}\theta}$ and given that $g(\xi)$ is an even function, the only term that contributes to the ξ-integral is $\quad|\xi|^2|z_t[\eta;x]|^2$. With this approximation (4.36) reduces to

$$\partial_t\tilde{\chi}_t[\eta]=\ \frac{\sigma_g^2\gamma}{L}\int_0^L \mathrm{d}x\left|\int_0^L \mathrm{d}y\,\big[\,\eta(y)a_t(x;y)+\eta^*(y)b_t(x;y)\,\big]\right|^2\tilde{\chi}_t[\eta], \tag{4.42}$$

where

$$\sigma_g^2=\int \mathrm{d}^2\xi\,|\xi|^2 g(\xi) \tag{4.43}$$

is the second moment of g.

The Fourier transform of (4.42) is

$$\begin{aligned}\partial_t\widetilde{W}_t[\lambda]=\ &\frac{\gamma\sigma_g^2}{L}\int_0^L \mathrm{d}x\int \mathrm{d}x_1\mathrm{d}x_2\int\mathcal{D}^2[\eta]\big[a_t(x;x_1)b_t^*(x;x_2)\,\eta(x_1)\eta(x_2)\\ &+a_t(x;x_1)\,a_t^*(x;x_2)\eta(x_1)\eta^*(x_2)+b_t(x;x_1)\,b_t^*(x;x_2)\eta^*(x_1)\eta(x_2)\\ &+b_t(x;x_1)\,a_t^*(x;x_2)\,\eta^*(x_1)\eta^*(x_2)\big]\,e^{\int \mathrm{d}z\,[\lambda(z)\eta^*(z)\quad\lambda^*(z)\eta(z)]}\tilde{\chi}_t[\eta].\end{aligned} \tag{4.44}$$

Since $\widetilde{W}_t[\lambda]$ is an analytic functional of λ and λ^*, the corresponding functional Wirtinger derivatives (see Section 2.2.6) are given by

$$\frac{\delta}{\delta\lambda(y)}\widetilde{W}_t[\lambda]=\int\mathcal{D}^2[\eta]\ \eta^*(y)\chi[\eta]\exp\!\left(\int \mathrm{d}z\,\big[\,\lambda(z)\eta^*(z)\quad\lambda^*(z)\eta(z)\,\big]\right), \tag{4.45}$$

and

$$\frac{\delta}{\delta\lambda^*(y)}\widetilde{W}_t[\lambda]=\ \int\mathcal{D}^2[\eta]\ \eta(y)\chi[\eta]\exp\!\left(\int \mathrm{d}z\,\big[\,\lambda(z)\eta^*(z)\quad\lambda^*(z)\eta(z)\,\big]\right). \tag{4.46}$$

These expressions follow from the identity (see Section 2.2.3)

$$\frac{\delta\lambda(z)}{\delta\lambda(y)}=\delta(z\quad y). \tag{4.47}$$

In terms of functional derivatives, Eq. (4.44) can thus be written as a Fokker–Planck equation,

$$\partial_t \widetilde{W}_t[\lambda] = \int \mathrm{d}x_1\,\mathrm{d}x_2 \Bigg[\mathcal{D}_t^{\lambda\lambda}(x_2 \quad x_1)\frac{\delta}{\delta\lambda(x_1)}\frac{\delta}{\delta\lambda(x_2)} + \mathcal{D}_t^{\lambda\lambda^*}(x_2 \quad x_1)\frac{\delta}{\delta\lambda(x_1)}\frac{\delta}{\delta\lambda^*(x_2)} + \mathcal{D}_t^{\lambda^*\lambda}(x_2 \quad x_1)\frac{\delta}{\delta\lambda^*(x_1)}\frac{\delta}{\delta\lambda(x_2)} + \mathcal{D}_t^{\lambda^*\lambda^*}(x_2 \quad x_1)\frac{\delta}{\delta\lambda^*(x_1)}\frac{\delta}{\delta\lambda^*(x_2)} \Bigg] \widetilde{W}_t[\lambda]. \tag{4.48}$$

The coefficients in front of the functional derivatives correspond to the infinite-dimensional generalization of the diffusion tensor,

$$\begin{aligned}
\mathcal{D}_t^{\lambda\lambda}(x_2 \quad x_1) &= \gamma\sigma_g^2 \int_0^L \frac{\mathrm{d}\,x}{L}\, b_t(x;x_1)a_t^*(x;x_2),\\
\mathcal{D}_t^{\lambda\lambda^*}(x_2 \quad x_1) &= \gamma\sigma_g^2 \int_0^L \frac{\mathrm{d}\,x}{L}\, b_t(x;x_1)b_t^*(x;x_2),\\
\mathcal{D}_t^{\lambda^*\lambda}(x_2 \quad x_1) &= \gamma\sigma_g^2 \int_0^L \frac{\mathrm{d}\,x}{L}\, a_t(x;x_1)a_t^*(x;x_2),\\
\mathcal{D}_t^{\lambda^*\lambda^*}(x_2 \quad x_1) &= \gamma\sigma_g^2 \int_0^L \frac{\mathrm{d}\,x}{L}\, a_t(x;x_1)b_t^*(x;x_2).
\end{aligned} \tag{4.49}$$

There are four coefficients because the coordinates in phase space are divided into two sets: the field amplitude $\varphi(y)$ and its canonically conjugate momentum $\pi(y)$. In this basis, the corresponding Fokker–Planck equation contains terms describing diffusion only of the field, diffusion of both the field and the canonically conjugate momentum, and diffusion only of the canonically conjugate momentum [24].

Following [93], for a given initial state the solution of Eq. (4.48) can be obtained using the functional generalization of the method of characteristics [22] to solve (4.42) and then taking the Fourier transform of the solution.

It is worth noting that the master equation associated to (4.48) results from formally expanding $\tilde{\mathrm{U}}_x(\xi)\tilde{\rho}_t\tilde{\mathrm{U}}_x^\dagger(\xi)$ to second order in ξ using the formula

$$e^{s\mathrm{A}}\mathrm{B}e^{\ s\mathrm{A}} = \mathrm{B} + s[\mathrm{A},\mathrm{B}] + \frac{s^2}{2}[\mathrm{A},[\mathrm{A},\mathrm{B}]] + \cdots, \tag{4.50}$$

with $s=1$, $\mathrm{B}=\tilde{\rho}_t$ and

$$\mathrm{A} = \mathrm{A}_t(x,\xi) = \int_0^L \mathrm{d}y\,[\Lambda_t(\xi,x;y)\Psi^\dagger(y) \quad \Lambda_t^*(\xi,x;y)\Psi(y)]. \tag{4.51}$$

The result is the Lindblad equation

$$\partial_t\tilde{\rho}_t = \gamma\int_0^L \frac{\mathrm{d}x}{L}\int \mathrm{d}^2\xi\, g(\xi)\Bigg[\mathrm{A}_t(x,\xi)\tilde{\rho}_t\mathrm{A}_t^\dagger(x,\xi) \quad \frac{1}{2}\Big\{\mathrm{A}_t^\dagger(x,\xi)\mathrm{A}_t(x,\xi),\tilde{\rho}_t\Big\}\Bigg]. \tag{4.52}$$

Since the Lindblad operators $\mathrm{A}_t(x,\xi)$ are linear in the field operators, this is a field-theoretic generalization of the quantum Brownian motion master equation [24].

4.3 Dynamics of the purity decay

In the Wigner representation quantum superpositions of macroscopically distinct field configurations are characterized by a quasiprobability distribution displaying strong oscillations between positive and negative values in a local phase-space region of volume $\hbar$ [64]. The decoherence of a superposition due to random phase-space kicks results in the blurring of these fine structures.

As shown in [94] for a finite number of degrees of freedom, in the diffusion limit the Wigner function turns positive after a finite time. Moreover, it is known that the only non-negative Wigner functions correspond to coherent states [63]. Since these results do not depend on the number of degrees of freedom of the quantum system, once the Wigner functional has become positive, the state of the field is indistinguishable from a mixture of classical field configurations.

In the general case of Eq. (4.38), however, it takes an infinite time until the Wigner functional becomes positive. This gradual loss of coherence will be quantified below through the decay of the purity of the state. For this purpose it is convenient to use the phase-space representation (4.12), as will become clear when considering different limit cases of the parameters characterizing the classicalization dynamics.

In the basis of the mode variables (4.11) the purity is given by

$$p_t = \int \mathcal{D}^2[\{\eta_k\}] \left|\tilde{\chi}_t[\{\eta_k\}]\right|^2. \tag{4.53}$$

This expression follows from

$$\text{Tr}\ \ \tilde{\rho}_t^2) = \int \mathcal{D}^2[\{\eta_k\}]\ \tilde{\chi}_t[\{\eta_k\}] \int \mathcal{D}^2[\{\zeta_k\}]\ \tilde{\chi}_t^*[\{\zeta_k\}]\ \text{Tr}\ \ \text{D}^\dagger[\{\eta_k\}]\text{D}[\{\zeta_k\}]\big), \tag{4.54}$$

by recognizing that the trace on the right side,

$$\text{Tr}\ \ \text{D}^\dagger[\{\eta_k\}]\text{D}[\{\zeta_k\}]\big) = \big\langle\{\zeta_k\}|\{\eta_k\}\big\rangle \int \mathcal{D}^2[\{\lambda_k\}] \exp\left(\sum_{k\in K} \lambda_k^*(\zeta_k \quad \eta_k) \quad \lambda_k(\zeta_k \quad \eta_k)^*\right), \tag{4.55}$$

involves the functional generalization of the Dirac delta,

$$\delta[\{\zeta_k \quad \eta_k\}] = \lim_{n\to\infty} \int \frac{\mathrm{d}^2\alpha_1 \cdots \mathrm{d}^2\alpha_n}{\pi^{2n}} \exp\left(\sum_{j=1}^{n} \alpha_j^*(\zeta_j \quad \eta_j) \quad \alpha_j(\zeta_j \quad \eta_j)^*\right). \tag{4.56}$$

Inserting (4.17) into (4.53) the purity is explicitly given by

$$p_t = \int \mathcal{D}^2[\{\eta_k\}] \left|\chi_0[\{\eta_k\}]\right|^2 \exp\left(\ \ 2\int_0^t \mathrm{d}\tau\ \ {}_\tau[\{\eta_k\}]\right), \tag{4.57}$$

with the decay rate ${}_\tau[\{\eta_k\}]$ defined in Eq. (4.27).

In order to perform analytical and numerical calculations of the purity I will assume, as in Section 3.2.3, that the kick-strength distribution is given by (4.19), with

$$\hat{G}(s) = \exp\left(\frac{s^2\sigma_g^2}{2} \right), \tag{4.58}$$

and the spread function is specified by the Fourier coefficients (3.55).

The initial state is assumed to be a superposition of single-mode coherent states in the mode $k=0$,

$$|\psi\rangle = \mathcal{N}^{1/2} \left(|\alpha\rangle_0 + |\beta\rangle_0 \right) \left| \{0\}_{k\neq 0} \right\rangle. \tag{4.59}$$

In terms of the relative coordinates $\Delta = \alpha - \beta$ and $2\mathcal{C} = (\alpha+\beta)$, the characteristic functional of the state at time $t=0$ is

$$\begin{aligned} \frac{\chi_0[\{\eta_k\}]}{\mathcal{N}} = {} & 2e^{\frac{1}{2}\sum_{k\neq 0}|\eta_k|^2} e^{\frac{1}{2}|\eta_0^2|} \cos\left(\mathrm{Im}\,\Delta\eta_0^* \right) e^{2i\mathrm{Im}\mathcal{C}\eta_0^*} \\ & + e^{\frac{1}{2}\sum_{k\neq 0}|\eta_k|^2} \exp\left(i\mathrm{Im}\left[2\mathcal{C}\eta_0^* + i\mathrm{Im}\,\mathcal{C}^*\Delta \right] \right) e^{\frac{1}{2}|\Delta+\eta_0|^2} \\ & + e^{\frac{1}{2}\sum_{k\neq 0}|\eta_k|^2} \exp\left(i\mathrm{Im}[2\mathcal{C}\eta_0^* - i\mathrm{Im}\,\mathcal{C}^*\Delta] \right) e^{\frac{1}{2}|\Delta - \eta_0|^2}. \end{aligned} \tag{4.60}$$

Its squared modulus is given by

$$\begin{aligned} \frac{\left|\chi_0[\{\eta_k\}]\right|^2}{\mathcal{N}^2} = {} & e^{\sum_{k\neq 0}|\eta_k|^2} \left(e^{|\Delta+\eta_0|^2} + e^{|\Delta-\eta_0|^2} \right) \\ & + 2e^{\sum_{k\neq 0}|\eta_k|^2} e^{|\eta_0^2|} \left(2\cos^2\left(\mathrm{Im}\,\Delta\eta_0^* \right) + \cos\left(2\mathrm{Im}\,\Delta\mathcal{C}^* \right) e^{|\Delta|^2} \right) \\ & + 4e^{\left|\frac{\Delta}{2}\right|^2} \cos\left(\mathrm{Im}\,\Delta\mathcal{C}^* \right) e^{\sum_{k\neq 0}|\eta_k|^2} \cos\left(\mathrm{Im}\,\Delta\eta_0^* \right) \\ & \times \left(e^{|\Delta/2+\eta_0|^2} + e^{|\Delta/2-\eta_0|^2} \right). \end{aligned} \tag{4.61}$$

The normalization constant, which ensures that $\chi_0[0]=1$, is

$$\mathcal{N} = \left[2 + 2\exp\left(-|\Delta|^2/2 \right) \cos(\mathrm{Im}\,\Delta\mathcal{C}^*) \right]^{-1}. \tag{4.62}$$

From Eqs. (3.55), (4.57), (4.58) and (4.61) it is clear that the purity decay depends on the three parameters characterizing the classicalizing dynamics, γ, σ and σ_g, and on the structure of the initial state. Since the expression (4.57) for the purity is in general not amenable to analytic calculation, in the following I will obtain analytic approximations to it for different limiting values of the above parameters. The resulting expressions will be compared with numerical calculations of the exact Eq. (4.57), carried out using the discrete-chain model of the quantum field discussed in Chapter 2, with $N=32$ harmonic degrees of freedom.

4.3.1 Full time evolution

In order to describe the purity decay analytically at all times, it is necessary to consider parameter regimes in which

$$ {}_{\tau}[\{\eta_k\}] = \gamma \quad \gamma\int_0^L \frac{\mathrm{d}x}{L}\exp\Big(\quad 2\sigma_g^2 L\Big|\sum_{k\in K}\Omega_k^+\tfrac{f_k}{\sqrt{L}}\,e^{\mathrm{i}kx}e^{\mathrm{i}\omega_k\tau}\,\eta_k+\Omega_k\tfrac{f_k}{\sqrt{L}}\,e \quad {}^{\mathrm{i}kx}e \quad {}^{\mathrm{i}\omega_k\tau}\,\eta_k^*\Big|^2\Big) \tag{4.63}$$

is time-independent, that is ${}_t[\{\eta_k\}] = \ [\{\eta_k\}]$. This is the case for a broad spread function and for a narrow kick distribution, as will be shown next.

If the width σ of the spread function is comparable to the size L of the region enclosing the quantum field, the Fourier coefficients (3.55) of f can be approximated as

$$f_k \simeq \sqrt{L}\,\delta_{0k}. \tag{4.64}$$

Since $\omega_0 = \omega$, it follows that $\Omega_0^+ = 1$, $\Omega_0 = 0$. Therefore, for $\sigma/L \simeq 1$ the purity decays as

$$p_t \simeq \int \mathcal{D}^2[\{\eta_k\}]\,\big|\chi_0[\{\eta_k\}]\big|^2 \exp\Big(\quad 2\gamma t\Big[1 \quad \exp \quad 2L\sigma_g^2|\eta_0|^2)\Big]\Big). \tag{4.65}$$

In the limiting case of a narrow kick distribution, such that $\sigma_g^2 L \ll 1$, the approximation

$$\exp \quad 2L\sigma_g^2|\eta_0|^2) \simeq 1 \quad 2L\sigma_g^2|\eta_0|^2 \tag{4.66}$$

leads to the analytically tractable expression for the purity

$$p_t \simeq \int \mathcal{D}^2[\{\eta_k\}]\,\big|\chi_0[\{\eta_k\}]\big|^2 \exp \quad 4\gamma t\,L\sigma_g^2|\eta_0|^2). \tag{4.67}$$

The phase-space integral in (4.67) can be readily calculated. For the modes with $k \neq 0$ it involves a Gaussian integral, and for the mode $k = 0$ one needs to evaluate the integrals

$$\begin{aligned}
\int \frac{\mathrm{d}^2\eta_0}{\pi}\,e \ {}^{|\eta_0|^2(1+\mu^2)}\,\tfrac{1}{2}\big[1+\cos\ 2\mathrm{Im}\,\Delta\,\eta_0^*\big)\big] &= \frac{1}{1+\mu^2}\,\frac{1}{2}\Big(1+e \ {}^{\frac{|\Delta|^2}{1+\mu^2}}\Big),\\
\int \frac{\mathrm{d}^2\eta_0}{\pi}\,e \ {}^{|\Delta/2\pm\eta_0|^2 \ |\eta_0|^2\mu^2}\cos\ \mathrm{Im}\,\Delta\,\eta_0^*\big) &= \frac{1}{1+\mu^2}\,e \ {}^{|\Delta|^2/4},\\
\int \frac{\mathrm{d}^2\eta_0}{\pi}\,e \ {}^{|\Delta\pm\eta_0|^2 \ |\eta_0|^2\mu^2} &= \frac{1}{1+\mu^2}\,e \ {}^{\frac{|\Delta|^2\mu^2}{1+\mu^2}},
\end{aligned} \tag{4.68}$$

where $\mu = 4\gamma t\sigma_g^2 L$. The purity of the state of the field for $\sigma/L \simeq 1$ and $\sigma_g^2 L \ll 1$ is therefore

$$p_t \simeq \frac{2\mathcal{N}^2}{1+\mu^2}\Big[1+e \ {}^{\frac{|\Delta|^2}{1+\mu^2}}+e \ {}^{\frac{|\Delta|^2\mu^2}{1+\mu^2}}+4e \ {}^{|\Delta|^2/2}\cos\ \mathrm{Im}\Delta\mathcal{C}^*\big)+e \ {}^{|\Delta|^2}\cos\ 2\mathrm{Im}\,\Delta\mathcal{C}^*\big)\Big]. \tag{4.69}$$

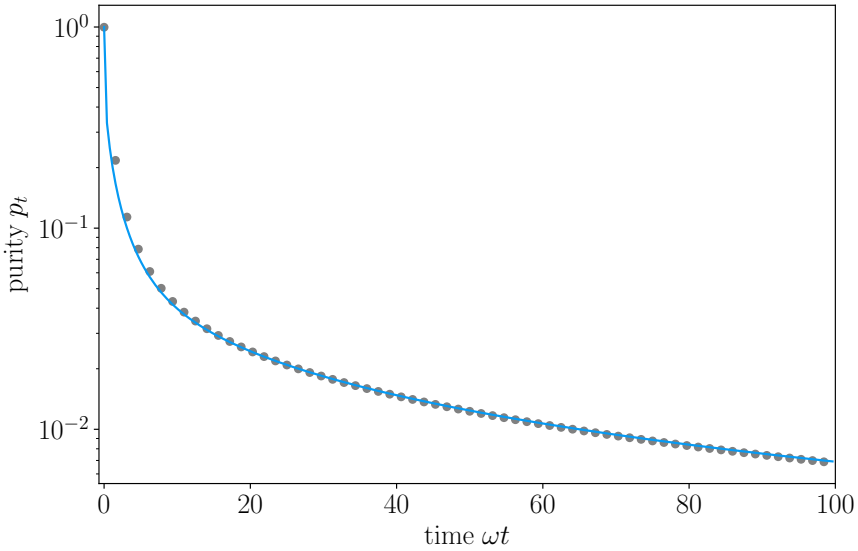

Figure 4.1. Purity decay of a superposition of single-mode coherent states $|\psi\rangle \propto (|\alpha\rangle_0 + |\ \ \alpha\rangle_0)|\{0\}_{k\neq 0}\rangle$ with $\alpha = 2+2\mathrm{i}$. The parameters are $v/L\omega = 0.01$, $\gamma/\omega = 0.2$, $\sigma/L = 1$ and $\sigma_g^2 L = 0.32$. The points correspond to the exact numerical calculation of Eq. (4.57). The solid line is the analytic approximation to this equation for $\sigma/L \simeq 1$ and $\sigma_g^2 L \ll 1$, given by Eq. (4.69).

As shown in Fig. 4.1, Eq. (4.69) is in excellent agreement with the exact numerical calculation of Eq. (4.57). The corresponding phase-space integrals were calculated using quasi-Monte Carlo integration based on a generalized Faure sequence. This numerical method is explained in detail in Chapter 5.

On the other hand, when $\sigma/L < 1$ and in the limit of a narrow kick distribution such that $\sigma_g^2 L \ll 1$, Eq. (4.63) can be approximated as

$$ {}_\tau[\{\eta_k\}] = 2\gamma\sigma_g^2 L \int_0^L \frac{\mathrm{d}x}{L} \left| \sum_{k\in K} \Omega_k^+ e^{\mathrm{i}kx} e^{\mathrm{i}\omega_k \tau} \frac{f_k}{\sqrt{L}} \eta_k + \Omega_k \, e^{\ \mathrm{i}kx} e^{\ \mathrm{i}\omega_k \tau} \frac{f_k}{\sqrt{L}} \eta_k^* \right|^2 . \tag{4.70} $$

Since the integral over x vanishes, the purity remains constant,

$$ p_t \simeq 1. \tag{4.71} $$

4.3.2 Short-time behavior

On physical grounds, it is expected that the decay rate of the purity of a quantum superposition of coherent states depends on their initial separation in phase space, as compared to the width of the kick distribution. From Eqs. (4.53) and (4.36) the initial purity decay rate $R_0 = \ \ \dot{p}_0$ is given by

$$ R_0 = 2 \int \mathcal{D}^2[\{\eta_k\}] \left| \chi_0[\{\eta_k\}] \right|^2 \ {}_0[\{\eta_k\}], \tag{4.72} $$

where

$$ {}_0[\{\eta_k\}] = \gamma \quad \gamma \int_0^L \frac{\mathrm{d}x}{L} \exp\Bigg(\quad 2\sigma_g^2 L \left| \sum_{k\in K} \Omega_k^+ \frac{f_k}{\sqrt{L}} e^{\mathrm{i}kx} \eta_k + \Omega_k \frac{f_k}{\sqrt{L}} e^{\ \mathrm{i}kx} \eta_k^* \right|^2 \Bigg). \tag{4.73} $$

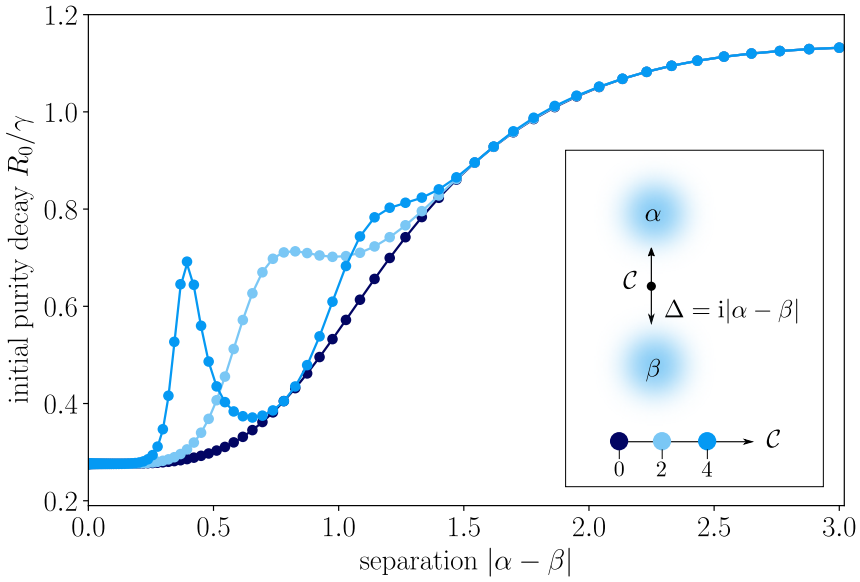

Figure 4.2. Initial purity decay rate, R_0/γ, of three superpositions of single-mode coherent states, $|\psi\rangle \propto (|\alpha\rangle_0 + |\beta\rangle_0)|\{0\}_{k\neq 0}\rangle$ as a function of the separation $|\alpha \quad \beta|$. The parameters are $v/L\omega = 0.01$, $\gamma/\omega = 1.0$, $\sigma/L = 1$ and $\sigma_g^2 L = 0.08$. The circles correspond to the exact numerical calculation of Eq. (4.72). The solid lines show the analytic approximation to this equation for $\sigma/L \simeq 1$, given by Eq. (4.75).

The integral in (4.72) can be readily calculated in the case of a broad spread function, that is for $\sigma/L \simeq 1$. From Eq. (4.65) the corresponding decay rate is given by

$$R_0 = 2\gamma \quad 2\gamma \int \mathcal{D}^2[\{\eta_k\}] \left|\chi_0[\{\eta_k\}]\right|^2 \exp \quad 2\sigma_g^2 L|\eta_0|^2), \tag{4.74}$$

which using Eqs. (4.68) has the explicit expression

$$R_0 = 2\gamma \quad \frac{4\gamma\mathcal{N}^2}{1+\mu^2}\Big[1 + e^{\ \frac{|\Delta|^2}{1+\mu^2}} + e^{\ \frac{|\Delta|^2\mu^2}{1+\mu^2}} + 4e^{\ |\Delta|^2/2}\cos\ \mathrm{Im}\Delta\mathcal{C}^*) + e^{\ |\Delta|^2}\cos\ 2\mathrm{Im}\Delta\mathcal{C}^*)\Big], \tag{4.75}$$

with $\mu^2 = 2\sigma_g^2 L$. This equation shows that for arbitrarily large separations the classicalization rate approaches the maximum value

$$\frac{R_{\max}}{\gamma} = 2 \quad \frac{1}{1+2\sigma_g^2 L}. \tag{4.76}$$

In Fig. 4.2 the initial purity decay rate is plotted as a function of the separation $2\Delta = |\alpha \quad \beta|$ for three different values of $\alpha + \beta = 2\mathcal{C}$. It exhibits oscillations for $|\alpha \quad \beta| < 1.5$, and for large separations it saturates at the value expected from Eq. (4.76). The circles correspond to the exact numerical calculation of Eq. (4.72). The solid lines represent the analytic approximation to this equation for the case of a broad spread function, as given by Eq. (4.75). The remarkable agreement between both highlights the adequacy of the chosen numerical method for calculating phase-space integrals in high dimensions.

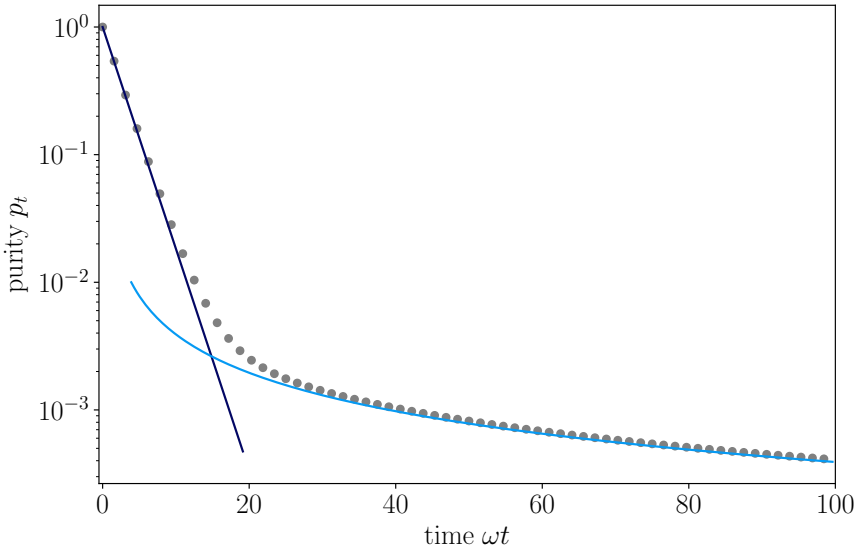

Figure 4.3. Purity decay of a superposition of single-mode coherent states $|\psi\rangle \propto (|\alpha\rangle_0 + |\ \ \alpha\rangle_0)|\{0\}_{k\neq 0}\rangle$ with $\alpha = 2 + 2\mathrm{i}$. The parameters are $v/L\omega = 0.01$, $\gamma/\omega = 0.2$, $\sigma/L = 1$ and $\sigma_g^2 L = 32$. The points correspond to the exact numerical calculation of Eq. (4.57). The straight line shows the short-time behavior $p_t \simeq \exp(\ \ 2\gamma t)$. The curve describing the long-time behavior, $p_t \simeq 1/4\sigma_g^2 L\gamma t$, was obtained using Laplace's method.

The initial decay of the purity (4.57) is given by an exponential with decay rate R_0. This follows from considering the Taylor series of $\log p_t$ to linear order in t,

$$\log p_t \simeq \log p_0 + \frac{\mathrm{d}}{\mathrm{d}t}(\log p_t)\Big|_{t=0} t, \tag{4.77}$$

where

$$\frac{\mathrm{d}}{\mathrm{d}t}(\log p_t)\Big|_{t=0} = \ \ R_0. \tag{4.78}$$

From Eq. (4.75), for a broad spread function and a broad kick distribution, such that $\sigma_g^2 L \gg 1$, the initial decay rate is $R_0 = 2\gamma$. The corresponding purity decay, $p_t \simeq \exp(\ \ 2\gamma t)$, is observed in Fig. 4.3 for times shorter than $10\,\omega^{\ \ 1}$.

4.3.3 Long-time behavior

For parameter regimes such that $\ \ _t[\{\eta_k\}] = \ \ [\{\eta_k\}]$ the purity (4.57) is given by a functional Laplace integral

$$p_t = \int \mathcal{D}^2[\{\eta_k\}]\, \big|\chi_0[\{\eta_k\}]\big|^2 \exp(\ \ 2t\ \ [\{\eta_k\}]). \tag{4.79}$$

The asymptotic behavior of the purity as $\gamma t \to \infty$ can thus be obtained using Laplace's method for functional integrals [95]

$$\int \mathcal{D}[Z]\, q[Z] e^{\ \ \tau h[Z]} \simeq q[Z_0]\, e^{\ \ \tau h[Z_0]} \exp\!\left(\ \ \frac{1}{2}\,\mathrm{Tr}\log\Lambda(Z_0)\right) \text{ as } \tau \to \infty, \tag{4.80}$$

where Z_0 is the solution of the functional equation (see Section 2.2)

$$\frac{\delta h[Z]}{\delta Z} = 0, \tag{4.81}$$

that satisfies

$$\frac{\delta}{\delta Z(y)}\frac{\delta}{\delta Z(x)}h[Z]\bigg|_{Z=Z_0} > 0, \tag{4.82}$$

and the operator $\Lambda(Z_0)$ is defined as

$$\Lambda(Z_0)\,h = \frac{\delta}{\delta Z}\frac{\delta}{\delta Z}h[Z]\bigg|_{Z=Z_0}. \tag{4.83}$$

In the case of a broad spread function, the asymptotic behavior of the purity is obtained from Eq. (4.65) using the multivariate version of Laplace's method [96]

$$\int_{\mathbb{R}^d} \mathrm{d}\mathbf{x}\; q(\mathbf{x})e^{\;\tau h(\mathbf{x})} \simeq q(\mathbf{x}_0)\left(\frac{2\pi}{\tau}\right)^{d/2}\frac{e^{\;\tau h(\mathbf{x}_0)}}{|H_h(\mathbf{x}_0)|^{1/2}} \;\text{ as } \tau\to\infty, \tag{4.84}$$

where H_h is the Hessian matrix of h and $\mathbf{x}_0$ is a global minimum of h, that is $\nabla h(\mathbf{x}_0)=\mathbf{0}$ and $|H_h(\mathbf{x}_0)|>0$. In the case considered here $d=2$,

$$h(\eta_0) = 2\big[1 \quad \exp\Big(\;\; 2L\sigma_g^2|\eta_0|^2\Big)\big], \tag{4.85}$$

which has a minimum at $\eta_0=0$, and

$$q(\eta_0) = \int \mathcal{D}^2[\{\eta_k\}_{k\neq 0}]\,\big|\chi_0[\{\eta_k\}]\big|^2. \tag{4.86}$$

From Eq. (4.61) it follows that $q(0)=1$. The asymptotic behavior of the purity for $\sigma/L\simeq 1$ is thus given by

$$p_t \simeq \frac{1}{4\sigma_g^2 L}\frac{1}{\gamma t} \quad \text{as } \gamma t\to\infty. \tag{4.87}$$

As shown in Fig. 4.3, this expression is in good agreement with the exact numerical calculation of Eq. (4.65) for times larger than $40\,\omega^{\;-1}$.

5 Beyond Monte Carlo integration

This chapter contains a brief review of the numerical methods available for approximating integrals in high-dimensional spaces. Special emphasis is made on low-discrepancy digital sequences, since the integration method used in Chapter 4 belongs to this class. For a comprehensive treatment of these techniques the reader is advised to consult [97, 98].

5.1 Classical integration methods

Before discussing integration methods based on low-discrepancy sequences, in this section I provide a brief summary of the more familiar methods based on product rules, analysis of variance and Monte Carlo sampling. In particular, I mention their shortcomings when calculating integrals in very high dimensions in order to show the motivation for the development of the methods described in the next section.

5.1.1 Product rules

Given a function $f\colon \Omega \subset \mathbb{R} \to \mathbb{R}$ one can approximate the integral

$$I(f) = \int_\Omega f(x)\,\mathrm{d}x \tag{5.1}$$

to great accuracy using different techniques. Newton–Cotes methods use a lattice of equally spaced points to evaluate the integrand, whereas Gaussian quadratures evaluate the function on the lattice of roots of a polynomial. The extension of these methods for functions of s variables consists in constructing a high-dimensional lattice using the s-fold Cartesian product of the one-dimensional rule. For this reason, the resulting method is called a *product rule*.

The main obstacle when calculating high-dimensional integrals with these techniques is the so-called curse of dimensionality: the cost to compute an approximation with a prescribed accuracy increases *exponentially* with the dimension of the integral. For this reason, several methods have been developed that avoid the curse of dimensionality to some extent.

5.1.2 Analysis of variance

In the *analysis of variance* (ANOVA) representation the integrand f of a s-dimensional integral is decomposed into a sum of 2^s terms, where each term describes the relative importance of a subset of variables with respect to the total variance of f [97].

In some applications, the integrals are of low effective dimension in the superposition sense, which means that they can be well approximated by a sum of functions defined in a subspace of low dimension. Moreover, coordinate transformations such as the *Brownian bridge* [97] can be used to exploit the underlying structure of the integral to single out the leading dimensions. In this case, the integrand is said to be of low effective dimension in the truncation sense, which means that only a few variables have a significant impact on the output of the function.

This class of methods also includes the *sparse grid methods*, which are based on a decomposition of a s-dimensional integral into an infinite telescopic sum that is truncated in a way that balances computational cost and accuracy [99].

5.1.3 Monte Carlo integration

Given the integral on the s-dimensional unit cube $B_s = [0,1)^s$:

$$I[f] = \int_{B_s} f(\mathbf{u})\,\mathrm{d}\mathbf{u}, \tag{5.2}$$

a *Monte Carlo estimator* of (5.2) uses N *random* points $\mathbf{u}_i$ independently and uniformly distributed in B_s:

$$Q_N = \frac{1}{N}\sum_{i=1}^{N} f(\mathbf{u}_i). \tag{5.3}$$

This estimator is unbiased since [97]

$$\mathrm{E}(Q_N) = \frac{1}{N}\sum_{i=1}^{N} \mathrm{E}(f(\mathbf{u}_i)) = I(f). \tag{5.4}$$

Moreover, from the central limit theorem it follows that [97]

$$\frac{Q_N \quad I(f)}{\sigma/\sqrt{N}} \Rightarrow \mathcal{N}(0,1), \tag{5.5}$$

where the arrow denotes convergence to the standard normal distribution and

$$\sigma^2 = \int_{[0,1)^s} (f(\mathbf{u}) \quad I(f))^2\,\mathrm{d}\mathbf{u} \tag{5.6}$$

is the variance of f.

Eq. (5.5) shows that the convergence rate of a Monte Carlo method is proportional to $N^{\ 1/2}$ independently of the dimension. As a consequence, in order to reduce the error by a factor of 10, the sample size N must increase by a factor of 100, which for many applications can be prohibitive.

In order to improve the convergence rate, variance-reduction techniques have been developed. The idea is to find another function ϕ whose integral is also $I(f)$, but has a smaller variance than f (5.6). A prominent example of this method is the VEGAS algorithm, which is based on importance sampling and has been successfully used in quantum electrodynamics [100, 101].

5.2 Quasi-Monte Carlo methods

An alternative approach to improve the convergence rate of Monte Carlo methods is to use quasi-random or low-discrepancy sampling. In the context of multi-variable integration this is referred to as a *quasi-Monte Carlo method*.

Informally, a low-discrepancy sample is a set of points distributed in a way that approximates the uniform distribution as closely as possible. However, unlike random samples, the points are not required to be independent and moreover they are deterministic. There are two main sources of low-discrepancy point sets: lattices and digital nets and sequences. In the following I will only consider digital sequences, since the integration method used in this thesis belongs to this class.

5.2.1 Digital sequences

One of the simplest examples of a low-discrepancy sequence is the van der Corput sequence in base $b \geq 2$

$$u_m = \phi_b(m \quad 1), \quad m \geq 1, \tag{5.7}$$

defined in terms of the radical inverse function in base b:

$$\phi_b(m) = \sum_{k=0}^{\infty} a_k(m) b^{\ k \ \ 1} \in [0,1), \tag{5.8}$$

where $a_k(m)$ is the k-th digit in the b-ary representation of the positive integer m

$$m = \sum_{k=0}^{\infty} a_k(m) b^k, \quad 0 \leq a_k(m) < b, \tag{5.9}$$

when infinitely many coefficients $a_k(m)$ are equal to zero. Compared to an equidistantly spaced grid, this sequence is space-filling and extensible. That is, the points in the sequence are ordered in such a way that they iteratively refine the partition of the unit interval and thus do not leave large gaps. Moreover, this allows adding more points later without having to reconstruct the point set. The first few terms of this sequence in base 5 are given by $u_1 = 0$, $u_2 = 1/5$, $u_3 = 2/5$, $u_4 = 3/5$, $u_5 = 4/5$, $u_6 = 1/25$, $u_7 = 6/25$, $u_8 = 11/25$.

Given a sample P_N of N points from a one-dimensional sequence, the deviation of P_N from uniformity is quantified by the so-called star discrepancy

$$D^*(P_N) = \sup_{x \in [0,1)} |F(x) \quad \hat{F}_N(x)|, \tag{5.10}$$

where $F(x) = x$ is the cumulative distribution function (CDF) of a $U(0,1)$ random variable and $\hat{F}_N(x)$ is the empirical CDF induced by P_N. That is,

$$\hat{F}_N(x) = \frac{1}{N} \sum_{i=1}^{N} \mathbf{1}_{u_i \leq x}, \tag{5.11}$$

gives the proportion of numbers $u_i \in P_N$ that are smaller than or equal to x. For a sample P_N obtained from the van der Corput sequence one has [97]

$$D^*(P_N) \leq C \frac{\log N}{N}. \tag{5.12}$$

A direct generalization of the van der Corput sequence in the s-dimensional unit cube B_s uses a different base b for each of the s coordinates. The result is the Halton sequence

$$\mathbf{u}_m = (\phi_{b_1}(m \quad 1), ..., \phi_{b_s}(m \quad 1)), \quad m \geq 1. \tag{5.13}$$

In order to assess the deviation of this sequence from uniformity, the multidimensional generalization of (5.10) is needed. Given a sample P_N of N points from a multidimensional sequence and a box anchored at the origin with sides $\mathbf{v} = (v_1, ..., v_s) \in B_s$

$$A(\mathbf{v}) = \{\mathbf{x} \in B_s : 0 \leq x_j \leq v_j, j = 1, ..., s\}, \tag{5.14}$$

the number of points $\mathbf{u}_i$ from P_N that fall into the box equals the cardinality of the set

$$\{\mathbf{u}_i : 0 \leq u_{i,j} \leq v_j, i = 1, ..., N\}, \tag{5.15}$$

which is denoted by $\#(P_N, A)$. The empirical CDF induced by P_N is given by $\#(P_N, A)/N$ and the CDF of the uniform distribution over I_s is $\prod_{j=1}^{s} v_j$. Comparing one to the other via the Kolmogorov–Smirnov statistic yields the star discrepancy [97]

$$D^*(P_N) = \sup_{\mathbf{v} \in I_s} \left| v_1 \cdots v_s \quad \frac{\#(P_N, A)}{N} \right|. \tag{5.16}$$

For the Halton sequence

$$D^*(P_N) \leq C \frac{(\log N)^s}{N}. \tag{5.17}$$

A sequence of points $\mathbf{u}_1, \mathbf{u}_2, ...$ is called a *low-discrepancy sequence* if $D^*(P_N) \in O(N^{\quad 1}(\log N)^s)$, and the finite point sets P_N obtained from such sequences are called *low-discrepancy point sets*.

The concept of discrepancy can be used to obtain a deterministic upper bound on the integration error. For a function f of finite variation $V(f)$ in the sense of Hardy and Krause [97], the absolute error of integration,

$$E_N = |Q_N \quad I(f)|, \tag{5.18}$$

is bounded according to the Koksma–Hlawka inequality

$$E_N \leq D^*(P_N) V(f). \tag{5.19}$$

Therefore, for a low-discrepancy sequence the integration error is in $O((\log N)^s / N)$. Compared to the probabilistic Monte Carlo error, which is in $O(N^{\quad 1/2})$, for fixed dimension s the quasi-Monte Carlo error converges considerably faster. This result is often mentioned as the motivation to prefer such methods.

However, one issue with the van der Corput and Halton sequences is that for large base b the space-filling property of the sequences degrades, since the points move very slowly from 0 to 1. To overcome this problem one can use the same base for each coordinate, but then the coordinates have to be calculated in a different way (otherwise they would all be equal). One possibility is to apply a linear transformation, called the generating matrix, to the coefficients $a_k(m)$ in (5.8). This idea is used in the Sobol' sequence [102], for which $b=2$, and in the Faure sequence discussed in the next section, which uses a prime $b \geq s$.

The sequences mentioned above belong to the class of digital sequences introduced by Niederreiter, who defined the concepts of (t,s)-sequences and (t,k,s)-nets [98]. Given the nonnegative integers $q_1,...,q_s$ such that $q=q_1+\cdots+q_s$, a point set P_N with $N=b^k$ points is $(q_1,...,q_s)$-equidistributed in base b if every elementary interval defined in terms of a Cartesian product as

$$\mathcal{I}(\mathbf{r})=\prod_{j=1}^{s}\left[\frac{r_j}{b^{q_j}},\frac{r_j+1}{b^{q_j}}\right), \quad 0\leq r_j<b^{q_j}, \quad j=1,...,s, \tag{5.20}$$

contains $b^{k\quad q}$ points from P_N. A point set that is $(q_1,...,q_s)$-equidistributed in base b is called a (t,k,s)-net in base b provided $q\leq k\quad t$. The smallest integer t for which this condition holds is the t-value of P_N and also of the sequence it was obtained from. The Faure sequence that will be discussed below was designed to have $t=0$. A (t,s)-sequence is a sequence of points for which each b-ary segment of the form $\mathbf{u}_{lb^k},...,\mathbf{u}_{(l+1)b^k\quad 1}$ with $k\geq t$ and $l\geq 0$ is a (t,k,s)-net in base b. Niederreiter showed that the discrepancy of the first N points of a (t,s)-sequence in base b satisfies

$$D^*(P_N)\leq C(t,s,b)\,(\log N)^s+O((\log N)^{s\quad 1}), \quad N\geq 2. \tag{5.21}$$

5.2.2 Faure sequences and their generalization

In 1982 Henri Faure presented [103] a method to construct a $(0,s)$-sequence in any prime base b. This is only possible if $s\leq b$. That is, b is the smallest prime number greater than or equal to s. The j-th coordinate of the point $\mathbf{u}_i$ in the Faure sequence is given by

$$u_{i,j}=\sum_{k=0}^{\infty}\tilde{a}_{j,k}(i)\,b^{\quad k\quad 1}, \quad j=1,...,s, \quad i\geq 1, \tag{5.22}$$

where

$$\tilde{a}_{j,k}(i)=\sum_{\ell=0}^{\infty}\binom{\ell}{k}(j\quad 1)^{\ell\quad k}a_\ell(i)(\mathrm{mod}\,b), \tag{5.23}$$

with

$$\binom{m}{n}=\begin{cases}\frac{m!}{n!\,(m\quad n)!}, & m\geq n,\\ 0, & \text{otherwise.}\end{cases} \tag{5.24}$$

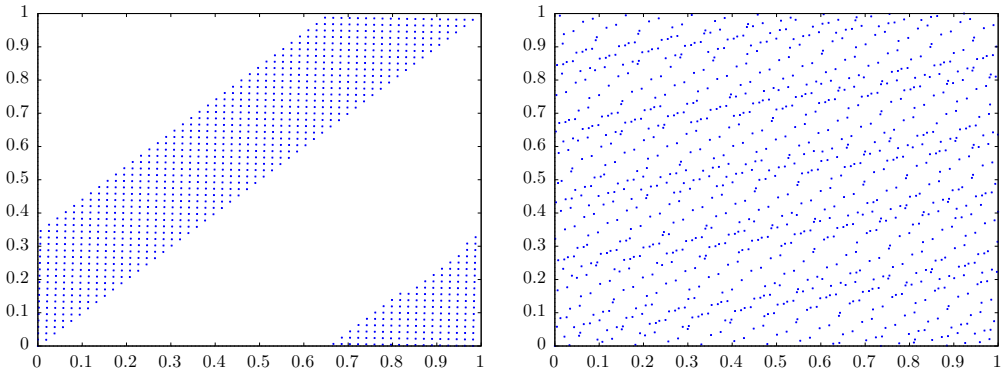

Figure 5.1. Coordinates 49 and 50 of the first 1,000 points in base 53 of a Faure sequence (left) and a generalized Faure sequence (5.28) (right).

In matrix form (5.23) is written

$$\begin{pmatrix} \tilde{a}_{j,0}(i) \\ \tilde{a}_{j,1}(i) \\ \vdots \end{pmatrix} = \mathbf{C}^{j \quad 1} \begin{pmatrix} a_0(i) \\ a_1(i) \\ \vdots \end{pmatrix} \bmod b, \tag{5.25}$$

where the generating matrices of the sequence are

$$\mathbf{C}^j(m,n) = \binom{n}{m} j^{n \quad m}, \tag{5.26}$$

that is, $\mathbf{C}^j$ is the j-th power of the Pascal matrix. The construction of the Faure sequence is described in detail in [104].

The Faure sequence is not extensible due to the condition $s \leq b$. Therefore, for different values of s new sequences must be constructed. Given a value of s the constant in (5.21) satisfies $\log C(t,s,b) \in O(\quad s \log s \log s)$ and thus it goes to zero exponentially fast with the dimension. By contrast, for the Sobol' sequence $\log C(t,s,b) \in O(s \log s \log s)$. As mentioned before, the t-value of this sequence is $t = 0$, which means that it achieves the best possible value of the uniformity parameter t. This is reflected in the one- and two-dimensional projections of the first b^2 points, which have optimal equidistribution in base b. However, the Faure sequence suffers from clustering around zero. As a workaround Faure suggested to discard the first $b^4 \quad 1$ points.

As shown in Figure 5.1, for large s the Faure sequence has gaps. In order to overcome this problem, Tezuka [105] introduced generalized Faure (GF) sequences by multiplying the generating matrices (5.26) from the left by nonsingular lower-triangular matrices. These matrices can be constructed in a deterministic way or randomly. In this thesis, the generating matrices of the Faure sequence are multiplied by random striped matrices [106],

$$\mathbf{R}^{(j)} = \begin{pmatrix} h_1 & 0 & 0 & 0 & \cdots \\ h_1 & h_2 & 0 & 0 & \cdots \\ h_1 & h_2 & h_3 & 0 & \cdots \\ h_1 & h_2 & h_3 & h_4 & \cdots \\ \vdots & \vdots & \vdots & \vdots & \ddots \end{pmatrix}, \quad j = 1, \ldots, s, \tag{5.27}$$

where each element h_i is uniformly distributed on $\mathbb{Z}_b^+$. This procedure, called a matrix scrambling of the Faure sequence, yields GF sequences with coefficients

$$\begin{pmatrix} \tilde{a}_{j,0}(i) \\ \tilde{a}_{j,1}(i) \\ \vdots \end{pmatrix} = \mathbf{R}^{(j)}\, \mathbf{C}^{j \quad 1} \begin{pmatrix} a_0(i) \\ a_1(i) \\ \vdots \end{pmatrix} \bmod b. \tag{5.28}$$

5.2.3 Integrals with a Gaussian kernel

In this thesis, the first N points from the GF sequence (5.28) were used to approximate integrals with a Gaussian kernel

$$I_s[f] = \int_{\mathbb{R}^s} f(\mathbf{x})\, e^{\quad \|\mathbf{x}\|^2} \mathrm{d}^s x. \tag{5.29}$$

Since the points $\mathbf{u}_i$ in this sequence belong to the unit hypercube $B_s = [0,1)^s$, the domain of integration, $\mathbb{R}^s$, has to be mapped onto B_s. Using the change of variables

$$y_j = \phi(\sqrt{2}x_j), \quad \mathrm{d}y_j = \sqrt{2}\phi'(\sqrt{2}x_j)\mathrm{d}x_j, \quad j = 1, ..., s, \tag{5.30}$$

where ϕ is the CDF of the standard normal distribution $\mathcal{N}(0,1)$,

$$\phi(t) = \frac{1}{\sqrt{2\pi}} \int_{\infty}^{t} e^{\quad x^2/2} \mathrm{d}x, \quad t \in (\quad \infty, \infty), \tag{5.31}$$

with

$$\phi'(t) = \frac{1}{\sqrt{2\pi}}\, e^{\quad t^2/2}, \tag{5.32}$$

the integral (5.29) transforms into

$$I_s[f] = \pi^{\frac{s}{2}} \int_{B_s} f\Big(\frac{\phi^{\quad 1}(y_1)}{\sqrt{2}}, ..., \frac{\phi^{\quad 1}(y_s)}{\sqrt{2}}\Big)\, \mathrm{d}^s y, \tag{5.33}$$

where $\phi^{\quad 1}$ is the quantile function of $\mathcal{N}(0,1)$, which has no analytical expression.

In order to demonstrate the high accuracy of quasi-Monte Carlo integration using the GF sequence (5.28), consider the s-dimensional integral

$$I_s[\cos] = \int_{\mathbb{R}^s} \cos(\|\mathbf{x}\|)\, e^{\quad \|\mathbf{x}\|^2} \mathrm{d}^s x, \tag{5.34}$$

which in spherical coordinates reduces to a one-dimensional quadrature,

$$I_s[\cos] = \frac{2\pi^{\frac{s}{2}}}{\frac{s}{2}\big)} \int_0^{\infty} \cos(r) e^{\quad r^2} r^{s \quad 1} \mathrm{d}r, \tag{5.35}$$

since the angular integral can be readily calculated [107],

$$\int_0^{2\pi} \mathrm{d}\varphi \int_0^{\pi} \mathrm{d}\theta_s \;{}_2\sin\theta_s \;{}_2 \cdots \int_0^{\pi} \mathrm{d}\theta_1 \sin^{s \quad 2}\theta_1 = \frac{2\pi^{\frac{s}{2}}}{\frac{s}{2}\big)}. \tag{5.36}$$

	s						
N	9	16	25	36	49	64	81
512	10^{-4}	10^{-3}	10^{-2}	10^{-2}	10^{-2}	10^{-3}	10^{-2}
1,024	10^{-4}	10^{-3}	10^{-3}	10^{-3}	10^{-2}	10^{-2}	10^{-2}
4,096	10^{-3}	10^{-3}	10^{-5}	10^{-3}	10^{-2}	10^{-2}	10^{-2}
16,384	10^{-3}	10^{-3}	10^{-4}	10^{-3}	10^{-2}	10^{-3}	10^{-3}
65,536	10^{-4}	10^{-4}	10^{-5}	10^{-3}	10^{-2}	10^{-3}	10^{-3}

Table 5.1. Order of magnitude of the relative error, as defined in (5.37), in the calculation of the integral (5.34) using a generalized Faure sequence.

The accuracy of the method can be quantified in terms of the relative error

$$\eta = \left| \frac{Q_N \quad I_s(\cos)}{I_s(\cos)} \right|, \tag{5.37}$$

with Q_N given by

$$Q_N = \pi^{\frac{s}{2}} \frac{1}{N} \sum_{i=1}^{N} \cos\left(\sqrt{\frac{1}{2} \sum_{j=1}^{s} \phi^{-1}(u_{ij})^2} \right). \tag{5.38}$$

As shown in Table 5.1, the order of magnitude of η is at most 10^{-2} over a wide range of values of N and s. This level of accuracy is sufficient for the calculations in Chapter 4. For the calculation of η, the quadrature in (5.35) was evaluated with the QAGI routine of QUADPACK [108] and the quasi-Monte Carlo calculation was carried out using the Java program discussed in Appendix C.

6 Conclusions and outlook

Quantum fields often provide an appropriate description of quantum systems with a large number of interacting constituents. Therefore, the objective of this research project was the development of a generic model that describes the decoherence dynamics of a non-relativistic bosonic quantum field towards a corresponding classical field theory, while minimally affecting the quantum field. The construction of such a model and its physical characterization turned out to be quite challenging, which was a great source of motivation throughout.

In this chapter I present a short summary of the results obtained, highlight the contributions of this thesis to the field of open quantum systems, and discuss possible extensions of the model introduced here.

Results

In Chapter 3 I introduced a generic Lindblad master equation that induces the gradual classicalization of a non-relativistic bosonic quantum field. On the one hand, this open-system dynamics induces a monotonic decay of the purity of any state of the field. In consequence, any quantum superposition of field configurations turns into a mixture. On the other hand, the Ehrenfest equations for the canonical field variables are identical to the corresponding classical field equations. Therefore, the classical superposition principle is not affected. In this sense, the model fulfills the requirement of minimal impact on the bosonic field. In addition to inducing decoherence, the master equation leads to an increase of the field energy with a constant and state-independent rate. Other decoherence models, such as spontaneous-collapse theories, have provided evidence that this energy increase is inevitable. The open-system dynamics induced by the master equation can be interpreted as arising from a Poisson process in which the unitary evolution is interrupted at random times by a minimally imprecise uninformative generalized measurement of the canonical field variables enclosed in a finite region. This measurement process amounts to subjecting the field to random kicks in the functional phase space of the field amplitude and its canonically conjugate momentum.

In Chapter 4 I analyzed the classicalization dynamics of the bosonic field using phase-space methods. As shown there, the time evolution of the Wigner functional in the functional phase space mentioned above is described by a generalized linear Boltzmann equation, which in the diffusion limit reduces to a Fokker–Planck equation. Assuming that the initial state of the field is a superposition of single-mode coherent states, I obtained approximate analytical expressions for the purity decay. They correspond to important limiting cases of the parameters in the master equation, and are in excellent agreement with the numerical calculation of the exact dynamics of the purity.

Contributions

To the best of my knowledge, the decoherence dynamics and the emergence of classical behavior in non-relativistic bosonic quantum fields had not been hitherto investigated using a field-theoretic Lindblad master equation. As mentioned in the introduction, previous works only considered relativistic bosonic quantum fields subject to phase-space dynamics described by a Fokker–Planck equation [19–23]. This thesis should encourage further investigations of the decoherence dynamics of non-relativistic and also relativistic quantum fields. In particular, the phase-space methods used to analyze the classicalization induced by the master equation serve as a starting point for several possible generalizations, as will be discussed below.

Another contribution of this work is the utilization of quasi-Monte Carlo integration based on generalized Faure sequences for the efficient and accurate calculation of expectation values in a high-dimensional phase space. Integration methods of this kind are better known in fluid mechanics and financial engineering. This thesis makes a strong case for their inclusion in the numerical toolbox of the quantum physicist.

Possible extensions

The field-theoretic classicalization model presented in this thesis can be applied to a non-relativistic scalar field in one spatial dimension. In order to develop classicalization models that can be applied to tensor fields, relativistic fields or fermionic fields, it is desirable to use a general framework that can handle all of these cases. In the following, I provide a brief summary of the methods that allow constructing quantum dynamical semigroups on bosonic and fermionic algebras.

The solution of the master equation introduced in this thesis was shown to be of the form $\tilde{\chi}_t[\eta] = \chi_0[\eta]\, f_t[\eta]$ in the Wigner phase-space representation. Here, $\chi_0[\eta]$ and $f_t[\eta]$ are a quantum and a classical function of positive type [109], given by the Fourier transform of the Wigner functional and of a classical probability measure, respectively. This is an example of a classical-quantum semigroup [110], that is, a one-parameter family of mappings of the form $S_t\, \chi_0[\eta] = \chi_0[\eta]\, f_t[\eta]$ where, in general, f_t is a convolution semigroup of measures.

In the 1970s the quasi-free dynamical semigroups on the CCR algebra were introduced [111]. They are completely positive semigroups that map Weyl operators onto Weyl operators. In the Fock representation, the generator of the semigroup is of Lindblad form [112]. Moreover, using the correspondence between Weyl operators and characteristic functionals in phase space, which was discussed in Chapter 2, a quasi-free semigroup corresponds to a classical-quantum semigroup.

In the 1980s a Poincaré-covariant quasi-free dynamical semigroup that describes the decay of unstable neutral scalar particles was introduced [20]. As expected, the corresponding generator is of Lindblad form. Building on this work, the emergence of classical electrodynamics from quantum electrodynamics could be investigated by constructing appropriate relativistic quasi-free semigroups. It is worth noting that this framework allows the direct construction of non-unitary dynamics

in phase space, which is the preferred representation to study the quantum-classical transition.

Phase space methods have also been developed for fermions [8, 113]. They are based on Grassmann or anticommuting variables, since fermion operators satisfy canonical anticommutation relations (CAR). Quasi-free semigroups on the CAR algebra have also been studied [114]. They are defined as mappings on monomials of the fermionic Fock operators, and have been used to describe the dynamics of infinite fermionic systems in contact with a thermal bath [115, 116]. To the best of my knowledge, decoherence in infinite fermionic systems has not yet been studied using phase space methods and quasi-free semigroups.

Of course, classicalization models for tensor, relativistic and fermionic fields can be constructed by specifying the Lindblad generator. But it would be interesting to determine what are the advantages, if any, of the framework of quasi-free semigroups. One should not forget that the road less traveled can lead to new insights and inspire many questions.

Epilogue

Many contemporary experiments prepare quantum superpositions of increasingly macroscopic and complex objects, which are in contact with an environment. Probing the physics at the quantum-classical border in these many-body systems allows testing classicalization models and yields insight into the decoherence processes that degrade the performance of quantum technologies.

Due to the above, it is clear that there will be an increased interest in the development of field-theoretic decoherence models. I hope that this thesis will serve as a reference to the existing literature on the subject and as a guide for future developments, since it provides a generic model that can be generalized in many different ways, it discusses useful analytic and numerical methods, and provides pointers to more than a hundred books and research articles.

Appendix A
Functional integration

As shown in Section 2.2, for countably infinite many variables the concept of the functional derivative can be defined as a straightforward generalization of the directional derivative for functions of n variables.

However, the integration of functions of a finite number of variables cannot be extended to infinitely many variables by defining the integration measure as

$$\mathcal{D}x = \prod_{i=1}^{\infty} \mathrm{d}x_i. \tag{A.1}$$

This is so because there is no Lebesgue measure on the infinite-dimensional vector space $V = L^2(\mathbb{R}^n)$ [117]. The well-defined measures in such a space are probability measures μ, which satisfy

$$\int_V \mathrm{d}\mu = 1. \tag{A.2}$$

These measures are defined through their inverse Fourier transform or characteristic functional [118]

$$\chi_\mu[f] = \int_V \mathrm{d}\mu(\phi)\, e^{\mathrm{i}\phi[f]}, \tag{A.3}$$

with f in the Schwartz space of test functions $\mathcal{S}(\mathbb{R}^n) \subset L^2(\mathbb{R}^n)$. The characteristic functional is continuous, positive definite and satisfies the normalization $\chi_\mu[0] = 1$.

In the case of free quantum fields the relevant measures are Gaussian, with their characteristic functional given by [118]

$$\chi_\mu[f] = \exp\Big(\tfrac{1}{2}\langle f, \mathrm{C} f\rangle_V \Big), \tag{A.4}$$

where C is called the covariance operator and $\langle\cdot,\cdot\rangle_V$ is the inner product in $L^2(\mathbb{R}^n)$,

$$\langle f, g\rangle = \int_{\mathbb{R}^n} f^*(x) g(x)\, \mathrm{d}^n x. \tag{A.5}$$

The measure corresponding to (A.4) is formally given by [118]

$$\mathrm{d}\mu_C = B \exp\Big(\tfrac{1}{2}\langle f, \mathrm{C}^{-1} f\rangle \Big)\, \mathcal{D}f, \tag{A.6}$$

where B is a constant and $\mathcal{D}f$ is a fictitious Lebesgue measure in V. In fact, none of the three factors is well-defined. The actual measure corresponding to (A.4) is given by the limit $n \to \infty$ of the finite-dimensional measure [118]

$$\mathrm{d}\mu_{C_\mathcal{F}} = \frac{\det \mathrm{C}_\mathcal{F}^{1/2}}{(2\pi)^{n/2}} \exp\Big(\tfrac{1}{2}\langle f, \mathrm{C}_\mathcal{F}^{-1} f\rangle \Big) \mathrm{d}x^n, \tag{A.7}$$

where $\mathcal{F}$ is a finite-dimensional subspace of V and $\mathrm{C}_{\mathcal{F}}$ is the restriction of C to $\mathcal{F}$. For the quantum field considered in this work the covariance operator is given by [119]

$$\mathrm{C} = (\omega^2/v^2 \quad \partial_x^2)^{1/2}, \tag{A.8}$$

which is related to the scalar product in the Hilbert space of solutions of the classical Klein–Gordon equation [120],

$$\langle f, g\rangle = \int \mathrm{d}x \left[f^*(x)\sqrt{\omega^2/v^2 \quad \partial_x^2}\, g(x) + \sqrt{\omega^2/v^2 \quad \partial_x^2}\, f^*(x)\, g(x)\right]. \tag{A.9}$$

For a finite number n of variables, the Fourier transform of a function f is defined as

$$\tilde{f}(k) = \frac{1}{(2\pi)^{n/2}} \int \mathrm{d}^n x\, e^{\ \mathrm{i}\sum_{j=1}^{n} k_j x_j} f(x_1, ..., x_n), \tag{A.10}$$

which is a pointwise well-defined integral. The corresponding Fourier transform for countably infinite variables is the limit $n \to \infty$ of (A.10). However, it is customary to write the formal expression [121]

$$\tilde{F}[\varphi] = \mathcal{C} \int \mathcal{D}g\ e^{\ \mathrm{i}\langle \varphi, g\rangle} F[g], \tag{A.11}$$

where $\mathcal{C}$ goes to zero when $n \to \infty$, but it is compensated by a diverging term contained in the fictitious Lebesgue measure $\mathcal{D}g$. Considering Eq. (A.11) as a linear mapping between functionals, it can be useful for performing analytic manipulations. But one should keep in mind that it is not a well-defined integral.

For a more comprehensive discussion of functional integration the reader should consult Ref. [121].

Appendix B

Fortran source code

The numerical calculations in Chapter 4 can be reproduced using the Fortran program contained in this appendix. This program takes advantage of several features in the Fortran 2008 standard [122]. In particular, it uses Fortran coarrays for parallelization. The free-software GNU Fortran compiler requires the installation of the OpenCoarrays library in order to support coarrays. On the Linux-based operating system Ubuntu 18.04 the required software can be installed with the commands

```
# apt update
# apt install gfortran libcoarrays-dev libopenmpi-dev open-coarrays-
  bin
```

The Fortran program consists of two modules and a front end. The module `Faure` (Figure B.2) executes the Java program discussed in Appendix C (Figure C.1) and loads the resulting binary file into an array. The module `Purity_mod` (Figures B.3 to B.9) contains the subroutines `purity`, which calculates the time evolution of the purity of a given initial state, and `purity_decay`, which calculates the purity decay as a function of the separation between the coherent states in a superposition. Of course, this module also contains the necessary code to perform these calculations. The front end in Figure B.1 allows performing the calculations in Chapter 4. The compilation and execution of the program is carried out with the commands

```
$ gfortran -c Faure.f90
$ gfortran -fcoarray=lib -O3 -c purity.f90 -lcaf_mpi
$ gfortran -fcoarray=lib Faure.o purity.o -lcaf_mpi main.f90 -o
  purity
$ cafrun -np 4 ./purity
```

The number 4 should be adjusted to the number of processor cores available. On a computer with 4 cores the run time of the program should be around 12 seconds.

Changing the parameters characterizing the kinematics and the dynamics of the quantum system involves recompiling the program. This can be avoided if the

parameters are written in a configuration file which is then passed as an argument to the `purity` executable. The JSON serialization format is a standard choice for such a task. In fact, there is a JSON library for Fortran. Another possibility to interact more easily with the program is to use the LFortran compiler, which is under development at the Los Alamos National Laboratory in the USA. This compiler extends the Fortran language providing an interactive commandline interface and also a web interface based on the Jupyter digital notebook. As a third option the reader might also consider translating the program to the Julia programming language. This is straightforward and leads to a reduction in code size due to Julia's type inference. However, since it is a young language, for archival purposes I chose to write the program in Fortran. In the following I will discuss some aspects of the code in order to make it more understandable.

The module `Purity_mod` (Figure B.3) uses global variables instead of passing these variables as arguments to all the subroutines and functions in the module. The `allocatable` arrays are declared specifying the number of dimensions using colons (`:`), but their size is determined at runtime. In fact, these arrays are allocated by the subroutine `setup_arrays` (Figure B.6). Correspondingly, at the end of the calculations the arrays are deallocated by the subroutine `deallocate_arrays` (Figure B.6).

The program is compiled with support for coarrays and is executed on N processor cores. However, in the present case it is not necessary to write the result of the calculations in parallel to a file. Therefore, in the subroutines `purity` (Figure B.4) and `purity_decay` (Figure B.5) only one of the processes (or images in Fortran parlance) writes the file with the results of the calculation. As shown in Figure B.5 the subroutine `write_params` adds a header to this file specifying the physical parameters of the simulation. The header can be parsed by a computer program, but if more structure is desired, it is recommended to use the JSON format.

The subroutine `eta_integrate` in Figure B.7 calculates the integral of a given function f in a high-dimensional space using the generalized Faure sequence provided by the `Faure` module. Since this calculation can be readily parallelized, it relies on Fortran coarrays. The dimension of a coarray corresponds to the number of elements it contains, whereas the codimension corresponds to the number of images (or processes) that read from or write to the coarray. This distinction is evident in the last section of code in the subroutine, where the results from all coarrays are combined in the coarray corresponding to the first image.

The integrands of the integrals carried out by the program are constructed using the function `chi_sq_sup_coh` (Fig. B.8), which contains all the terms present in the squared modulus of the characteristic functional of a superposition of coherent states. This function takes a function as an argument in order to avoid repeating code. For calculating the decay of the purity the integrand is determined by `chi_sq_sup_coh_states` (Fig. B.8) and for the calculation of the time evolution of the purity the integrand is specified by `chi_sq_sup_coh_t` (Fig. B.9).

The function `g_r` in Figure B.9 implements the core of the decoherent dynamics. It is also the part of the code that determines its performance. The reason for this is that it involves a function of three physical variables: time, position and Fourier modes. A typical imperative implementation would use three nested loops to calculate this function. Whereas in Julia this algorithm is efficient, in Fortran it is more performant to precalculate the function and store it in a three-dimensional array, which is done by the subroutine `setup_arrays` (Fig. B.6), and use a single loop to extract two-dimensional sub-arrays. It is important to keep in mind that in both Fortran and Julia arrays are stored in memory column-wise.

The source code in this Appendix should allow the interested reader to reproduce the results of Chapter 4. Moreover, it can be used as a starting point to perform calculations with other superposition states or to study different decoherent dynamics. In order to facilitate this, the Java and Fortran files are available permanently at [123].

```
program main
  use Faure
  use Purity_mod

  implicit none

  integer, parameter :: dp = kind(0.0D0)
  integer :: i, N, eta_points, t_points, N_states, mode_alpha, mode_beta
  real(dp) :: Gamma, sigma_g, C, sigma_f, max_separation, T_final
  complex(dp) :: alpha_ini, beta_ini
  complex(dp), allocatable :: eta(:,:)
  real(dp), allocatable :: t(:), d(:)
  type(t_state) :: state
  type(t_params) :: params

  N = 32                        ! Number of oscillators in the chain
  eta_points = 2**12            ! Discretization of phase space
  t_points = 64                 ! Discretization of time
  T_final = 100.0               ! Calculate the purity until T_final

  Gamma = 0.2                   ! Kick rate
  sigma_g = 1.0                 ! Width of the kick distribution
  C = 0.01                      ! Dimensionless coupling constant
  sigma_f = 1.0                 ! A name for sigma_x/L

  alpha_ini = (2.0D0, 2.0D0)  !  2.0 + 2.0i
  beta_ini = (-2.0D0, -2.0D0) ! -2.0 - 2.0i
  mode_alpha = 0
  mode_beta = mode_alpha

  N_states = 99                 ! Number of superposition states
  max_separation = 3.0          ! Maximum separation between the coherent states

  state = t_state(alpha_ini, beta_ini, mode_alpha, mode_beta)
  params = t_params(Gamma, C, sigma_f, sigma_g)

  allocate(eta(N,eta_points))
  eta = faure_eta(eta_points, 2*N)

  allocate(t(t_points+1))
  t = T_final*[(1.0D0/t_points*i, i=0,t_points)]

  allocate(d(N_states+1))
  d = max_separation*[(1.0D0/N_states*i, i=0,N_states)]

  call purity(eta, state, params, t, "purity.dat")
  call purity_decay(eta, state, params, d, "purity_decay.dat")
end program main
```

Figure B.1. Fortran program to perform the calculations of Chapter 4 (`main.f90`).

```
module Faure

  implicit none

  integer, private, parameter :: dp = kind(0.0D0)

contains

  function faure_eta(points, dims)
    integer :: points, dims, i, j, status, fileunit, rec_len
    character(128) :: cmd, filename
    logical :: file_exists

    real(dp), dimension(points*dims) :: eta_1D
    real(dp), dimension(points,dims) :: eta_2D
    complex(dp), dimension(points*dims/2) :: eta_C_1D
    complex(dp), dimension(dims/2,points) :: faure_eta

    rec_len = storage_size(eta_1D)/8*size(eta_1D)

    write(filename, "(*(g0))") "Faure_eta", "_", points, "_", dims, ".dat"
    filename = trim(filename)

    inquire(file=filename, exist=file_exists)

    if (.not. file_exists) then
       write(cmd, "(*(g0))") "FaureGen_eta", " ", points, " ", dims
       call execute_command_line("java -cp ssj.jar:. " // trim(cmd))
       call exit(0)
    endif

    open(newunit=fileunit, file=filename, convert='big_endian',&
         access='direct', recl=rec_len, iostat=status)

    if (status .eq. 0) then
       read(unit=fileunit, rec=1) eta_1D
       close(fileunit)
    else
       print *, "Error reading " // filename
       call exit(0)
    endif

    eta_2D = reshape(eta_1D/sqrt(2.0), [points, dims])
    eta_C_1D = [((cmplx(eta_2D(i,j), eta_2D(i,j+1)), i=1,points), j=1,dims,2)]
    faure_eta = transpose(reshape(eta_C_1D, [points, dims/2]))
  end function faure_eta

end module Faure
```

Figure B.2. Source code of the module `Faure` (`Faure.f90`).

```
module Purity_mod

  implicit none

  public :: purity, purity_decay
  public :: t_state, t_params

  private

  integer, parameter :: dp = kind(0.0D0)
  real(dp), parameter :: Pi = 4*atan(1.0D0)
  complex(dp), parameter :: Im = (0.0D0, 1.0D0)

  integer  :: N, eta_points, t_points, N_states
  real(dp) :: Gamma, sigma_g, C, sigma_f

  complex(dp), allocatable :: exp_jtq(:,:,:)
  real(dp), allocatable :: W_sqrt(:), Fq(:), qs(:)

  complex(dp) :: c1, c2
  complex(dp), allocatable :: alpha_tilde(:)
  real(dp) :: Norm_sq

  integer :: mode_alpha, mode_beta
  complex(dp) :: alpha_ini, beta_ini

  type t_state
     complex(dp) alpha_ini
     complex(dp) beta_ini
     integer  mode_alpha
     integer  mode_beta
  end type t_state

  type t_params
     real(dp) Gamma
     real(dp) C
     real(dp) sigma_f
     real(dp) sigma_g
  end type t_params

contains

    ! The subroutines and functions contained in the module will be
    ! presented in separate listings. When writing the file purity.f90,
    ! they must be included here.

end module Purity_mod
```

Figure B.3. Source code of the module `Purity_mod` (`purity.f90`).

```
subroutine purity(eta, state, params, t, filename)
    complex(dp) :: eta(:,:)
    type(t_state) :: state
    type(t_params) :: params
    real(dp) :: t(:)
    character(len=*) :: filename

    real(dp) :: p_t(size(t))
    integer :: unit, i

    N = size(eta, 1)
    eta_points = size(eta, 2)
    t_points = size(t)

    call setup_state_params(state, params)

    call setup_arrays(t)

    call setup_state()

    call eta_integrate(chi_sq_sup_coh_t, eta, t, p_t)

    if (this_image() == 1) then
       open(newunit=unit, file=filename)
       call write_params(unit)
       write(unit, "(*(g0))") "# ", "time, ", "purity"
       write(unit, "(*(g0))") (t(i), " ", p_t(i), new_line("A"), i=1,size(t))
       close(unit)
    endif

    call deallocate_arrays()
end subroutine purity


subroutine setup_state_params(state, params)
    type(t_state) :: state
    type(t_params) :: params

    alpha_ini = state%alpha_ini
    beta_ini = state%beta_ini
    mode_alpha = state%mode_alpha
    mode_beta = state%mode_beta

    Gamma = params%Gamma
    C = params%C
    sigma_f = params%sigma_f
    sigma_g = params%sigma_g
end subroutine setup_state_params
```

Figure B.4. Source code of the subroutines `purity` and `setup_state_params`.

```
subroutine purity_decay(eta, state, params, d, filename)
    complex(dp) :: eta(:,:)
    type(t_state) :: state
    type(t_params) :: params
    real(dp) :: d(:)
    character(len=*) :: filename

    real(dp) :: p_d(size(d))
    integer :: unit, i

    N = size(eta, 1)
    eta_points = size(eta, 2)
    t_points = 1
    N_states = size(d)

    call setup_state_params(state, params)

    call setup_arrays([0.0D0])

    call eta_integrate(chi_sq_sup_coh_states, eta, d, p_d)

    if (this_image() == 1) then
       open(newunit=unit, file=filename)
       call write_params(unit)
       write(unit, "(*(g0))") "# ", "2|delta| = |alpha - beta|, ", "purity"
       write(unit, "(*(g0))") (d(i), " ", p_d(i), new_line("A"), i=1,size(d))
       close(unit)
    endif

    call deallocate_arrays()
end subroutine purity_decay

subroutine write_params(unit)
    integer :: unit

    write(unit, "(*(g0))") "# N: ", N
    write(unit, "(*(g0))") "# eta_points: ", eta_points
    write(unit, "(*(g0))") "# Gamma: ", Gamma
    write(unit, "(*(g0))") "# sigma_x/L: ", sigma_f
    write(unit, "(*(g0))") "# C: ", C
    write(unit, "(*(g0))") "# sigma_g: ", sigma_g
    write(unit, "(*(g0), SP)") "# alpha: ", real(alpha_ini), " ",&
         aimag(alpha_ini), "i"
    write(unit, "(*(g0))") "# mode_alpha: ", mode_alpha
    write(unit, "(*(g0), SP)") "# beta: ", real(beta_ini), " ",&
         aimag(beta_ini), "i"
    write(unit, "(*(g0))") "# mode_beta: ", mode_beta
    write(unit, *)
end subroutine write_params
```

Figure B.5. Source code of the subroutines `purity_decay` and `write_params`.

```
subroutine setup_arrays(t)
    real(dp) :: t(t_points)
    integer :: i,j,k

    allocate(alpha_tilde(N))

    allocate(qs(N))
    qs = 2*Pi*mode_range(N)/N

    allocate(W_sqrt(N))
    W_sqrt = sqrt(sqrt(1.0 + 2.0*C**2*(1.0 - cos(qs))))

    allocate(exp_jtq(N, t_points, N))
    exp_jtq = reshape([(((exp(Im*(qs(i)*j + W_sqrt(i)**2*t(k))), j=1,N),&
        k=1,t_points), i=1,N)], [N,t_points,N])

    allocate(Fq(N))
    Fq = exp(-sigma_f**2*qs**2*N**2/2.0)
    Fq = sqrt(N*1.0D0)*Fq/sum(Fq)
end subroutine setup_arrays

subroutine deallocate_arrays()
    deallocate(alpha_tilde)
    deallocate(W_sqrt)
    deallocate(Fq)
    deallocate(qs)
    deallocate(exp_jtq)
end subroutine deallocate_arrays

subroutine setup_state()
    complex(dp) :: sum_alpha_tilde_conj_Z
    complex(dp) :: abs_sq_alpha_tilde
    complex(dp), dimension(N) :: alpha, beta, Z
    integer :: i

    alpha = [(merge(alpha_ini, 0.0*Im, qs(i) == mode_alpha), i=1,N)]
    beta = [(merge(beta_ini, 0.0*Im, qs(i) == mode_beta), i=1,N)]
    Z = (alpha + beta)/2.0

    alpha_tilde = alpha - Z
    sum_alpha_tilde_conj_Z = sum(alpha_tilde*conjg(Z))
    abs_sq_alpha_tilde = sum(alpha_tilde*conjg(alpha_tilde))

    c1 = 2.0*cos(4.0*aimag(sum_alpha_tilde_conj_Z))*exp(-4.0*abs_sq_alpha_tilde)
    c2 = 4.0*cos(2.0*aimag(sum_alpha_tilde_conj_Z))*exp(-abs_sq_alpha_tilde)

    Norm_sq = 1.0/(2.0 + 2.0*exp(-1.0/2*sum(abs(alpha - beta)**2))*&
        cos(aimag(sum(conjg(alpha)*beta))))**2
end subroutine setup_state
```

Figure B.6. Source code of the subroutines `setup_arrays`, `deallocate_arrays` and `setup_state`.

```
function mode_range(N)
    integer :: N, i
    real(dp), dimension(N) :: mode_range

    if (modulo(N,2) == 0) then
       mode_range = [(i, i=-N/2+1, N/2)]
    else
       mode_range = [(i, i=-(N-1)/2, (N-1)/2)]
    endif
end function mode_range

! Only part of the code that involves coarrays (indexed with square brackets)
subroutine eta_integrate(f, eta, x, p)
     abstract interface
       function chi_sq_f(eta_i, v)
         complex(kind(0.0D0)) :: eta_i(N)
         real(kind(0.0D0)) :: v(size(x)), chi_sq_f(size(x))
       end function chi_sq_f
    end interface

    procedure(chi_sq_f) :: f

    complex(dp), intent(in) :: eta(:,:)
    real(dp), intent(in) :: x(:)
    real(dp), intent(out) :: p(size(x))

    real(dp), allocatable :: s(:)[:]
    integer :: eta_points, img, i

    eta_points = size(eta, 2)
    allocate (s(size(x))[*])
    s = 0.0D0
    img = this_image()

    do i = img, eta_points, num_images()
       s = s + f(eta(:,i), x)
    enddo

    sync all

    if (img == 1) then
       do i = 2, num_images()
          s(:) = s(:) + s(:)[i]
       enddo
       s = s/eta_points
       p = s
    endif
  end subroutine eta_integrate
```

Figure B.7. Source code of the function `mode_range` and the subroutine `eta_integrate`.

```
function chi_sq_sup_coh(f, eta_i, t) result(chi_sq)
    abstract interface
       function f_inter(eta_i, v)
         complex(kind(0.0D0)) :: eta_i(N)
         real(kind(0.0D0)) :: v(size(t)), f_inter(size(t))
       end function f_inter
    end interface

    procedure(f_inter) :: f
    real(dp), dimension(t_points) :: chi_sq, t
    complex(dp), dimension(N) :: eta_i
    complex(dp) :: im_a_tilde_c_eta_i

    im_a_tilde_c_eta_i = aimag(sum(alpha_tilde*conjg(eta_i)))
    chi_sq = f(eta_i,t)*(2.0 + 2.0*cos(4.0*im_a_tilde_c_eta_i) + c1)
    chi_sq = c2*cos(2.0*im_a_tilde_c_eta_i)*f(eta_i - alpha_tilde,t) + chi_sq
    chi_sq = c2*cos(2.0*im_a_tilde_c_eta_i)*f(eta_i + alpha_tilde,t) + chi_sq
    chi_sq = f(eta_i + 2*alpha_tilde,t) + f(eta_i - 2*alpha_tilde,t) + chi_sq
    chi_sq = chi_sq*Norm_sq
end function chi_sq_sup_coh

function chi_sq_sup_coh_states(eta_i, d) result(chi_sq_sep)
    complex(dp), dimension(N) :: eta_i
    real(dp), dimension(N_states) :: d, chi_sq_sep

    complex(dp) :: sep, delta_unit, Z
    integer :: i

    sep = abs((alpha_ini - beta_ini)/2.0)
    delta_unit = (alpha_ini - beta_ini)/(2.0*sep)
    Z = (alpha_ini + beta_ini)/2.0

    do i = 1,N_states
       alpha_ini = Z + d(i)*delta_unit
       beta_ini = Z - d(i)*delta_unit
       call setup_state()
       ! The decay rate is minus the time derivative of the purity
       ! sum is used to extract the only element of the array
       chi_sq_sep(i) = -sum(chi_sq_sup_coh(dec_kernel_t0, eta_i, [0.0D0]))
    enddo

contains
    function dec_kernel_t0(eta_i, t)
      real(dp), dimension(t_points) :: t, dec_kernel_t0
      complex(dp), dimension(N) :: eta_i

      dec_kernel_t0 = -2.0*Gamma*(1.0 - sum(real(g_r(eta_i)))/N)
    end function dec_kernel_t0
end function chi_sq_sup_coh_states
```

Figure B.8. Source code of the functions `chi_sq_sup_coh` and `chi_sq_sup_coh_states`.

```
function chi_sq_sup_coh_t(eta_i, t) result(chi_sq)
    real(dp), dimension(t_points) :: chi_sq, t
    complex(dp), dimension(N) :: eta_i

    chi_sq = chi_sq_sup_coh(dec_kernel_t, eta_i, t)

  contains

    function dec_kernel_t(eta_i, t)
      complex(dp), dimension(N) :: eta_i
      real(dp), dimension(t_points) :: dec_kernel_t, t

      dec_kernel_t = exp(-2.0*Gamma*t_int(1.0-sum(real(g_r(eta_i)),1)/N,t))
    end function dec_kernel_t

end function chi_sq_sup_coh_t

function g_r(eta_i)
    complex(dp), dimension(N) :: eta_i
    complex(dp), dimension(N, t_points) :: g_r
    integer :: i

    g_r = (0.0D0, 0.0D0)
    do i=1,N
       g_r = g_r + Fq(i)*(real(eta_i(i)*exp_jtq(:,:,i))/W_sqrt(i) +&
            Im*aimag(eta_i(i)*exp_jtq(:,:,i))*W_sqrt(i))
    enddo

    g_r = exp(-2.0*abs(g_r)**2*sigma_g**2)
end function g_r

function t_int(integrand, t)
    real(dp), dimension(t_points) :: t_int, integrand, t
    integer :: n

    t_int = cumsum(integrand)*t/[(n, n=1,t_points)]
end function t_int

function cumsum(x) result(s)
    real(dp) :: x(:)
    real(dp) :: s(size(x))
    integer :: i

    s(1) = x(1)
    do i=2,size(x)
       s(i) = x(i) + s(i-1)
    enddo
end function cumsum
```

Figure B.9. Source code of the functions `chi_sq_sup_coh_t`, `g_r`, `t_int`, and `cumsum`.

Appendix C
Generating Faure sequences with SSJ

The library Stochastic Simulation in Java (SSJ) [124] contains a generator of Faure sequences and also implements random striped matrices. Therefore, it allows constructing the GF sequence in Eq. (5.28). Since it also implements the inverse function of (5.31), after applying this transformation to the points in the sequence they can be readily used for performing the quasi-Monte Carlo integration in (5.38). However, unlike a software library written in the programming language C, a Java library cannot be easily used from other programming languages. On the positive side, Java excels at reproducibility. This means that on every major operating system (Linux-based, macOS, or Windows) a Java library can be readily used after installing the Java Development Kit.

In order to take advantage of SSJ for performing quasi-Monte Carlo integration in any programming environment, it is necessary to write a short Java program that generates the first N points of a GF sequence in s dimensions and stores them in a file. For compactness, it is convenient to write the file in binary format. Java uses big-endian format, wherein the binary representation of a number begins with the most significant byte.

Assuming that the source code in Figure C.1 is stored in the file `FaureGen.java`, located in the same directory as the Java archive `ssj.jar`, the command

```
$ javac -cp ssj.jar FaureGen.java
```

compiles the program to Java byte code, generating the file `FaureGen.class`. For $N = 4096$ and $s = 64$, the command

```
$ java -cp ssj.jar:. FaureGen 4096 64
```

executes the program `FaureGen`, that generates the file `FaureGen_4096_64.dat` which can be read by most programming environments. When executing the last command in Windows the colon (:) must be replaced with a semicolon (;).

For example, the above Java program can be used for calculating the quasi-Monte Carlo integral (5.38). This can be done using the free and open-source computer algebra system Maxima. The program in Figure C.2 shows how to do this. First, the function `GF` executes the Java program `FaureGen` and reads the resulting file `FaureGen_points_dim.dat` into a one-dimensional array, which is then reshaped into an $N \times s$ array. This array is then converted into a matrix, which in Maxima is implemented as a list of lists and can thus be processed using functional programming, a programming paradigm based on the λ-calculus that

```
import umontreal.ssj.probdist.NormalDist;
import umontreal.ssj.rng.*;
import umontreal.ssj.hups.*;
import java.io.*;

public class FaureGen {
    public static void main(String[] args) throws IOException {
         String msg = "Usage: java -cp ssj.jar:. FaureGen points
dimension";
         if (args.length < 2){
            System.out.println(msg);
            System.exit(0);
         }

         int points = Integer.parseInt(args[0]);
         int dim    = Integer.parseInt(args[1]);
         String filename = String.format("Faure_eta_%d_%d.dat",
points, dim);

         DigitalNet faure = new FaureSequence(points, dim);
         RandomStream RNG = new MRG32k3a();
         NormalDist normal = new NormalDist();
         double[] point = new double[dim];

         faure.stripedMatrixScramble(RNG);
         PointSetIterator iter = faure.iterator();

         // Skip the first point, (0,..,0), where
normal.inverseF is not defined
         iter.nextPoint(point, dim);

         // Write the coordinates of the points in binary format
         DataOutputStream dos =
             new DataOutputStream(new
FileOutputStream(filename));

        for (int i = 0; i < points; i++) {
            iter.nextPoint(point, dim);

            for (Double coord : point)
                dos.writeDouble(normal.inverseF(coord));
        }
    }
}
```

Figure C.1. Java program that generates a generalized Faure sequence using the SSJ library.

```
load(numericalio)$
load(stringproc)$

I(s):= (quad:quad_qagi(cos(r)*exp(-r^2)*r^(s-1),r,0,inf)[1],
    float(2*%pi^(s/2)*quad/gamma(s/2)))$

GF(points, dim):= block(
    system(simplode(["java -cp ssj.jar:. FaureGen", points,
dim], " ")),
    filename: sconcat(simplode(["Faure_eta", points, dim], "_"),
".dat"),
    array(GF_arr, flonum, points*dim),
    read_binary_array(openr_binary(filename), GF_arr),

    GF_Ns: make_array(flonum, points, dim),
    fillarray(GF_Ns, GF_arr),
    genmatrix(GF_Ns, points-1, dim-1, 0, 0))$

f(y):= cos(sqrt(apply("+", map(lambda([y_i], y_i^2/2), y))))$

Q(points, dim):= block([fPi: float(%pi)],
    apply("+", maplist(f,
rest(GF(points,dim)))))/points*fPi^(dim/2))$

eta(points, dim):= abs((I(dim) - Q(points,dim))/I(dim))$
```

Figure C.2. Maxima program for calculating the quasi-Monte Carlo integral (5.38) and the relative error (5.37).

allows expressing computations in a similar way to mathematics [125]. This is illustrated by the function `f`, which performs the mapping

$$\mathbf{u}_i = (u_{i1}, \ldots, u_{is}) \xrightarrow{f} \cos\left(\sqrt{\frac{1}{2}\sum_{j=1}^{s} \phi^{-1}(u_{ij})^2}\right) \tag{C.1}$$

on a given point of the GF sequence, and the function `Q`, which maps the N points of the sequence into the quasi-Monte Carlo integral (5.38).

Assuming that the source code in Figure C.2 is stored in the file `Faure.mac`, located in a directory that contains `ssj.jar` and `FaureGen.class`, Maxima should be invoked as

```
$ maxima --init-mac=Faure.mac
```

in order to obtain an interactive session. Calling the function `eta` for given values of N and s yields the relative error (5.37).

Bibliography

[1] H.-P. Breuer, F. Petruccione, The Theory of Open Quantum Systems, Oxford University Press, 2002.

[2] C. Gardiner, P. Zoller, The Quantum World of Ultra-Cold Atoms and Light Book I, Imperial College Press, 2014.

[3] C. Gardiner, P. Zoller, The Quantum World of Ultra-Cold Atoms and Light Book II, Imperial College Press, 2015.

[4] C. Gardiner, P. Zoller, The Quantum World of Ultra-Cold Atoms and Light Book III, Imperial College Press, 2017.

[5] M. Devoret, B. Huard, R. Schoelkopf, L. Cugliandolo, Quantum Machines: Measurement and Control of Engineered Quantum Systems, Ecole De Physique Des Houches, Oxford University Press, 2014.

[6] M. Arndt, K. Hornberger, Testing the limits of quantum mechanical superpositions, Nat. Phys. 10 (4) (2014) 271.

[7] H. Jeong, M. Sasaki (Eds.), Macroscopic quantumness: Theory and applications in optical sciences, Vol. 337 of Opt. Commun., 2015.

[8] B. Dalton, J. Jeffers, S. Barnett, Phase Space Methods for Degenerate Quantum Gases, Oxford University Press, 2015.

[9] B. Rauer, S. Erne, T. Schweigler, F. Cataldini, M. Tajik, J. Schmiedmayer, Recurrences in an isolated quantum many-body system, Science 360 (6386) (2018) 307–310.

[10] M. Blasone, P. Jizba, G. Vitiello, Quantum Field Theory and Its Macroscopic Manifestations: Boson Condensation, Ordered Patterns, and Topological Defects, Imperial College Press, 2011.

[11] P. M. Preiss, R. Ma, M. E. Tai, A. Lukin, M. Rispoli, P. Zupancic, Y. Lahini, R. Islam, M. Greiner, Strongly correlated quantum walks in optical lattices, Science 347 (6227) (2015) 1229–1233.

[12] A. B. Shkarin, A. D. Kashkanova, C. D. Brown, S. Garcia, K. Ott, J. Reichel, J. G. E. Harris, Quantum optomechanics in a liquid, Phys. Rev. Lett. 122 (2019) 153601.

[13] A. Schmitt, Introduction to Superfluidity: Field-theoretical Approach and Applications, Springer International Publishing, 2014.

[14] L. Childress, M. P. Schmidt, A. D. Kashkanova, C. D. Brown, G. I. Harris, A. Aiello, F. Marquardt, J. G. E. Harris, Cavity optomechanics in a levitated helium drop, Phys. Rev. A 96 (2017) 63842.

[15] R. Riedinger, A. Wallucks, I. Marinković, C. Löschnauer, M. Aspelmeyer, S. Hong, S. Gröblacher, Remote quantum entanglement between two micromechanical oscillators, Nature 556 (7702) (2018) 473.

[16] C. Ockeloen-Korppi, E. Damskägg, J. Pirkkalainen, M. Asjad, A. Clerk, F. Massel, M. Woolley, M. Sillanpää, Stabilized entanglement of massive mechanical oscillators, Nature 556 (7702) (2018) 478.

[17] C. Monroe, J. Kim, Scaling the ion trap quantum processor, Science 339 (6124) (2013) 1164–1169.

[18] C. F. Ockeloen-Korppi, E. Damskägg, J.-M. Pirkkalainen, A. A. Clerk, M. J. Woolley, M. A. Sillanpää, Quantum backaction evading measurement of collective mechanical modes, Phys. Rev. Lett. 117 (2016) 140401.

[19] J. R. Anglin, W. H. Zurek, Decoherence of quantum fields: pointer states and predictability, Phys. Rev. D 53 (1996) 7327–7335.

[20] R. Alicki, M. Fannes, A. Verbeure, Unstable particles and the poincare semigroup in quantum field theory, J. Phys. A: Math. Gen. 19 (6) (1986) 919.

[21] E. Calzetta, B. Hu, Correlations, decoherence, dissipation, and noise in quantum field theory, arXiv preprint hep-th/9501040 (1995).

[22] R. Graham, H. Haken, Functional fokker-planck treatment of electromagnetic field propagation in a thermal medium, Z. Phys. A: Hadrons Nucl. 234 (3) (1970) 193–206.

[23] S. Albeverio, O. G. Smolyanov, Infinite-dimensional stochastic schrödinger-belavkin equations, Russ. Math. Surv. 52 (4) (1997) 822–823.

[24] B. Vacchini, Quantum optical versus quantum brownian motion master equation in terms of covariance and equilibrium properties, J. Math. Phys. 43 (11) (2002) 5446–5458.

[25] E. Joos, H.-D. Zeh, C. Kiefer, D. Giulini, J. Kupsch, I. Stamatescu, Decoherence and the Appearance of a Classical World in Quantum Theory, Springer Berlin Heidelberg, 1996.

[26] A. Bassi, K. Lochan, S. Satin, T. P. Singh, H. Ulbricht, Models of wave-function collapse, underlying theories, and experimental tests, Rev. Mod. Phys. 85 (2013) 471–527.

[27] S. Nimmrichter, Macroscopic Matter Wave Interferometry, Springer International Publishing, 2014.

[28] H. Goldstein, C. Poole, J. Safko, Classical Mechanics, Addison Wesley, 2002.

[29] R. D'Auria, M. Trigiante, From Special Relativity to Feynman Diagrams: A Course in Theoretical Particle Physics for Beginners, Springer, 2015.

[30] I. Gelfand, S. Fomin, Calculus of Variations, Dover Publications, 2012.

[31] E. Zeidler, Quantum Field Theory I: Basics in Mathematics and Physics: A Bridge between Mathematicians and Physicists, Springer Science & Business Media, 2007.

[32] E. Engel, R. Dreizler, Density Functional Theory: An Advanced Course, Springer Science & Business Media, 2011.

[33] W. Fischer, I. Lieb, A Course in Complex Analysis: From Basic Results to Advanced Topics, Springer Science & Business Media, 2012.

[34] J. Lopuszanski, Introduction To Symmetry And Supersymmetry In Quantum Field Theory, World Scientific, 1991.

[35] J. Klauder, Beyond Conventional Quantization, Cambridge University Press, 2005.

[36] N. Bogolubov, A. Logunov, A. Oksak, I. Todorov, General Principles of Quantum Field Theory, Kluwer Academic Publishers, 1990.

[37] V. Tarasov, Quantum Mechanics of Non-Hamiltonian and Dissipative Systems, Elsevier Science, 2008.

[38] F. Strocchi, Elements of Quantum Mechanics of Infinite Systems, International School for Advanced Studies Lecture Series, World Scientific, 1985.

[39] R. Streater, A. Wightman, PCT, Spin and Statistics, and All That, Princeton University Press, 2000.

[40] J. M. Cook, The mathematics of second quantization, Proc. Natl. Acad. Sci. U.S.A. 37 (7) (1951) 417–420.

[41] R. Honegger, A. Rieckers, Photons In Fock Space And Beyond (In 3 Volumes), World Scientific, 2015.

[42] M. Schönberg, Application of second quantization methods to the classical statistical mechanics, Il Nuovo Cimento (1943-1954) 9 (12) (1952) 1139–1182.

[43] M. Doi, Second quantization representation for classical many-particle system, J. Phys. A: Math. Gen. 9 (9) (1976) 1465–1477.

[44] K. R. Parthasarathy, An Introduction to Quantum Stochastic Calculus, Modern Birkhäuser Classics, Springer Basel, 2012.

[45] C. Gardiner, P. Zoller, Quantum Noise: A Handbook of Markovian and Non-Markovian Quantum Stochastic Methods with Applications to Quantum Optics, Springer series in Synergetics, Springer, 2000.

[46] G. G. Emch, Algebraic Methods in Statistical Mechanics and Quantum Field Theory, Dover Publications, 2009.

[47] F. Berezin, The Method of Second Quantization, Academic Press, 1966.

[48] I. H. Deutsch, A basis-independent approach to quantum optics, Am. J. Phys. 59 (9) (1991) 834–839.

[49] A. Arai, Analysis On Fock Spaces And Mathematical Theory Of Quantum Fields, World Scientific Publishing Company, 2017.

[50] V. Bargmann, Remarks on a hilbert space of analytic functions, Proc. Natl. Acad. Sci. U.S.A. 48 (2) (1962) 199–204.

[51] I. E. Segal, Mathematical characterization of the physical vacuum for a linear bose-einstein field, Illinois J. Math. 6 (3) (1962) 500–523.

[52] A. Verbeure, E. Verboven, States of infinitely many oscillators, Physica 37 (1) (1967) 1–22.

[53] W. O. Kermack, W. H. McCrea, On professor whittaker's solution of differential equations by definite integrals: part ii: applications of the methods of non-commutative algebra, Proceedings of the Edinburgh Mathematical Society 2 (4) (1931) 220–239.

[54] R. Puri, Mathematical Methods of Quantum Optics, Springer Science & Business Media, 2001.

[55] R. J. Glauber, Coherent and incoherent states of the radiation field, Phys. Rev. 131 (1963) 2766–2788.

[56] A. C. Vutha, E. A. Bohr, A. Ransford, W. C. Campbell, P. Hamilton, Displacement operators: the classical face of their quantum phase, Eur. J. Phys. 39 (2) (2018) 25405.

[57] J. R. Klauder, Weak correspondence principle, J. Math. Phys. 8 (12) (1967) 2392–2399.

[58] A. Ashtekar, A. Magnon-Ashtekar, A curiosity concerning the role of coherent states in quantum field theory, Pramana 15 (1) (1980) 107–115.

[59] W. Louisell, Quantum Statistical Properties of Radiation, Wiley, 1990.

[60] H. Linde, A new way of visualising quantum fields, Eur. J. Phys. 39 (3) (2018) 35401.

[61] G. S. Agarwal, E. Wolf, Calculus for functions of noncommuting operators and general phase-space methods in quantum mechanics. i. mapping theorems and ordering of functions of noncommuting operators, Phys. Rev. D 2 (1970) 2161–2186.

[62] S. Mrówczyński, B. Müller, Wigner functional approach to quantum field dynamics, Phys. Rev. D 50 (1994) 7542–7552.

[63] R. Hudson, When is the wigner quasi-probability density non-negative?, Rep. Math. Phys. 6 (2) (1974) 249–252.

[64] W. Schleich, Quantum Optics in Phase Space, Wiley-VCH Verlag, 2001.

[65] R. F. Bishop, A. Vourdas, Displaced and squeezed parity operator: its role in classical mappings of quantum theories, Phys. Rev. A 50 (1994) 4488–4501.

[66] L. Cohen, Generalized phase-space distribution functions, J. Math. Phys. 7 (5) (1966) 781–786.

[67] R. Aldrovandi, Special Matrices of Mathematical Physics: Stochastic, Circulant, and Bell Matrices, World Scientific, 2001.

[68] F. Schwabl, Advanced Quantum Mechanics, Springer Science & Business Media, 2008.

[69] M. Vetterli, J. Kovačević, V. Goyal, Foundations of Signal Processing, Cambridge University Press, 2014.

[70] R. de la Madrid, A. Bohm, M. Gadella, Rigged hilbert space treatment of continuous spectrum, Fortschr. Phys. 50 (2) (2002) 185–216.

[71] G. Lindblad, On the generators of quantum dynamical semigroups, Commun. Math. Phys. 48 (2) (1976) 119–130.

[72] V. Gorini, A. Kossakowski, E. C. G. Sudarshan, Completely positive dynamical semigroups of n-level systems, J. Math. Phys. 17 (5) (1976) 821–825.

[73] P. Aniello, A. Kossakowski, G. Marmo, F. Ventriglia, Brownian motion on lie groups and open quantum systems, J. Phys. A: Math. Theor. 43 (26) (2010) 265301.

[74] A. Kossakowski, On quantum statistical mechanics of non-hamiltonian systems, Rep. Math. Phys. 3 (4) (1972) 247–274.

[75] M. Bolaños, B. A. Stickler, K. Hornberger, Decoherence of nonrelativistic bosonic quantum fields, Phys. Rev. A 99 (2019) 60103.

[76] P. Ehrenfest, Bemerkung über die angenäherte gültigkeit der klassischen mechanik innerhalb der quantenmechanik, Zeitschrift für Physik 45 (7) (1927) 455–457.

[77] D. I. Bondar, R. Cabrera, R. R. Lompay, M. Y. Ivanov, H. A. Rabitz, Operational dynamic modeling transcending quantum and classical mechanics, Phys. Rev. Lett. 109 (2012) 190403.

[78] L. E. Ballentine, Y. Yang, J. P. Zibin, Inadequacy of ehrenfest's theorem to characterize the classical regime, Phys. Rev. A 50 (1994) 2854–2859.

[79] V. V. Albert, L. Jiang, Symmetries and conserved quantities in lindblad master equations, Phys. Rev. A 89 (2014) 22118.

[80] D. Lidar, A. Shabani, R. Alicki, Conditions for strictly purity-decreasing quantum markovian dynamics, Chem. Phys. 322 (1) (2006) 82–86.

[81] P. Busch, P. Lahti, J. Pellonpää, K. Ylinen, Quantum Measurement, Springer, 2016.

[82] K. Jacobs, D. A. Steck, A straightforward introduction to continuous quantum measurement, Contemp. Phys. 47 (5) (2006) 279–303.

[83] J. von Neumann, Mathematical Foundations of Quantum Mechanics, Princeton University Press, 1955.

[84] M. Schlosshauer, Decoherence: and the Quantum-To-Classical Transition, Springer Science & Business Media, 2007.

[85] J. D. Cresser, S. M. Barnett, J. Jeffers, D. T. Pegg, Measurement master equation, Opt. Commun. 264 (2) (2006) 352–361.

[86] T. Heinosaari, J.-P. Pellonpää, Generalized coherent states and extremal positive operator valued measures, J. Phys. A: Math. Theor. 45 (24) (2012) 244019.

[87] J. R. Klauder, E. C. G. Sudarshan, Fundamentals of Quantum Optics, W.A. Benjamin, Inc., 1968.

[88] C. Carmeli, T. Heinosaari, J.-P. Pellonpää, A. Toigo, Optimal covariant measurements: the case of a compact symmetry group and phase observables, J. Phys. A: Math. Theor. 42 (14) (2009) 145304.

[89] K. Husimi, Some formal properties of the density matrix, Nippon Sugaku-Buturigakkwai Kizi Dai 3 Ki 22 (4) (1940) 264–314.

[90] F. Hanson, Applied Stochastic Processes and Control for Jump-Diffusions: Modeling, Analysis, and Computation, Society for Industrial and Applied Mathematics, 2007.

[91] B. Vacchini, K. Hornberger, Quantum linear boltzmann equation, Phys. Rep. 478 (4) (2009) 71–120.

[92] R. F. Pawula, Approximation of the linear boltzmann equation by the fokker-planck equation, Phys. Rev. 162 (1967) 186–188.

[93] M. C. Wang, G. E. Uhlenbeck, On the theory of the brownian motion ii, Rev. Mod. Phys. 17 (1945) 323–342.

[94] L. Diósi, C. Kiefer, Exact positivity of the wigner and p functions of a markovian open system, J. Phys. A: Math. Gen. 35 (11) (2002) 2675–2683.

[95] C. M. Bender, F. Cooper, G. S. Guralnik, Path integral formulation of mean-field perturbation theory, Ann. Phys. 109 (1) (1977) 165–209.

[96] N. Bleistein, R. Handelsman, Asymptotic Expansions of Integrals, Dover Publications, 1986.

[97] C. Lemieux, Monte Carlo and Quasi-Monte Carlo Sampling, Springer Science & Business Media, 2009.

[98] H. Niederreiter, Random Number Generation and Quasi-Monte Carlo Methods, Society for Industrial and Applied Mathematics, 1992.

[99] M. Holtz, Sparse Grid Quadrature in High Dimensions with Applications in Finance and Insurance, Springer Science & Business Media, 2010.

[100] T. Kinoshita, Quantum Electrodynamics, World Scientific, 1990.

[101] G. P. Lepage, A new algorithm for adaptive multidimensional integration, J. Comput. Phys. 27 (2) (1978) 192–203.

[102] I. M. Sobol', On the distribution of points in a cube and the approximate evaluation of integrals, Zhurnal Vychislitel'noi Matematiki i Matematicheskoi Fiziki 7 (4) (1967) 784–802.

[103] H. Faure, Discrépance de suites associées à un système de numération (en dimension s), Acta Arithmetica 41 (4) (1982) 337–351.

[104] P. Glasserman, Monte Carlo Methods in Financial Engineering, Springer Science & Business Media, 2004.

[105] S. Tezuka, Uniform Random Numbers: Theory and Practice, Springer Science & Business Media, 1995.

[106] A. B. Owen, Variance with alternative scramblings of digital nets, ACM Trans. Model. Comput. Simul. 13 (4) (2003) 363–378.

[107] S. Scherer, M. Schindler, A Primer for Chiral Perturbation Theory, Springer Science & Business Media, 2011.

[108] R. Piessens, E. de Doncker-Kapenga, C. Überhuber, D. Kahaner, Quadpack: A Subroutine Package for Automatic Integration, Springer Science & Business Media, 1983.

[109] P. Aniello, Square integrable representations, an invaluable tool, in: J.-P. Antoine, F. Bagarello, J.-P. Gazeau (Eds.), Coherent States and Their Applications, Springer International Publishing, 2018, pp. 17–40.

[110] P. Aniello, Classical-quantum semigroups, J. Phys.: Conf. Ser. 563 (2014) 12002.

[111] B. Demoen, P. Vanheuverzwijn, A. Verbeure, Completely positive maps on the ccr-algebra, Lett. Math. Phys. 2 (2) (1977) 161–166.

[112] P. Vanheuverzwijn, Generators for quasi-free completely positive semi-groups, Annales de l'I.H.P. Physique théorique 29 (1) (1978) 123–138.

[113] K. E. Cahill, R. J. Glauber, Density operators for fermions, Phys. Rev. A 59 (1999) 1538–1555.

[114] D. E. Evans, Completely positive quasi-free maps on the car algebra, Commun. Math. Phys. 70 (1) (1979) 53–68.

[115] A. Frigerio, V. Gorini, J. V. Pulé, Open quasi-free systems, J. Stat. Phys. 22 (4) (1980) 409–433.

[116] M. Fannes, F. Rocca, A class of dissipative evolutions with applications in thermodynamics of fermion systems, J. Math. Phys. 21 (2) (1980) 221–226.

[117] A. Skorohod, Integration in Hilbert Space, Springer Science & Business Media, 1974.

[118] J. Glimm, A. Jaffe, Quantum Physics: A Functional Integral Point of View, Springer Science & Business Media, 1987.

[119] J. Velhinho, Canonical quantization of the scalar field: the measure theoretic perspective, Adv. Math. Phys. 2015 (2015).

[120] S. Schweber, An Introduction to Relativistic Quantum Field Theory, Row, Peterson and Company, 1961.

[121] J. Klauder, A Modern Approach to Functional Integration, Birkhäuser Boston, 2010.

[122] W. Brainerd, Guide to Fortran 2008 Programming, Springer London, 2015.

[123] M. Bolaños Puchet, Decoherence of nonrelativistic bosonic quantum fields - Fortran code, available at https://doi.org/10.5281/zenodo.3359879 (Aug 2019).

[124] P. L'Ecuyer, L. Meliani, J. Vaucher, SSJ: a framework for stochastic simulation in Java, in: E. Yücesan, C.-H. Chen, J. L. Snowdon, J. M. Charnes (Eds.), Proceedings of the 2002 Winter Simulation Conference, IEEE Press, 2002, pp. 234–242, available at http://simul.iro.umontreal.ca/ssj/indexe.html.

[125] P. Selinger, Lecture notes on the lambda calculus, arXiv:0804.3434 (2008).

This dissertation was typeset by GNU TEXMACS 1.99.12